UNIVERSIDAD AUTÓNOMA DE MADRID
FACULTAD DE CIENCIAS
DEPARTAMENTO DE BIOLOGÍA MOLECULAR

Regulation of cancer cell viability by p38 MAPK

Report submitted by **Carmen Lorena Pereira Pérez**
to obtain the PhD degree at the Autónoma University of Madrid

Thesis Director:
Dr. Ángel Rodríguez Nebreda

Centro Nacional de Investigaciones Oncológicas (CNIO), Madrid
Institut de Recerca Biomèdica (IRB Barcelona), Barcelona

Abbreviations

∅	Diameter
APS	Ammonium persulfate
ASK1	Apoptosis signal-regulating kinase 1
a.u.	Arbitrary units
Bcl-2	Breakpoint cluster region 2
BH3	Bcl-2 homology region 3
BSA	Bovine serum albumin
CDDP	cis-diammine-dichloro-platinum (cisplatin)
cDNA	Complementary DNA
COX-2	Cyclooxygenase 2
DAB	3,3-di-amino-benzidine
DABCO	1,4-Diazabicyclo[2.2.2]octane
DAPI	4',6-diamidino-2-phenylindole
DCFDA	2′,7′-dichlorofluorescin diacetate
DMEM	Dulbecco's Modified Eagle Medium
DMSO	Dimethyl sulfoxide
DNA	Deoxyribonucleic acid
dNTPs	Deoxyribonucleotides triphosphate
DPI	Diphenyleneiodonium chloride
DPNH	2,4-dinitrophenylhydrazine
DTT	DL-dithiothreitol or Cleland's reagent
DUSP	Dual-specificity phosphatase
EDTA	Ethylenediamine tetraacetic acid
eEF-2	Eukaryotic translation elongation factor 2
EGTA	Ethylene glycol tetraacetic acid
ER	Estrogen receptor
FBS	Fetal bovine serum
FITC	Fluorescein isothiocyanate
FW	Forward
GAPDH	Glyceraldehyde 3-phosphate dehydrogenase
GPX	Glutathione peroxidase
GSH	Glutathione
GSR	Glutathione reductase
GST	Glutatione S-transferase
HMBS	Hydroxymethylbilane synthase
HSP27	Small heat shock protein
IF	Immunofluorescence
IgG	Immunoglobulin G
IHC	Immunohistochemistry
IKK2	Inhibitor of nuclear factor kappa-B kinase subunit beta
IPTG	Isopropyl β-D-1-thiogalactopyranoside

JNK	Jun N-terminal kinase
KO	Knock-out
LB	Luria-Bertani broth
LSB	Loading sample buffer
LPO	Lactoperoxidase
MAPK	Mitogen-activated protein kinase
MAPKAPK	Mitogen-activated protein kinase-activated protein kinase
MEFs	Mouse embryonic fibroblasts
MK2	Mitogen-activated protein kinase-activated protein kinase 2
MKK	Mitogen-activated protein kinase kinase
mRNA	Messenger RNA
MS	Mass spectrometry
mTOR	Mammalian target of rapamycin
MTT	3-(4,5-Dimethylthiazol-2-yl)-2,5-diphenyltetrazolium bromide
MWM	Molecular weight marker
N/A	Not applicable
NAC	*N*-acetyl-L-cysteine
NADPH	Nicotinamide adenine dinucleotide phosphate-oxidase
Nox	NADPH oxidases
NP-40	Nonidet NP-40
OD	Optical density
O/N	Over night
PARP	Poly (ADP-ribose) polymerase
PBS	Phosphate buffer solution
PCR	Polymerase chain reaction
PI	Propidium iodide
PI3K	Phosphatidylinositol 3-kinase
PFA	Paraformaldehyde
PKC	Protein kinase C
PMSF	Phenylmethanesulfonyl fluoride
PTGS2	Prostaglandin-endoperoxide synthase 2
PTP	Protein tyrosine phosphatase
PTPN	Protein tyrosine phosphatase non-receptor type
PXDNL	Peroxidasin homolog (Drosophila)-like
qRT-PCR	Quantitative real time PCR
RefSeq	NCBI Reference Sequence Database
Resazurin	7-Hydroxy-3*H*-phenoxazin-3-one 10-oxide
RNA	Ribonucleic acid
RNase	Ribonuclease
ROS	Reactive oxygen species
RT	Room temperature

RV	Reverse
SDS	Sodium dodecyl sulfate
SDS-PAGE	Sodium dodecyl sulphate-polyacrylamide gel electrophoresis
shRNA	Short hairpin RNA
siRNA	Small interfering RNA
SOC	Super optimal broth with catabolite repression
SOD	Superoxide dismutase
TAE	Tris base - acetic acid - EDTA buffer solution
TEMED	*N,N,N´,N´*-tetramethylethylenediamine
TUNEL	Terminal deoxynucleotidyl transferase dUTP nick-end labelling
TXNDC2	Thioredoxin domain containing 2
UV	Ultraviolet radiation
WB	Western blot
WT	Wild type

Abstract

Regulation of the redox state is essential to maintain cellular homeostasis. In fact, dysregulated reactive oxygen species (ROS) production has been associated with enhanced tumorigenicity in epithelial cells. However, the pro-tumorigenic effect of the accumulation of ROS can turn out to be a double-edged sword, since high levels of these species may lower the apoptotic threshold for cytotoxicity. Therefore, redox regulation plays an important role in tumor cell survival.

The p38α protein kinase is an important regulator of many cellular responses. It is well established that p38α signaling negatively regulates epithelial cell transformation, but enhanced p38α kinase activity has been also correlated with bad clinical prognosis in some tumor types. This, together with the fact that p38α has been implicated in the proliferation of some cancer cell lines, led us to hypothesize that this protein kinase could be a good target for cancer therapy.

We performed a screening to try to identify synthetic lethal partners of p38α, but we only found one potential candidate. We also investigated the role of p38α in the response of tumor cells to chemotherapeutic agents that induce DNA damage. Our results provide genetic and pharmacological evidence showing that inhibition of p38α cooperates with the chemotherapeutic agent cisplatin to kill tumor cells. We show that p38α inhibition results in ROS upregulation, which in turn activates the JNK pathway via inactivation of phosphatases, sensitizing human tumor cells to cisplatin-induced apoptosis. Using a mouse model for breast cancer, we also show that inhibition of p38α cooperates with cisplatin treatment to reduce tumor size and malignancy *in vivo*. Taken together, our results illustrate a new function of p38α that helps tumor cells to survive chemotherapeutic drug treatments by inducing the expression of antioxidant enzymes, and reveal that the combination of p38α inhibitors with cisplatin can be potentially exploited for cancer therapy.

Introduction

Cancer, an ancient and worldwide disease

Cancer can quite easily be thought of as a modern disease, but it has existed for many centuries indeed. It has been clearly identified in studies of Egyptian mummies (Granville, 1825) and even depicted in pieces of art along the centuries (Vaidya, 2007). However, it is a more common phenomenon nowadays than previously, in large extent due to the growth of the world's population and the advances in civilization. The improvement in life expectancy has contributed to making cancer such a common disease worldwide, as it is more frequent in elderly ages than in younger ones.

During the last quarter of century, research has generated a rich and complex body of knowledge, revealing cancer to be a disease involving dynamic changes in the genome. There are already several clearly identified causes of cancer (Boyle et al., 2003; Peto, 2001) although this is a complex disease that is very variable at the cellular and molecular level. The same heterogeneity and variability exist in its presentation, development and outcome from one patient to the other, so a lot of questions remain to be answered yet.

Tumorigenesis is a multistep process that reflects genetic alterations that drive the progressive transformation of normal cells into highly malignant derivatives, which have defects in regulatory circuits that govern normal cell proliferation and homeostasis. There are more than 100 distinct types of cancer and subtypes of tumors can be found within specific organs. This complexity provokes a number of questions, like how many distinct regulatory circuits within each type of target cell must be disrupted in order for such a cell to become cancerous? Or, which of these circuits operate on a cell-autonomous basis, and which are coupled to the signals that cells receive from their surrounding microenvironment within a tissue?

1. Molecular traits

Culture of cancer cells *in vitro* and dissection of their molecular components has yielded much of the knowledge we currently possess about the molecular processes underlying cancer development. Hanahan and colleagues suggested

that the vast catalog of cell genotypes is a manifestation of six essential alterations in cell physiology that collectively dictate malignant growth: self-sufficiency in growth signals, insensitivity to growth-inhibitory signals, evasion of apoptosis, limitless replicative potential, sustained angiogenesis and tissue invasion, and metastasis (Hanahan and Weinberg, 2000). Acquisition of these biological capabilities appears in widely variable sequences, both among tumors of the same type and certainly between tumors of different types. But in addition to cancer cells, tumors exhibit another dimension of complexity: they contain a repertoire of recruited normal cells that contribute to the acquisition of these hallmark traits by creating the "tumor microenvironment". This implies the addition of two more hallmarks of cancer involved in the pathogenesis of perhaps all cancers. One involves the capability to reprogram cellular metabolism in order to most effectively support neoplastic proliferation. The second allows cancer cells to evade immunological destruction (**Fig.1**).

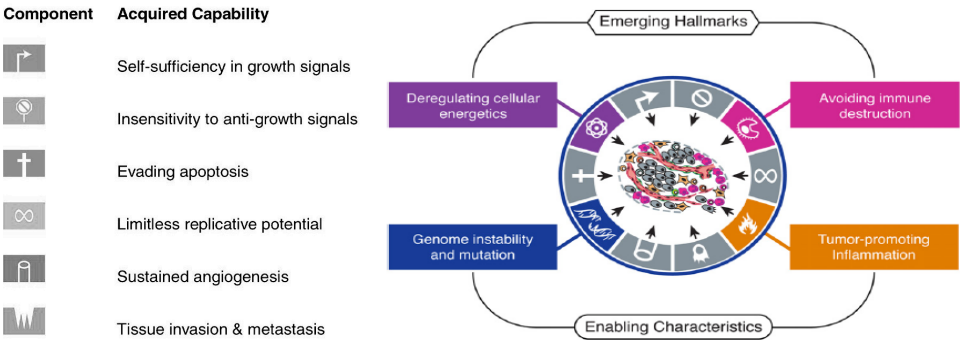

Figure 1. Schematic representation of the hallmarks of cancer. Hanahan and colleagues propose six biological capabilities, together with two other emerging hallmarks and enabling characteristics, to explain the cell transformation process and cancer progression. (Hanahan and Weinberg, 2011).

2. Mouse models

The laboratory mouse (*Mus musculus*) has revolutionized our ability to study gene function *in vivo* and our understanding of the molecular mechanisms of cancer pathogenesis. As a model system, mice have several important advantages over other mammalian models: they are small in size and relatively inexpensive to

maintain, they reproduce rapidly and have large litters, and they can be genetically manipulated. Currently, numerous techniques for genetic manipulation are available (Cheon and Orsulic, 2011) and this has allowed the generation of a number of mouse models to recapitulate human diseases (Frese and Tuveson, 2007). Here we will just describe one of the mouse models that have been generated for breast cancer, the MMTV-PyMT.

MMTV-PyMT model of breast cancer

Breast cancer is by far the most common cancer diagnosed in women worldwide (ranking second in both sexes combined), as it represents nearly a quarter (23%) of all cancers diagnosed in women around the world. Besides, it is also the most common cause of death from cancer in women worldwide (Cancer Research UK, 2011).

Genetically engineered mouse models of breast cancer exhibit many features of human breast cancer and thus provide valuable models to investigate the biology and pathogenesis of this disease. Nonetheless, because of the complexity and heterogeneity of breast cancer, no individual model recapitulates all aspects of this disease.

Murine polyomavirus (PyV) can cause a wide variety of tumors in different types of cells (Dawe et al., 1987; Fluck and Haslam, 1996). The most important transforming protein that they produce is the middle T (PyMT) oncoprotein, whose transgenic expression can cause tumors in a broad range of tissues (Cecena et al., 2006; Guy et al., 1992; Rassoulzadegan et al., 1990; Tehranian et al., 1996). When PyMT cDNA is expressed under the control of the MMTV mammary gland promoter, metastatic carcinomas are induced (Guy et al., 1992). Another advantage of the PyMT mouse model is the focal induction of tumors, in contrast to the equally metastatic ErbB2/Neu models, in which the whole mammary gland coalesces into a large tumor. Thus, it provides a relatively good model for the human disease (Lin et al., 2003).

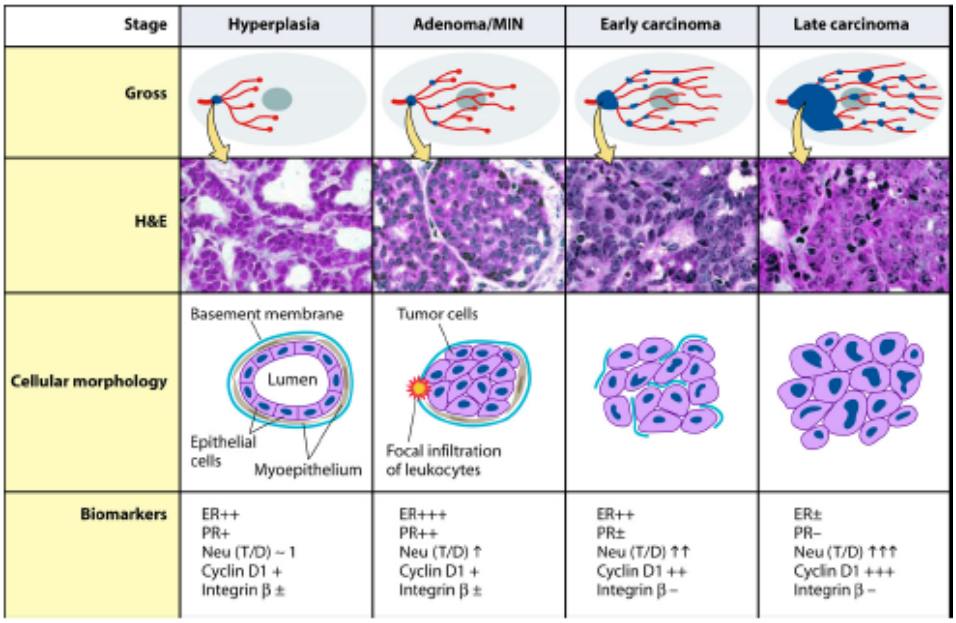

Figure 2. Summary of tumor progression and biomarker expression in the MMTV-PyMT mouse model of breast cancer. Four tumor stages are observed at different ages of the mice and in ducts that are at different stages of development. At the earliest stage (2 to 4 weeks after birth), growth of the short, underdeveloped prepubertal ducts takes place from the bulbous end buds under the influence of growth factors. In sexually mature mice (from 6 weeks on, when adenomas are observed), ducts continue to grow from the end buds under the control of estrogen and growth factors until they reach the confines of the gland. The "Gross" panel displays the overall development of lesions in mammary glands of PyMT mice. Tumor lesions are indicated by blue dots. The "H&E" panel displays the corresponding histology of primary lesions at different stages of tumor progression. The "Cellular morphology" panel schematically illustrates changes in the cytology of the cells as well as the integrity of the basement membrane and the presence or absence of myoepithelial and focal inflammation. Moreover, the changes in biomarkers during tumor progression are summarized in the panel of "Biomarkers". "T/D", the ratio of Neu expression between lesions and normal ducts in age-matched mammary glands. (Fluck and Schaffhausen, 2009)

In MMTV-PyMT mice, the earliest hyperplastic lesions arise at a very early age and are located very close to the nipple. The early lesion involves prepubertal, nipple-proximal buds (end buds) at the ends of growing immature ducts surrounding the main collecting duct. Following prepubertal growth, the ducts elongate further under hormonal influence, and new lesions arise on the distal end buds. The most distal foci arise at a stage of ER-dependent growth. At late stages, the nipple-proximal tumor fuses with numerous distal foci. Four stages with similarities to

human tumors were identified. These stages—hyperplasia, adenoma/mammary intraepithelial neoplasia (MIN), carcinoma *in situ*, and invasive carcinoma—and their timing, associated properties, and markers are described in **figure 2**.

MMTV-PyMT tumors display a large number of deregulated genes, including many implicated in breast cancer. These define a number of upregulated pathways: the glycolytic pathway; elongation translation factors plus structural RNAs; cell cycle regulators; signaling receptors and their effectors, including G proteins; and downstream transcription factors (Desai et al., 2002). Hierarchical clustering analyses of the MMTV-PyMT tumors along with classified human tumors suggest the placement of these tumors in a luminal group. In the human case, the luminal group generally expresses ER and ER-dependent genes (Perou et al., 2000) (**Fig. 3**). This is not the case of MMTV-PyMT tumors. However, the luminal subgroup B, that expresses only low levels of ER and overexpresses ErbB2, has been defined and they show a poor prognosis (Sorlie et al., 2003). This matches better the status of the PyMT tumors (Fluck and Schaffhausen, 2009).

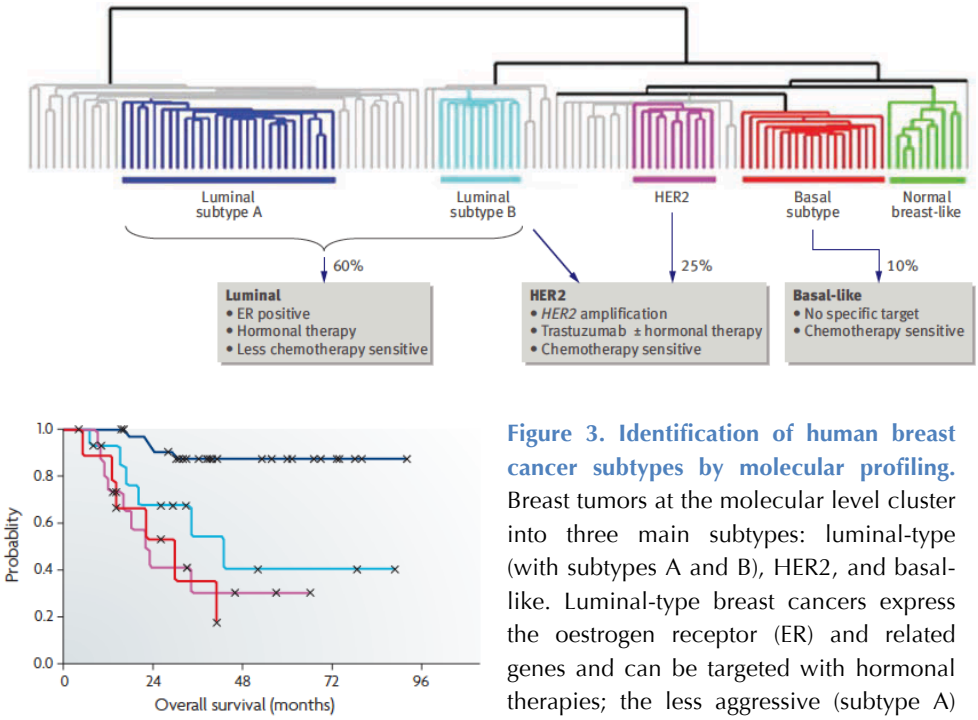

Figure 3. Identification of human breast cancer subtypes by molecular profiling. Breast tumors at the molecular level cluster into three main subtypes: luminal-type (with subtypes A and B), HER2, and basal-like. Luminal-type breast cancers express the oestrogen receptor (ER) and related genes and can be targeted with hormonal therapies; the less aggressive (subtype A)

cancers may be less sensitive to chemotherapy than the more aggressive ones (type B) cancers. HER2 breast cancers, characterized by overexpression of the growth factor receptor HER2 with amplification of the HER2 gene, are aggressive with a poor prognosis. HER2 positive cancers can be targeted with the monoclonal antibody trastuzumab and also may be highly chemotherapy sensitive. About half of the HER2 positive cancers express the oestrogen receptor. Basal-like cancers do not usually express either of the hormone receptors or overexpress the growth factor receptor HER2, a phenotype named "triple negative". Basal-like cancers are highly proliferative and have poor prognosis, although many are highly sensitive to chemotherapy. There is no subtype specific targeted therapy. (Turner and Jones, 2008; Vargo-Gogola and Rosen, 2007)

The MAPK signaling cascade

Cells need to be constantly aware of changes in the extracellular milieu to respond accordingly, so they have developed a wide variety of mechanisms to receive signals, transmit the information and orchestrate the appropriate responses. These are often mediated through the activation of transcription factors, which, in turn, induce the necessary cellular processes. However, most extracellular agents cannot cross the plasma membrane in order to activate their corresponding genes. Instead, these agents use intracellular "communication lines," which are known as "signaling pathways", to transmit their signals to various cytoplasmic and nuclear targets.

1. Canonical activation

In many cases, signaling pathways operate through sequential phosphorylation events that are termed protein kinase cascades. This type of signaling mechanism is used by the mitogen-activated protein kinase (MAPK) signaling cascades, which are a superfamily of evolutionary-conserved serine/threonine protein kinases. Four canonical mammalian MAPK cascades have been identified in the last 20 years, and those are usually named according to the MAPK components that are the central building blocks of each of the cascades. These are the extracellular signal-regulated kinase 1/2 (ERK1/2) (Boulton et al., 1991), c-Jun N-Terminal kinase 1-3 (JNK 1-3) (Derijard et al., 1994; Kyriakis et al., 1994), p38 MAPK α, β, γ, ∂ (p38α-∂) (Freshney et al., 1994; Han et al., 1994; Rouse et al., 1994), and ERK5 (Lee et al., 1995; Zhou et al., 1995) pathways (**Fig. 4**). Each of these cascades consists of a core module of three tiers of protein kinases termed MAPK, MAP2K, and MAP3K,

but often two additional tiers, the upstream MAP4K and the downstream MAPKAPK, which are not always present, can complete five tiers of each cascade in certain cell contexts.

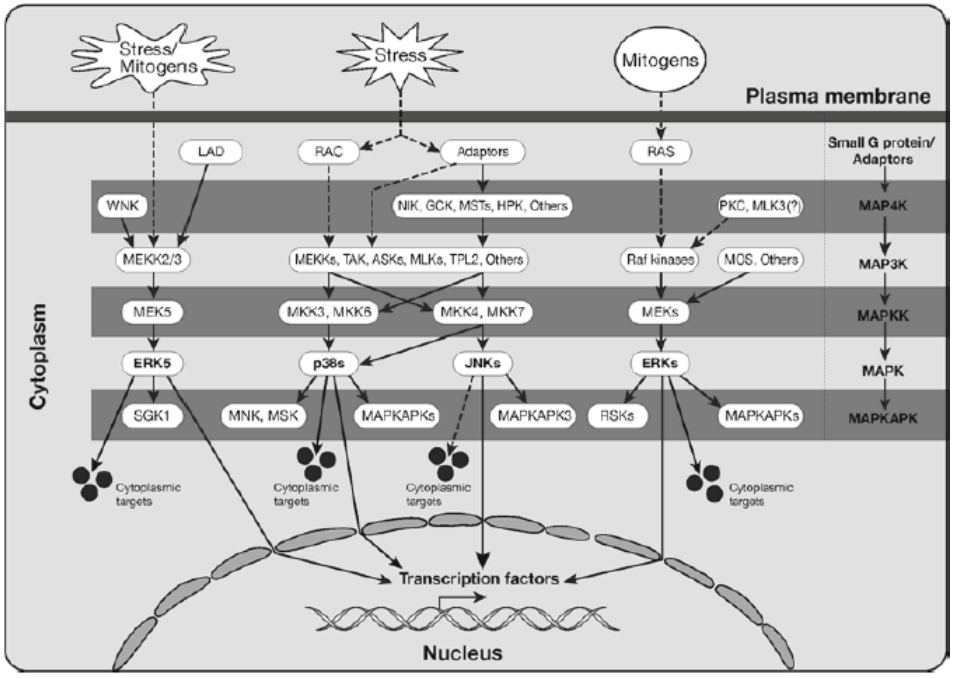

Figure 4. Schematic representation of the MAPK signaling cascades. (Keshet and Seger, 2010)

About 70 genes are known today to encode close to 200 distinct components that compose the entire MAPK system. This multiplicity of components allows the extended specificity and tight regulation, which are hallmarks of these cascades. Usually, the ERK1/2 cascade plays a role in proliferation and differentiation, meanwhile JNK and p38 MAPK pathways are activated mainly by cellular stresses, and therefore they are termed stress-activated protein kinases (SAPKs). The ERK5 cascade seems to respond equally to certain stresses and mitogenic signals (Keshet and Seger, 2010).

The transmission of the signal via each cascade is mediated by sequential phosphorylation and activation of the components in the sequential tiers.

Therefore, they cooperate in transmitting various extracellular signals and thus control a large number of distinct and even opposing cellular processes, such as proliferation, differentiation, survival, development, stress response, and apoptosis, depending on the cell type and stimulation (Avruch, 2007; Krishna and Narang, 2008; Raman et al., 2007). In fact, their mis-regulation often leads to diseases like cancer, diabetes or inflammation (Dhillon et al., 2007; Jeffrey et al., 2007; Zick, 2005).

2. The p38 MAPK pathway

The first member of the p38 MAPK family was identified as a 38 kDa protein (p38) that was rapidly phosphorylated on tyrosine in response to LPS (lipopolysaccharide) stimulation (Han et al., 1994). This protein was found to be the homologue of *Saccharomyces cerevisiae* Hog1, an important regulator of the osmotic response, and is now referred to as p38α (*MAPK14*). Additional p38 MAPK family members, which are approximately 60% identical in their amino acid sequence, were subsequently cloned and named p38β (*MAPK11*), p38γ (*MAPK12*) and p38∂ (*MAPK13*) (Enslen et al., 1998; Goedert et al., 1997; Jiang et al., 1996; Jiang et al., 1997; Lechner et al., 1996; Mertens et al., 1996). The four p38 MAPKs are encoded by different genes and have different tissue expression patterns, with p38α being ubiquitously expressed at significant levels in most cell types, whereas the others seem to be expressed in a more tissue-specific manner (Cuadrado and Nebreda, 2010).

Inhibitors and therapeutic implications

Despite their high sequence homology, p38 MAPK isoforms differ in their sensitivity to chemical inhibitors (Coulthard et al., 2009). The discovery of pathological conditions in which p38 MAPKs are involved (**Fig. 5**) supports the potential therapeutic interest of modulating the activity of these kinases. Pyridinyl-imidazole drugs, such as SB203580, were the first p38 MAPK inhibitors to be identified and they were designed to fit the ATP-binding site (**Fig. 6**). At low concentrations, these compounds inhibit p38α and p38β, but not p38γ and p38∂ (Cuenda et al., 1997; Goedert et al., 1997). Several of the compounds have proven

efficacy in preclinical models and good pharmacological properties and therefore have reached clinical trials (Cohen, 2009), like is the case for PH-797804 (Goldstein et al., 2010).

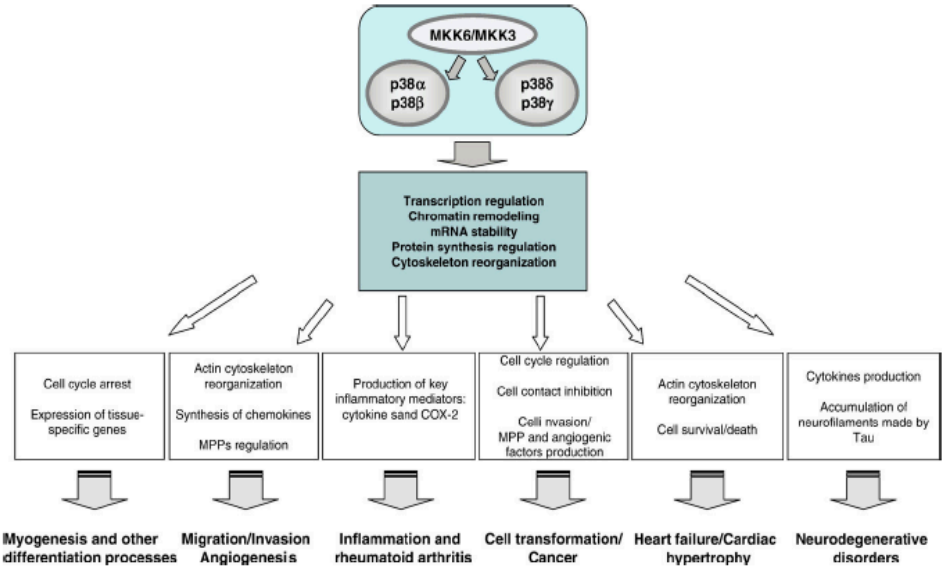

Figure 5. Physiological roles and pathological implications of p38 MAPKs pathways. p38 MAPKs play a central role in the regulation of many biological functions, so their deregulation can lead to the development of several pathological conditions. (Cuenda and Rousseau, 2007).

p38 MAPK in cancer

During the last few years, members of the p38 MAPK family have joined the group of signaling pathways involved in the regulation of the cell transformation process. It has been shown that p38 MAPK pathway could be involved in some of the alterations observed in the physiology of transformed cells: self-sufficiency in growth signals, unlimited replication potential, protection against apoptotic cell death, *de novo* angiogenesis, and tissue invasion and metastasis (Hanahan and Weinberg, 2000), being most frequently associated with a tumor-suppressor function. This role of p38 MAPK can largely be attributed to the inhibitory effects of the p38α and p38β isoforms on G1/S and G2/M cell-cycle-checkpoint controls (Ambrosino and Nebreda, 2001), to promote growth arrest and induction of apoptosis (Bulavin and Fornace, 2004; Kummer et al., 1997; She et al., 2001) or

cellular senescence (Bulavin et al., 2002; Haq et al., 2002; Wang et al., 2002). Collectively, these data suggest that inactivation of the p38 MAPK pathway will enhance cellular transformation by negatively regulating cell proliferation and inducing apoptosis.

However, this tumor-suppressor function seems to be mainly operative at the onset of cellular transformation (Dolado et al., 2007; Hui et al., 2007; Ventura et al., 2007), as enhanced p38 MAPK phosphorylation has been correlated with poor overall survival in patients with HER-2 negative breast cancer (Esteva et al., 2004) or with hepatocellular carcinoma (Wang et al., 2012). A few publications have provided evidence for an oncogenic potential of this cascade, as overexpression or over activation of p38α has been reported in transformed follicular lymphomas (Elenitoba-Johnson et al., 2003) and in thyroid neoplasms (Pomerance et al., 2006). Nonetheless, the potential pro-tumorigenic roles of p38α signaling are not only based on correlations with bad prognosis in cancer, but there is also evidence that this pathway may contribute to the survival or proliferation of cancer cell lines from different origins, including breast (Chen et al., 2009), colorectal (Chiacchiera et al., 2009), prostate (Ricote et al., 2006) or skin (Schindler et al., 2009).

Crosstalk between different signaling pathways is a common theme in cell regulation, which is usually highly dependent on cell context. The JNK and p38 MAPK pathways share several upstream regulators (**Fig. 4**), and accordingly there are multiple stimuli that simultaneously activate both cascades, although interplays at the levels of downstream target have also been described in several contexts (Wagner and Nebreda, 2009).

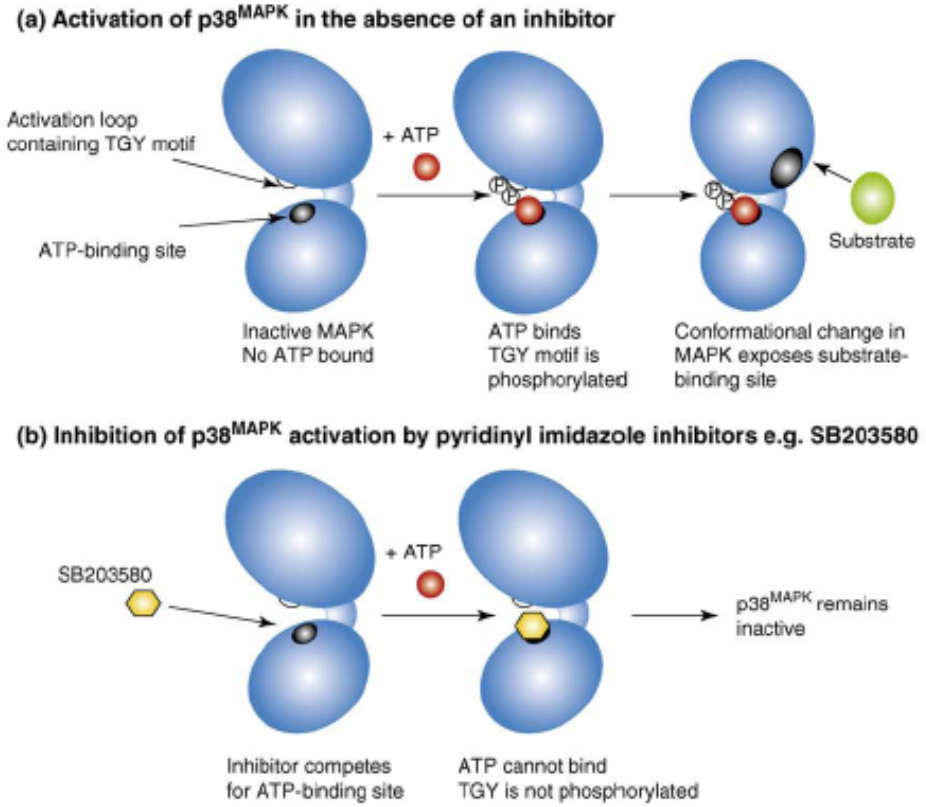

Figure 6. p38 MAPK activation and inhibition. (a) p38 MAPK is activated in multiple steps. ATP is required for phosphorylation of the TGY motif on the activation loop. Once this has occurred, there is a conformational change in the kinase, exposing a binding site for a substrate. (b) Classical pyridinyl imidazole inhibitors (e.g. SB203580) are similar in shape to ATP molecules and compete for ATP-binding site. Once the inhibitor is bound, ATP is blocked and phosphorylation of the TGY motif does not occur, leaving p38 MAPK inactive. (Coulthard et al., 2009).

3. The JNK cascade

MAPK8, *MAPK9* and *MAPK10* genes encode JNK1, JNK2 and JNK3 proteins respectively, which are alternatively spliced to create at least 10 isoforms (Dreskin et al., 2001; Gupta et al., 1996). In most cells the 46 kDa proteins are mainly JNK1 isoforms, the 54 kDa proteins are mainly JNK2, the 52 kDa band represents only JNK3, and this is often the simplified nomenclature used for JNK bands upon SDS-PAGE (Keshet and Seger, 2010). JNK1 and JNK2 are believed to be expressed in

every cell and tissue type, whereas JNK3 is found primarily in brain and to a lesser extent in heart and testis (Bode and Dong, 2007).

The pro-apoptotic role of JNK

As mentioned above, the JNK pathway is activated by the exposure of cells to stress. Nonetheless, its specific role may depend on the cellular context, as it has been implicated in both apoptosis and survival signaling (Ip and Davis, 1998). Regarding its apoptotic role, it has been demonstrated that JNK is required for stress-induced apoptosis mediated by the mitochondrial/caspase-9 pathway in response to UV radiation (**Fig. 7**), as JNK depletion causes failure to release cytochrome *c* and further caspase-3 activation (Tournier et al., 2000). It is also known that JNK-mediated apoptosis involves recruitment and regulation of members of the Bcl-2 family, which is itself antiapoptotic. Bcl-2 activity is blocked by the related BH3-only protein Bim when it is phosphorylated by JNK, thereby promoting apoptosis (Kyriakis and Avruch, 2012).

However, most forms of environmental stress do not cause apoptosis under conditions that are sufficient for JNK activation. This is partly because the JNK-dependent apoptotic signaling pathway can be blocked by activation of survival pathways, such as NF-κB, Akt and ERK. Thus, JNK pathway functions within the overall context of the state of activation of other signaling pathways. The absence of an apoptotic response also appears to correlate with the time course of JNK activation, being its sustained (but not transient) activation associated with apoptosis (Chen and Tan, 2000).

Response of JNK to cisplatin treatment

Cytotoxic activity of *cis*-diamminedichloroplatinum (II), or cisplatin (CDDP), was recognized more than 35 years ago. It is a small, neutral inorganic complex that becomes activated after entering into the cell, replacing its cis-chloro ligands with water molecules (el-Khateeb et al., 1999; Kelland, 2000). Such aquated form of CDDP is very reactive towards nucleophilic centers of biomolecules like proteins, RNA and DNA molecules, membrane phospholipids and microfilaments. Despite

the growing evidence on the binding of CDDP to non-DNA targets and their importance in CDDP-toxicity, it is generally accepted that the binding of CDDP to DNA is largely responsible for its antitumour properties (Fuertes et al., 2003; Jamieson and Lippard, 1999). Today it is one of the most effective and commonly used chemotherapeutics for the treatment of many solid tumors, including ovarian, testicular, bladder, lung and head and neck tumors (Boulikas and Vougiouka, 2003).

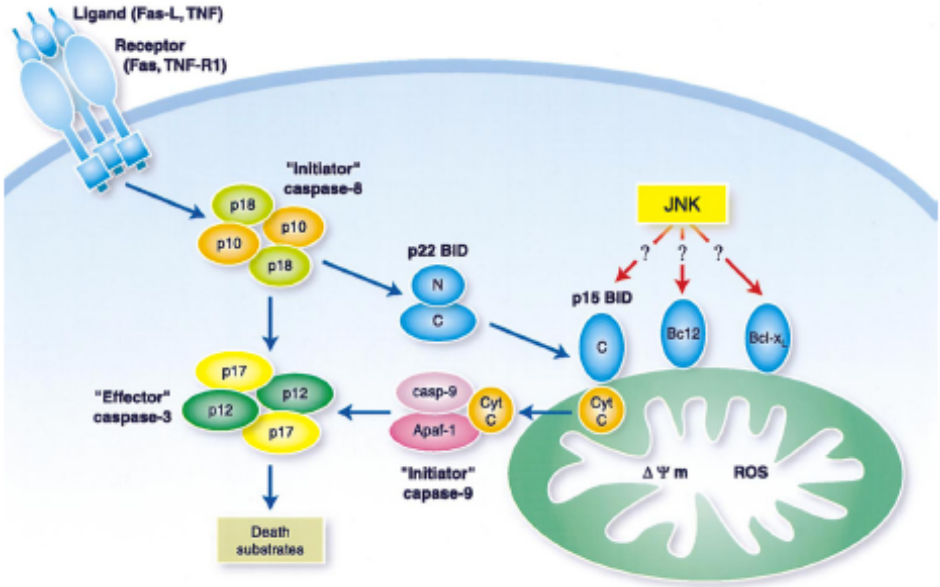

Figure 7. Role of the JNK signaling pathway in stress-induced apoptosis. The caspase apoptotic machinery is illustrated in a simplified cartoon. Effector caspases, including caspase-3, are activated by initiator caspases that are activated by cell surface death receptors (caspase-8) and by the mitochondrial pathway (caspase-9). JNK is not required for death receptor signaling, but it is required for caspase-9 activation by the mitochondrial pathway. Potential targets of JNK include members of the Bcl2 group of apoptotic regulatory proteins. (Davis, 2000).

Different tumour cell lines and experimental approaches have been used to study the causes and consequences of CDDP-induced MAPK activation. It seems that proteins involved in recognition of a platinum atom linked to DNA, are important regulators in triggering MAPK signaling pathways. For instance, CDDP and its analogue oxaliplatin activate different MAPK, which are further responsible for

their cytotoxic effects. CDDP-induced JNK activation seems to be a key pro-apoptotic mediator of cell death on a panel of four colon adenocarcinoma cell lines (Vasilevskaya et al., 2004), whereas upon oxaliplatin exposure this role was played by p38 MAPK (Rakitina et al., 2003).

There are several repair systems involved in recognition and repair of CDDP adducts like nucleotide excision repair (NER), homologous recombination (HR) repair and mismatch repair (MMR) (Brabec and Balcarova, 1993; Jordan and Carmo-Fonseca, 2000). Activation of JNK induced by CDDP is substantially greater in MMR proficient than in MMR deficient tumor cells (Nehme et al., 1997). The activation of MAPK also depends on the nature of the platinum drug. CDDP activates JNK slowly and persistently, while transplatin activates this kinase rapidly and briefly, or (in some cases) does not activate it at all (Levresse et al., 2002; Persons et al., 1999; Sanchez-Perez et al., 1998). The pro-death or pro-survival role of MAPK in response to CDDP could depend on the type of activated MAPK, but in most of the investigated cell systems JNK activation has a pro-death role (Koyama et al., 2006; Krilleke et al., 2003; Li et al., 2005; Mansouri et al., 2003; Sanchez-Perez et al., 2002; Sanchez-Perez et al., 1998; Sanchez-Perez and Perona, 1999). The time course of MAPK activity appears to be also important, because it will decide the fate of CDDP treated cells. Thus, lack of prolonged activation of JNK in CDDP-resistant cells determined their survival upon CDDP treatment, which was not the case in the sensitive cell line (Li et al., 2005).

The role of c-Jun in CDDP-induced apoptosis was documented in NIH3T3 fibroblasts derived from mouse embryos lacking c-jun. CDDP induces sustained JNK activation that occurs via the MEKK1/SEK1 cascade, causing cell death (Sanchez-Perez and Perona, 1999). CDDP resistant mouse fibroblasts lacking c-Jun became sensitive after re-expression of c-Jun (Toh et al., 2004). Activation of MEKK1 may upregulate pro-apoptotic pathways through c-Jun-dependent FasL transcription and simultaneous downregulation of survival pathways that are NF-κB transcription-dependent (Sanchez-Perez et al., 2002). The timing of JNK activity is essential, because it will determine whether cells will survive or undergo

apoptosis (Mansouri et al., 2003).

Despite the activation of p38 and ERK by CDDP, the JNK pathway actually represents a primary target for the modulation of CDDP lethality in p53 deficient/mutated cells (Bae et al., 2006).

Signaling pathways are integrated in a very complex network and the final response depends on the balance of activity of several of these networks, the cell type, as well as proliferation and differentiation status of tumour cells. The important questions are whether MAPK are also indeed *in vivo* determinants of tumour cell response to cisplatin- based therapy, and whether they could be used as potential prognostic factors.

4. Pathway inactivation

Since MAPK cascades are key mediators of most stimulation-induced cellular processes, their downregulation is critical to achieve transient activation and to regulate signal intensity, which in turn results in specific outcomes. Termination of the kinase catalytic activity involve the action of the protein tyrosine phosphatase (PTP) superfamily, which are potentially candidate tumor suppressors due to their opposing role to the MAPKs (Julien et al., 2011).

The PTP superfamily

The PTP superfamily comprises 107 members that are broadly grouped into four separate families on the basis of their amino acid sequences of their catalytic domains (Alonso et al., 2004) (**Fig. 8**). The first and largest PTP family contains type-I cysteine-based PTPs. These phosphatases can be divided further into subgroups depending on the similarity of the catalytic domains, comprising either tyrosine-specific classical PTPs or the dual-specificity phosphatases (DUSP). The second PTP family contains only one phosphatase, low-molecular-mass PTP (LMWPTP), that is type-II cysteine-based and tyrosine-specific. It is related to low-molecular-mass bacterial phosphatases that are evolutionarily conserved (Alonso et al., 2004). The third PTP family consists of rhodanese-related type-III cysteine-

based phosphatases that are both tyrosine- and threonine-specific (Alonso et al., 2004; Russell and Nurse, 1986). This group consists of three cell cycle regulators: Cdc25A, Cdc25B and Cdc25C, which dephosphorylate cyclin-dependent kinases (Karlsson-Rosenthal and Millar, 2006). The fourth PTP family consists of aspartic acid-based PTPs, which comprises the eyes absent (EyA) tyrosin specific phosphatases and haloacid dehalogenase (HAD) family phosphatases (Moorhead et al., 2007). The HAD family is a heterogeneous group of phosphatases that can be either tyrosine- (Rebay et al., 2005) or serine- (Gohla et al., 2005; Yeo et al., 2003) specific and have various substrates, including proteins, phospholipids, sugars and nucleotides (Lunn et al., 2000; Roberts et al., 2004). Below we will describe type-I PTPs.

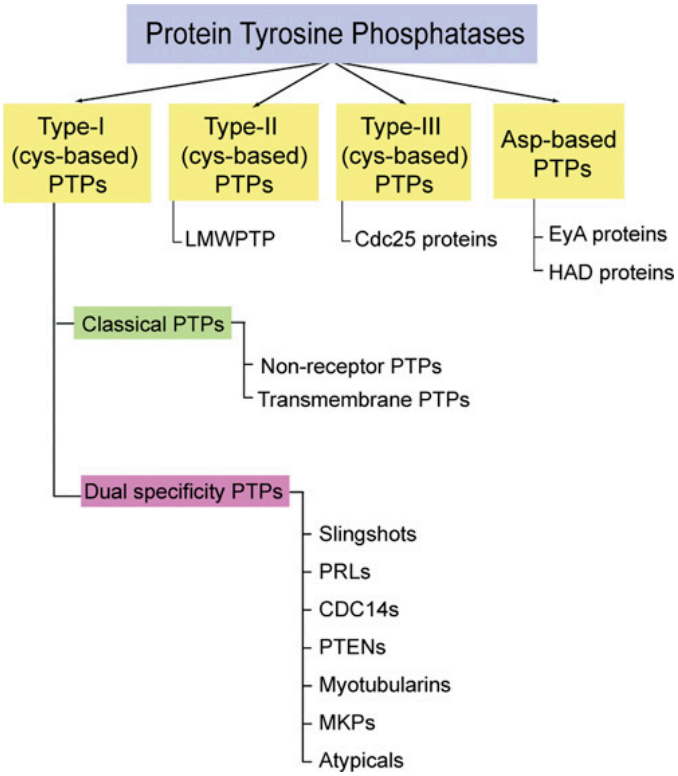

Figure 8. Classification of PTPs. PTPs can be classified into four subgroups on the basis of their sequence similarity and presence of functional or binding domins. EyA, eyes absent; LMWPTP, low molecular mass PTP. (Patterson et al., 2009).

Classical PTPs

Classical PTPs can be categorized as receptor PTPs (RPTPs) or non-receptor PTPs. (**Fig. 9**). RPTPs have the potential to regulate signaling through ligand-controlled

protein tyrosine dephosphorylation. Many of them display features of cell-adhesion molecules in their extra-cellular segment and have been implicated in processes that involve cell-cell and cell-matrix contact. Cytoplasmic PTPs are characterized by regulatory sequences that flank the catalytic domain and control activity either directly, by interactions at the active site that modulate activity or by controlling substrate specificity.

Dual-specificity PTPs

This is a very large and heterogeneous subgroup whose unique feature is the ability to dephosphorylate both tyrosine and serine/threonine residues within one substrate. There are 61 DUSP of very different forms and functions, which can be grouped on the basis of the presence of specific domains and sequence similarity. One of the best characterized subgroups is the mitogen-activated protein kinase phosphatases (MKP), which contains ten protein that can dephosphorylate MAPKs at both phospho-threonine and phospho-tyrosine residues simultaneously (**Table 1**).

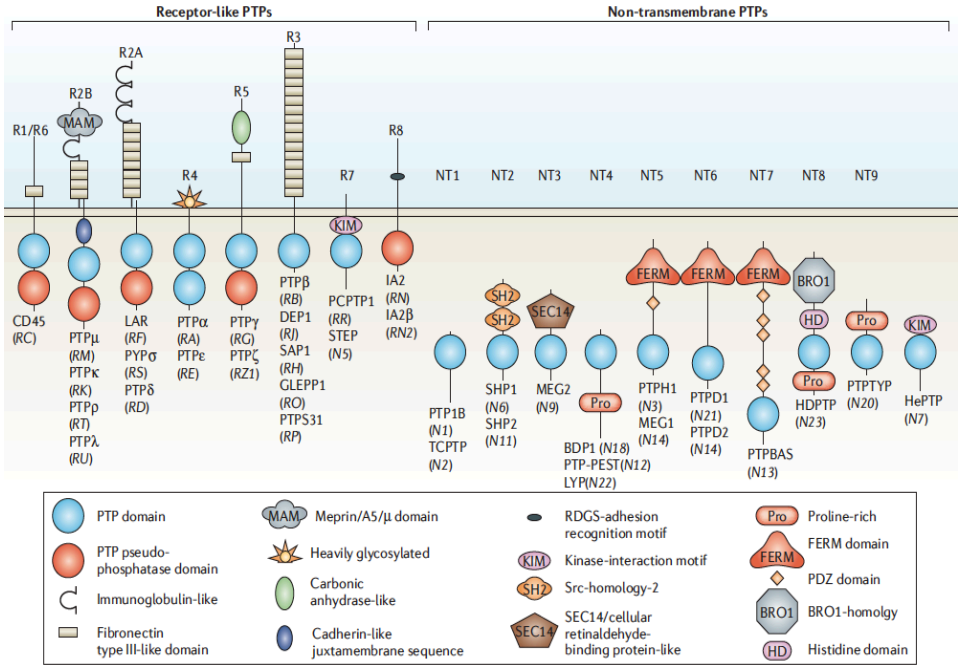

Figure 9. The classical PTPs. Classical PTPs can be categorized as receptor-like (R) or non-transmembrane (NT) proteins, although this is not an absolute distinction. (Tonks, 2006).

Individual MKPs show substrate specificity preference for one or more of the MAPKs, ERK, JNK or p38 (**Fig. 10**), although the MAPK substrate preference for individual MKPs *in vitro* does not always reflect that *in vivo*. Many MKPs are inducible or early-response genes and demonstrate low expression in resting or unstressed cells, with their expression rapidly increasing upon appropriate stimulation, e.g. with various cytokines, growth factors or serum. However, the kinetics and magnitude of the response of individual MKPs to these stimuli can be cell-type and context-specific (Brondello et al., 1997; Ekerot et al., 2008; Keyse, 2000; Wu et al., 2006). This induction is often dependent on MAPK activation and hence is thought to be a negative-feedback mechanism for down-regulating mitogenic signaling. In addition, MKPs can be subject to post-translational modification. Owing to the presence of the catalytic cysteine residue in the catalytic cleft, the enzymatic activity of PTPs including MKPs is sensitive to reversible oxidation and inactivation. Reversible oxidation of the conserved cysteine within the DUSP catalytic domain abolishes its nucleophilic properties and leads to profound changes in the conformation of the catalytic cleft, rendering the phosphatase inactive (Kamata et al., 2005). This may be mediated by the regulated production of reactive oxygen species such as H_2O_2 within the cell (Chiarugi and Cirri, 2003; Lambeth, 2004; Tonks, 2005) although the regulation of this process under normal physiological conditions, as well as in particular disease states, requires further clarification.

Table 1. Nomenclature of MKPs

Gene	MKP	Trivial names	Localisation	Substrate MAPKs
DUSP1	MKP-1	CL100, 3CH134, erp, hVH1	Nuclear	ERK1/2, p38, JNK
DUSP4	MKP-2	hVH2, TYP1, STY8	Nuclear	ERK1/2, p38, JNK
DUSP2	N/A	PAC1	Nuclear	ERK1/2, p38
DUSP5	N/A	hVH3, B23	Nuclear	ERK1/2
DUSP6	MKP-3	PYST1, rVH6	Cytoplasmic	ERK1/2
DUSP7	MKP-X	PYST2, B59	Cytoplasmic	ERK1/2
DUSP9	MKP-4	PYST3	Cytoplasmic	ERK1/2 > p38
DUSP8	N/A	hVH5, HB5, M3/6	Nuclear/cytoplasmic	JNK, p38
DUSP10	MKP-5	N/A	Nuclear/cytoplasmic	JNK, p38
DUSP16	MKP-7	N/A	Nuclear/cytoplasmic	JNK, p38

MKPs are listed here according their official HUGO Gene Nomenclature Committee name. Alternative names are also listed. The MAPK substrate specificity is listed in order of

preference; however, for DUSP2, preference *in vitro* differs from that *in vitro*. *In vivo*, DUSP2 inhibits JNK preferentially. Note that MK-STYX is catalytically inactive. The subcellular localization of these MKPs is also listed, with the nuclear MKPs most likely to be inducible. Adapted from (Dickinson and Keyse, 2006).

Reversible oxidation of PTPs

The production of reactive oxygen species (ROS), such as hydrogen peroxide, and the resulting post-translational modification of proteins by reversible oxidation have been implicated in the regulation of tyrosine phosphorylation-dependent signaling pathways that are initiated by a wide variety of stimuli, including growth factors, hormones, cytokines and cellular stresses (Finkel, 2003; Lambeth, 2004; Rhee et al., 2005). Attention was drawn to the PTPs as targets of ROS because the signature motif of this family contains an invariant cysteine residue that, due to the unique environment of the PTP active site, is characterized by an extremely low pKa (den Hertog et al., 2005; Salmeen and Barford, 2005; Tonks, 2005). The low pKa at the bottom of the catalytic cleft maintains the conserved cysteine residue in a negatively charged thiolate form, allowing nucleophilic attack on the substrate phosphate. On the other hand, being negatively charged makes the cysteine particularly sensitive to oxidative stress, which inactivates the enzyme activity by inducing profound changes in the catalytic site architecture.

Unlike the classical PTPs, the dual-specificity phosphatases contain a second cysteine residue within the active site. Following oxidation of the nucleophilic cysteine within the signature motif, a disulfide bond is formed with the neighboring cysteine protecting the enzymes from the irreversible inactivation that would result from higher oxidized species (Salmeen and Barford, 2005). The S–S bond can be readily reduced, which ensures the transient nature of the modification and returns the enzymes to their active form.

The current model is that physiological stimuli, such as growth factors or engagement of antigen receptors, trigger localized production of ROS. This leads to oxidation and inactivation of those PTPs that normally function to attenuate the

signaling response. Oxidation is transient, with the PTPs being reduced back to their active state by the action of cellular reducing agents such as thioredoxin or glutathione, leading to signal termination. Although particularly exciting as a new tier of control of pTyr-dependent signalling, there are several issues that must be resolved before the physiological importance of redox regulation of PTPs can be established. For instance, since the active site cysteine is particularly sensitive, it is likely that there will be intrinsic differences in sensitivity to oxidation between individual PTPs (Groen et al., 2005). It is also likely that those PTPs that are colocalized with sites of ROS production will be preferentially oxidized. For example, it has been shown that Nox4 regulates the oxidation of PTP1B in response to insulin (Goldstein et al., 2005) and colocalizes with PTP1B on intracellular membranes (Martyn et al., 2006). Therefore, it will be important to define further where in the cell oxidation occurs, the precise source of ROS, such as Nox (NADPH oxidases) enzymes (Goldstein et al., 2005) or mitochondria (Kamata et al., 2005), and how the localization of the PTPs is regulated.

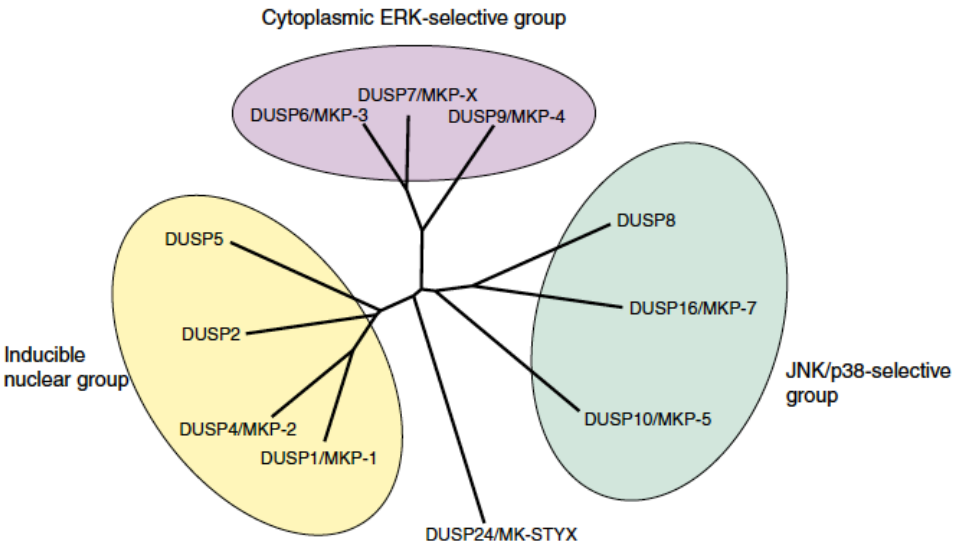

Figure 10. Classification and phylogenetic analysis of the MKPs. The three subgroups of DUSP proteins together with defining properties are indicated by the coloured ovals. (Dickinson and Keyse, 2006).

Oxidative stress

Oxidative stress refers to a situation of an imbalance between pro-oxidant and antioxidant factors controlled by multiple components, which might lead to cellular damage. Reactive oxygen species (ROS), such as superoxide anion ($O_2^{\cdot-}$), hydrogen peroxide (H_2O_2) and hydroxyl radical (HO·), consist of radical and non-radical oxygen species formed by the partial reduction of oxygen, which are key players in oxidative stress. This results in direct or indirect ROS-mediated damage of nucleic acids, proteins or lipids, and has been implicated in carcinogenesis (Trachootham et al., 2009), neurodegeneration (Andersen, 2004; Shukla et al., 2011), atherosclerosis, diabetes (Paravicini and Touyz, 2006), and aging (Haigis and Yankner, 2010).

1. Cellular sources of ROS

In cancer cells high levels of reactive oxygen species can result from increased metabolic activity, mitochondrial dysfunction, peroxisome activity, increased cellular receptor signaling, oncogene activity, increased activity of oxidases, cyclooxygenases, lipoxigenases and thymidine phosphorylase or through cross-talk with infiltrating immune cells (Storz, 2005; Szatrowski and Nathan, 1991).

In mitochondria, ROS are produced as an inevitable byproduct of oxidative phosphorylation (**Fig. 11**). The electron transport chain encompasses complexes I–IV and ATP synthase on the mitochondrial inner membrane. Superoxide is generated at complexes I and III and released into the inter-membrane space (~80% of the generated superoxide) or the mitochondrial matrix (~20%) (Han et al., 2001). The mitochondrial permeability transition pore (MPTP) in the outer membrane of the mitochondrion allows the leakage of superoxide into the cytoplasm (Crompton, 1999; Storz, 2006). Superoxide is dismutated to H_2O_2, either in the mitochondrial matrix (by MnSOD) or in the cytosol (by Cu/ ZnSOD). H_2O_2 is a *bona fide* second messenger that is highly diffusible. Recent data suggest that H_2O_2 may cross cellular membranes through specific members of the aquaporin family (Bienert et al., 2007).

Growth factors and cytokines stimulate the production of ROS to exert their diverse biological effects in cells (Bae et al., 2000; Goustin et al., 1986; Sundaresan et al., 1995). For example, an elevation of hydrogen peroxide and nitrite oxide levels was detected in tumor cells in response to interferon γ (IFN γ) and TNFα (Lo and Cruz, 1995; Tiku et al., 1990). Further, platelet-derived growth factor (PDGF), epidermal growth factor (EGF), insulin, transforming growth factor β (TGFβ), interleukin-1 (IL-1), tumor necrosis factor α (TNFα), angiotensin and lysophosphatidic acid all induce the formation of superoxide (Bae et al., 2000; Griendling et al., 1994; Roy et al., 2006; Sundaresan et al., 1995). Activation of the small GTPase K-ras downstream of growth factors or its oncogenic mutation has been associated with increased generation of superoxide and the incidence of various cancers (Aunoble et al., 2000; Minamoto et al., 2000; Minamoto et al., 2002). Dependent on the cellular system, growth factors and mutant K-ras elevate intracellular superoxide levels through NADPH oxidase or mitochondria (Storz, 2005). NADPH oxidase can also be activated via the RhoGTPase Rac-1 (Chiarugi and Fiaschi, 2007). Rac-1-mediated generation of superoxide is induced by cell surface receptors including c-Met (Ferraro et al., 2006).

2. Cellular detoxification from ROS

Under normal physiological conditions, the intracellular levels of ROS are steadily maintained to prevent cells from damage. Detoxification from ROS is facilitated by non-enzymatic molecules (i.e. glutathione, flavenoids and vitamins A, C and E) or through antioxidant enzymes, which specifically scavenge different kinds of ROS (**Fig. 11**). Superoxide dismutases (SODs) are metalloenzymes that catalyze the dismutation of superoxide anion to oxygen and hydrogen peroxide. These enzymes exist ubiquitously in eukaryotes and prokaryotes. Superoxide dismutases utilize metal ions such as copper (Cu^{2+}), zinc (Zn^{2+}), manganese (Mn^{2+}) or iron (Fe^{2+}) as cofactors. The different SOD enzymes are located in different compartments of the cell and are highly specific in regulating linked biological processes (Copin et al., 2000).

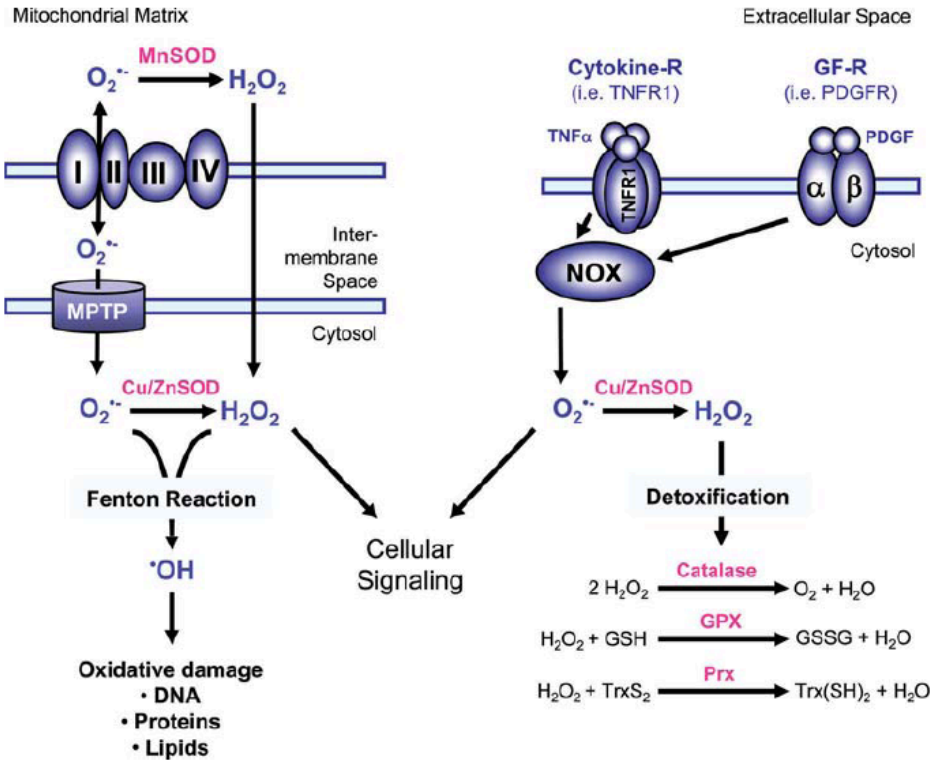

Figure 11. Major mechanisms of ROS generation and detoxification. Superoxide ($O2^{\bullet-}$) radicals are generated at the inner membrane of the mitochondria as a byproduct of the electron transport chain and then release into the mitochondrial matrix or the cytosol via the mitochondrial permeability transition pore (MPTP). Superoxide is also generated through activation of NADPH oxidases (NOX), for example in response to growth factor receptor (GF-R) or cytokine receptor activation. SOD enzymes, such as MnSOD in the mitochondrial matrix or Cu/ZnSOD in the cytosol, reduce superoxide to H_2O_2. Several cytosolic antioxidant systems, including catalase, glutathione peroxidase (GPX) and peroxiredoxins (Prx), detoxify cells from hydrogen peroxide by reducing it to water. Both hydrogen peroxide and superoxide contribute to cellular signaling but also can form hydroxyl radicals ($^{\bullet}OH$). Hydroxyl radicals are generated from $O^{\bullet-}$ and H_2O_2 in the Fenton reaction and have damaging functions for proteins, DNA and lipids. (Liou and Storz, 2010).

Catalase facilitates the transformation of H_2O_2 to H_2O and O_2. The major localization of catalase in most eukaryotes is in the cytosol and peroxisomes (Bendayan and Reddy, 1982; Hashimoto and Hayashi, 1990; Litwin et al., 1987). Peroxiredoxins are thioredoxin peroxidases that catalyze the reduction of H_2O_2, organic hydroperoxides and peroxynitrite (Hofmann et al., 2002; Rhee et al., 1999; Wood et al., 2003). The thioredoxin system consists of thioredoxin and

thioredoxin reductase. In its active state, thioredoxin scavenges reactive oxygen species and keeps proteins in their reduced state (Arner and Holmgren, 2000). Thioredoxin is regenerated by thioredoxin reductases, which utilize NADPH as an electron donor (Mustacich and Powis, 2000).

The glutathione system includes glutathione (GSH), glutathione reductase, glutathione peroxidases (GPX) and glutathione S-transferases (GST). Glutathione protects cells from oxidative stress by reducing disulphide bonds of cytoplasmic proteins to cysteines. During this process, glutathione is oxidized to glutathione disulphide (GSSG). Glutathione peroxidases (GPX) catalyze the breakdown of hydrogen peroxide and organic hydroperoxides (Brigelius-Flohe, 1999; Ursini et al., 1995). Glutathione reductase reduces GSSG and refills GSH pools (Carlberg and Mannervik, 1975). Under physiological conditions, glutathione almost exclusively exists in its reduced form because of a constitutive activity of glutathione reductase in cells (Beutler, 1969). Glutathione S-transferases are detoxification enzymes that catalyze the conjunction of GSH to a variety of exogenous and endogenous electrophilic compounds (Hayes et al., 2005; Sharma et al., 2004; Townsend and Tew, 2003).

3. Adaptation to high ROS levels in cancer cells

Cells can adapt to survive under certain levels of oxidative stress. As cancer cells actively produce high levels of ROS and are consistently exposed to such endogenous oxidants, one would expect that the intrinsic oxidative stress may exert selective pressure to enrich the population of cells that are capable of stress adaptation (Kim et al., 2006; Schneider and Kulesz-Martin, 2004). Those cells that survive oxidative stress are likely to have acquired adaptive mechanisms to counteract the potential toxic effects of elevated ROS and to promote cell-survival pathways (Irmak et al., 2003). For example, oncogenic *H-Ras*-transformed cells, which exhibited increased superoxide and hydrogen peroxide levels, were shown to express higher levels of antioxidants compared with their non-tumorigenic parental cells (Young et al., 2004). Their enhanced antioxidant capability is likely to serve as a key mechanism to evade ROS-induced apoptosis, as evidenced by

the resistance to hydrogen peroxide-induced cell death that was observed in the *Ras*-transformed cells (Young et al., 2004). These were also found to be more sensitive to depletion of glutathione (GSH), leading to ROS accumulation and cell death (Trachootham et al., 2006), suggesting a crucial role of antioxidants in cell survival.

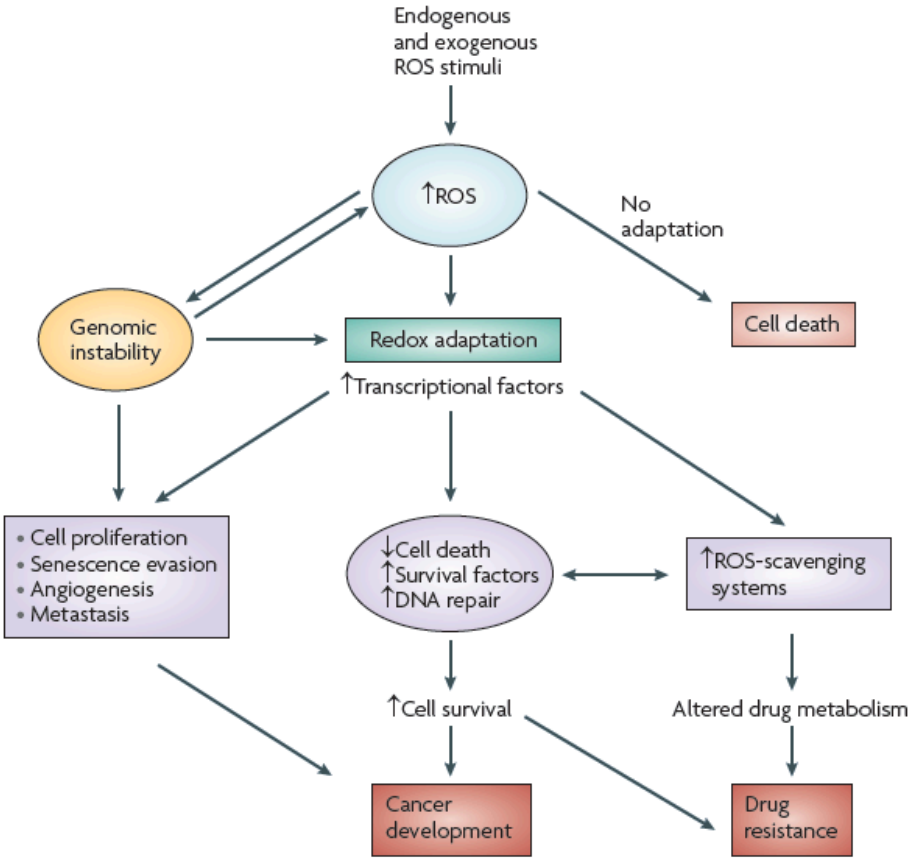

Figure 12. Redox adaptation in cancer development. Severe accumulation of ROS under various endogenous and exogenous stress stimuli may induce lethal damage in cells that have inadequate stress responses or adaptation. In certain cancer cells, persistent ROS stress may induce adaptive stress responses including activation of redox-sensitive transcription factors, leading to an increase in the expression of ROS-scavenging enzymes, elevation of survival factors, and inhibition of cell death factors, such as caspases. ROS-mediated DNA mutations or deletions promote genomic instability and thus provide an additional mechanism for stress adaptation. All these events enable cells to survive with the high level of ROS and maintain cellular viability. As these transcription factors also have roles in regulating the expression of genes that are responsible for proliferation, senescence evasion, angiogenesis and metastasis, the redox adaptation processes may promote cancer development. Furthermore, the increase in glutathione during adaptation can enhance the

export of certain anticancer drugs and their inactivation. This altered drug metabolism together with enhanced cell survival may render cancer cells more resistant to chemotherapeutic agents. (Trachootham et al., 2009).

Thus, it is conceivable that during malignant transformation the oncogenic signals both induce ROS generation to stimulate cell proliferation through redox-sensitive transcriptional factors, and promote antioxidant adaptive mechanisms to minimize oxidative damage. As shown in **figure 12**, redox adaptation by activating ROS-scavenging enzymes to counteract increased ROS generation seems to be a major mechanism by which cancer cells maintain redox homeostasis. Therefore, abrogation of this adaptation mechanism could be an attractive strategy to preferentially affect cancer cells and may therefore have therapeutic implications.

Aim of the work

p38α is known to have a tumor suppressor role based on its ability to negatively regulate cell proliferation and to induce cell death. However, most of these studies have focused on the investigation of p38α functions during tumor initiation, and we still do not fully understand the roles of p38α in tumor progression.

The aim of this work was to determine whether p38α might be necessary for the survival of cancer cells to chemotherapy treatments following two approaches:

- Identify synthetic lethal partners of p38α
- Determine if the inhibition of p38α synergizes with chemotherapeutic treatments to induce tumor cell death.

Materials & Methods

Buffers and solutions

Laboratory common stock solutions and buffers were prepared as described in Current Protocols in Cell Biology (2001), unless purchased, in which case references are provided in the "Commercial Reagents and Kits" section. Therefore, only unique solutions for this thesis are specified below.

Antioxidants (100 mM stock)

It is extremely important to adjust pH to 7.5 in both cases. Aliquot solutions and store at -20 ºC. Do not freeze again after thawing.

- GSH: 0.61 g GSH + 20 ml PBS
- NAC: 0.65 g NAC + 40 ml PBS

Buffer B (to resuspend bacterial pellets)

50 mM Tris-HCl pH 8.0
1 mM EDTA
1 mM DTT
10 µg/ml leupeptin
10 µg/ml pepstatin A
2.5 mM benzamidine
1 mM PMSF

Buffer D (for dialysis)

50 mM Tris-HCl pH 7.5
0.1 mM EDTA
2 mM DTT
50 mM NaCl
50% glycerol

Buffer H (high salt concentration)

50 mM Tris-HCl pH 8.0
1 mM EDTA
1 mM DTT
1% Triton X-100
500 mM NaCl
1 mM PMSF

Buffer L (low salt concentration)

50 mM Tris-HCl pH 8.0
1 mM EDTA
1 mM DTT
50 mM NaCl
1 mM PMSF

HBS buffer (2x)

Filter through 0.5 µm, aliquot and store at -20ºC

10 ml of 1M HEPES

11.2 ml of 5 M NaCl

0.3 ml of 1 M $Na_2HPO_4.2H_2O$

H_2O up to 180 ml (set pH to 7.12 with NaOH)

H_2O up to 200 ml

Kinase buffer

50 mM Tris-HCl pH 7.5

10 mM $MgCl_2$

1 mM DTT

Lysis buffer

Either store in aliquots at -20 ºC or add the inhibitors right before use

50 mM Tris-HCl pH 7.5

150 mM NaCl

1% NP-40

5 mM EDTA

5 mM EGTA

20 mM NaF

0.1 mM Na_3VO_4

1 µM microcystin

Protease Inhibitor Cocktail Set III

Mowiol

2.4 g Mowiol

6.0 g Glycerol

6.0 ml water

Vortex well and shake for approximately 2 h at RT. Add 12 ml 0.2 M Tris-HCl pH 8.5. Incubate at 50 ºC for approximately 3 h, with occasional mixing until most of the Mowiol is dissolved (it will never dissolve completely). Centrifuge at 5000 xg for 15 min to remove the sedimented Mowiol. Add DABCO antifading to 2.5%, aliquot and store at -20 ºC (it is stable for at least 1 year). Heat at 40 ºC before use (once heated, store at 4 ºC, it can be used for 1 month).

PBS-T

PBS + 0.1% (v/v) Tween-20

Phosphatase buffer

50 mM Tris-HCl pH7.5
250 mM NaCl
1% (v/v) Triton X-100
1 mM PMSF
10 µg/ml pepstatin
1.4 µg/ml aprotinin
10 µg/ml leupeptin

Either store in aliquots at -20 ºC or add the inhibitors right before use

Tissue lysis buffer

50 mM Tris-HCl pH 7.5
150 mM NaCl
1% NP-40
5 mM EDTA
5 mM EGTA
1 mM DTT
1 mM PMSF
10 µg/ml pepstatin
1.4 µg/ml aprotinin
10 µg/ml leupeptin
20 mM NaF
0.1 mM Na_3VO_4
1 µM microcystin

Either store in aliquots at -20 ºC or add the inhibitors right before use

TNB buffer

100 mM Tris-HCl pH 7.5
150 mM NaCl
0.5% Blocking Reagent (see "Commercial Reagents and Kits")
(Optional: 0.05% sodium azide to prevent contamination)

Shake for 1 h at 60 ºC to dissolve the Blocking Reagent. Aliquot and store at -20 ºC

Cell lines

Human cancer cells

We used cell lines derived from breast (MCF7, MDA-MB-231), cervix (HeLa), colon (HCT116, HCT116 p53 KO, HT-29, RKO, SW620) and osteosarcoma (U2OS). HEK293-derived 293T cells, provided by M. Serrano (CNIO, Madrid), were used to produce shRNA-expressing viruses.

Commercial Reagents and Kits

Article	Brand	Reference
40% Acrylamide/Bis (29:1)	Bio-Rad	161-0146
Ampicillin sodium salt	Sigma	A9518
Annexin V	BD Biosciences	556547
Aprotinin	Sigma	A6279
APS	Sigma	A3678
ASK1 inhibitor	Otava	7214191049
BSA	Sigma	A7906
Benzamidine	Sigma	B6506
Blocking Reagent	Boehringer Manheim	1096176
β-mercaptoethanol	Sigma	M7154
BrightVision poly-HRP anti-IgG	ImmunoLogic	DPVO110HRP
Cell Death Detection ELISA^{PLUS} kit	Roche	11 920 685 001
Cisplatin (for cells, 0.5 mg/ml)	Ferrer Farma	657932
Cisplatin (for mice, 1.0 mg/ml)	Accord	683046-8
Citrate	Merck	1-06448-5000
DAPI	Invitrogen	MP-36930
DAB	Dako	K3468
DABCO antifading reagent	Sigma	D2522
DCFDA	Sigma	D6883
Dharmafect 1	Dharmacon	T-2001
DMEM	Sigma	D5796
DMSO (for cell culture)	Sigma	276855
DMSO (for MTT assays)	Fisher Scientific	W03448
DNase I	Roche	4716728a
dNTPs mix (10 mM)	Fermentas	R0192
Doxorubicin	Sigma	D1515
DPI	Sigma	D2926
DTT	GE Healthcare	17-1318-02
Eosin (1% yellowish solution)	Panreac	251301-1611
Etoposide	Sigma	E1383

FBS	Thermo Scientific	E6541L
Formalin 10% (buffered)	Sigma	HT501128
Glutathione	Sigma	G6013
Glutathione Sepharose 4B beads	GE Healthcare	17-0756-01
Glycerol	Fluka	49782
Hematoxylin (Mayer's)	Panreac	254766-1611
IPTG	Sigma	I6758
LB	Invitrogen	12795-084
Leupeptin	Sigma	L2884
L-Glutamine 200 mM	LabClinics	M11-004
Library of inhibitors	Merck Millipore	539746
LY294002	Merck Millipore	440202
Methyl cellulose	Sigma	M7140
Microcystin-LR	Enzo Life Sciences	ALX350012
Mowiol	Calbiochem	475904
Mr. Frosty Freezing Container	Thermo Scientific	5100-0001
MTT	Sigma	M2128
MycoAlert	Lonza	LT07-318
NAC	Sigma	A9165
Neocarzinostatin	Sigma	N9162
Nitrocellulose 0.2 µm membrane	Protran	10401396
NP-40	AppliChem	A1694-0250
Oxidative Stress PCR Array	SABiosciences	PAHS-065Z
Oxyblot	Millipore	S7150
PBS 10x	Sigma	D1408
Penicillin/Streptomycin (100x)	LabClinics	P11-010
Pepstatin A	Sigma	P4265
Peroxidase	Dako	S2023
PFA 16%	EMS	15710
PH-797804	Selleckchem	S2726
Phenol:chloroform	Sigma	P2069
Phosphatase Assay (Ser/Thr)	Promega	V2460

Phosphatase Assay (Tyr)	Promega	V2471
PI	Sigma	P4864
PMSF	Sigma	P7626
Polybrene	Sigma	H9268
Protease Inhibitor Cocktail Set III	Merck Millipore	539134
Random primers	Invitrogen	48190011
Rapamycin	Merck Millipore	553210
Reagent A	Bio-Rad	500-0113
Reagent B	Bio-Rad	500-0114
Reagent S	Bio-Rad	500-0115
Resazurin	Sigma	R7017
RNA Mini Kit (Pure Link)	Ambion	12183-018A
RNeasy Mini Kit	Qiagen	74104
RNase A	Roche	109 169
Rotenone	Sigma	R8875
SB203580	Axon MedChem	1363
siRNA Negative Control	Ambion	4390843
siRNA DUSP8	Ambion	4390824
siRNA DUSP10	Ambion	4392420
siRNA DUSP16	Sta. Cruz Biotech.	sc-61052
siRNA MAPK14	Ambion	AM51333
siRNA PTPN12	Dharmacon	L008064-00
SOC	Invitrogen	15544-034
Sodium Fluoride	Sigma	S7920
Sodium Orthovanadate	Sigma	S6508
SP600125	Calbiochem	420119
SuperScript II Reverse Transcriptase	Invitrogen	18064-022
Sybr Green Supermix	Bio-Rad	1708886
Taq polymerase	Bioline	BIO-21040
TEMED	Sigma	T9281
Triton X-100	Sigma	T9284
Trypsin-EDTA	Sigma	T3924

TUNEL	Roche	11684795910
Tween-20	Sigma	P7949
U0126	Merck Millipore	662005

Laemmli polyacrylamide gels

	Stacking 5%	Resolving 10%	Resolving 12%
40% Acrylamyde/Bis	625 µl	2.5 ml	3 ml
1M Tris-HCl pH 6.8	940 µl	-	-
1M Tris-HCl pH 8.8	-	3.75 ml	4.5 ml
10% SDS	50 µl	100 µl	100 µl
H_2O	3.4 ml	3.6 ml	2.35 ml
10% APS	25 µl	40 µl	40 µl
TEMED	6 µl	10 µl	10 µl

Oligonucleotides

qRT-PCR

RefSeq	Gene	Sequence (5′-3′)
NM_004420	DUSP8	FW: GATGACGCAAAATGGAATAAGC
		RV: CTTCACGAACCTGTAGGCG
NM_144729	DUSP10	FW: TGAACATCGGCTACGTCATC
		RV: TGGTGTAAGGATTCTCGGTG
NM_030640	DUSP16	FW: CAGAATGGGATTGGTTATGTG
		RV: TAGGCGATAGCGATGGTGG
NM_002046	GAPDH	FW: GTCGGAGTCAACGGATTTGG
		RV: TGAGCCCCAGCCTTCTCC
NM_002083	GPX2	FW: CCTCCCCACCCCTCTAATAG
		RV: TCTACCTTCTCCCCATCCAG
NM_002084	GPX3	FW: TGTCAATGGAGAGAAAGAGCAG
		RV: TCTCAAAGTTCCAGCGGATG
NM_001509	GPX5	FW: ACATCCTGGCGTACTTGAAG
		RV: GGGAGAGCAAGTCATTAGGTG
NM_000190	HMBS	FW: GGAGTATTCGGGGAAACCTC

		RV: AAGCAGAGTCTCGGGATCG
NM_006151	LPO	FW: TGAAAAGACAAGGCACTGGG
		RV: TGAAGCAAGATGAGGGAAGC
NM_000963	PTGS2	FW: ACAGGCTTCCATTGACCAG
		RV: TCACCATAGAGTGCTTCCAAC
NM_002827	PTPN1	FW: AGAAGGACGAGGACCATGCAC
		RV: AGTGGAGGAGGGTCAGGCTAT
NM_002835	PTPN12	FW: GATGGTGCTGTGACCAGGAAC
		RV: TCATGTCCATTCTGAAGGTGG
NM_144651	PXDNL	FW: CCAAGTGATTCCCCAGAGAAG
		RV: GTTGCTTAAGTCAGTGGTTTCC
NM_032243	TXNDC2	FW: TGATGCCAGTGAATGCGTAG
		RV: CGTTGCTGGACAGGACTAG

siRNA (customed)

RefSeq	Gene	Sequence (5'-3')
NM_002827	PTPN1	Sense: UAGGUACAGAGACGUCAGUdTdT
		Antisense: ACUGACGUCUCUGUACCUAdTdT

Primary antibodies:

	Antigen	Brand and reference	Dilution (Time / °C)	Host
- flow cytometry	γ-H2AX	Upstate, 05-636	1:200 (2 h / 37)	Mouse
- IF	P-JNK	BD Biosciences, 612541	1:25 (1 h / 37)	Mouse
- IHC	Ki67	Novacastra	1:500 (1 h / RT)	Rabbit

- WB

Antigen	Brand and reference	Dilution	Time / °C	Host
Catalase	Abgent, AM2118a	1:1000	4 h / RT	Mouse
Cleav. caspase 3	Cell Signaling, 9661	1:500	O/N / 4	Rabbit
γ-H2AX	Upstate, 05-636	1:500	O/N / 4	Mouse
HSP27	Sta. Cruz, sc1049	1:1000	4 h / RT	Goat
JNK	Sta. Cruz, sc-571	1:1000	4 h / RT	Rabbit
p38α	Sta. Cruz, sc-535	1:1000	4 h / RT	Goat

p53	Cell Signaling, 2524	1:1000	1 h / RT	Mouse
p85 PARP	Promega, G734	1:500	O/N / 4	Rabbit
P-Hsp27 (tissue)	Cell Signaling, 2401	1:500	O/N / 4	Rabbit
P-Hsp27 (cells)	StressGene, ADI-SPA-523	1:500	O/N / 4	Rabbit
P-JNK (cells)	BD Biosciences, 612541	1:500	O/N / 4	Mouse
P-JNK (tissue)	Cell Signaling, 9251	1:500	O/N / 4	Rabbit
P-MK2	Cell Signaling, 3007	1:500	O/N / 4	Rabbit
P-p38	Cell Signaling, 9211	1:500	O/N / 4	Rabbit
Ras	BD Biosciences, 610001	1:1000	4 h / RT	Mouse
SOD2	Abcam, ab13533	1:1000	4 h / RT	Rabbit
Tubulin	Sigma, T9026	1:5000	1 h / RT	Mouse

Secondary antibodies

Antigen	Brand and reference	Time / ºC	Host
Goat IgG (Alexa Fluor 680)	Invitrogen, A21084	1 h / RT	Donkey
Mouse IgG (Alexa Fluor 488)	Invitrogen, A11001	1 h / RT	Goat
Mouse IgG (Alexa Fluor 680)	Invitrogen, A21057	1 h / RT	Goat
Mouse IgG (Alexa Fluor 800)	Rockland, 610-731-124	1 h / RT	Donkey
Rabbit IgG (Alexa Fluor 680)	Invitrogen, A21076	1 h / RT	Goat
Rabbit IgG (Alexa Fluor 800)	Rockland, 611-131-122	1 h / RT	Goat

(All secondary antibodies were used at 1:5000 dilution)

For commercial kits, only those protocols that either vary from the published datasheets or are not fully specified, are detailed here.

All the experiments that involve cell culture were done in sub-confluent conditions (unless otherwise specified).

Annexin V staining

This kit was used to quantitatively determine the percentage of cells within a population that are undergoing apoptosis by detecting their exposed phosphatidylserines. Counterstaining with PI is used to distinguish between viable and non-viable cells, since viable cells with intact membranes exclude PI.

1. Collect the supernatant of the cells, wash once with cold PBS and collect the washing solutions as well). Trypsinize with the minimum possible amount of trypsine (since it can alter the cell membrane integrity)

2. Pellet the cells (200 xg for 5 min at 4 ºC) and wash once more with PBS

3. Resuspend cells in ~1 ml of 1x Binding Buffer (dilute the 10x stock in water), count cells and adjust the concentrations to 10^6 cells/ml with 1x Binding Buffer

4. Transfer 100 µl of the solution (10^5 cells) to a cytometer tube

5. Add 5 µl of FITC Annexin V

6. Gently vortex the cells and incubate for 20 min at RT in the dark

7. Add 5 µl of PI right before going to analyze by flow cytometry

8. Add 400 µl of 1x Binding Buffer to each tube

9. Analyze by flow cytometry within 1 h

Bacterial transformation

1. Add up to 50 ng of DNA to 50 µl of chemo-competent cells and incubate them on ice for 30 min

2. Heat shock in a waterbath at 42 ºC for 45 s

3. Put back the tubes on ice for 2 min

4. Add 250 µl of SOC medium (do not mix!) and incubate for 1 h at 37 ºC with light shaking

5. Plate 80 – 100 µl on pre-warmed plates containing antibiotics and incubate O/N at 37 ºC

Clonogenic assays

This is a cell survival assay based on the ability of single cells to grow into colonies. It is used to determine cell death after treatment with cytotoxic agents.

Cancer cells were incubated O/N with 10 μM SB203580 and treated for 1 h with cisplatin either 50 μM (HT-29, MCF7) or 10 μM (SW620). Then, 500 cells (HT-29, MCF7) or 1000 cells (SW620) were plated per well in 6-well plates. Cells were allowed to grow until visible colonies were formed (about two weeks) and were processed as follows:

1. Wash the cells twice with PBS

2. Fix the cells for 30 min with 4% PFA

3. Wash cells twice with H_2O

4. Stain cells for 15 min with 0.05% crystal violet

5. Wash twice with H_2O

6. Drain cells inverted for a couple of minutes

7. Dishes can be photographed or scanned for colony counting (colonies can be counted several months after staining).

DNA oligonucleosomes quantification

The Cell Death Detection kit ELISA^{PLUS} is used to quantify histone-complexed DNA fragments (mono- and oligonucleosomes) that are released into the cytoplasm after the induction of apoptosis. Manufacturer's instructions (Roche) were followed exactly (**Fig. 13**).

Expression and purification of GST-tagged proteins

I. Expression

1. Transform BL21 (DE3) *Escherichia coli* bacterial strain with the expression construct DNA for your recombinant protein (see "Bacterial transformation" section)

2. Next morning, keep at 4 ºC the plates containing the bacterial colonies (to prevent the growth of "satellite" colonies)

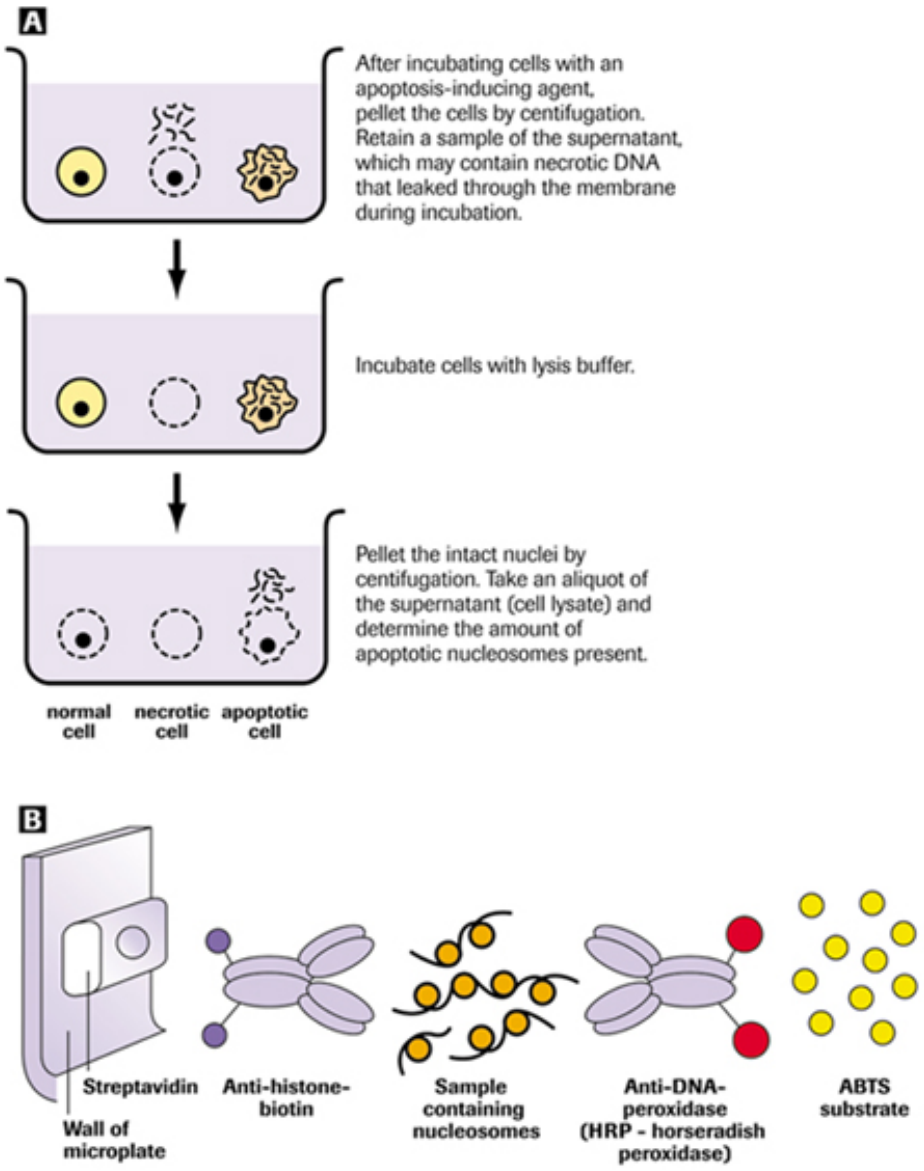

Figure 13. Overview of how DNA oligonucleosomes were detected. Cell Death Detection ELISA^{PLUS} kit was used following manufacture's instructions, which are cartooned here.

3. In the afternoon, pick one middle-sized colony and grow it in pre-warmed 25 ml of LB containing antibiotic (ampicillin 50 µg/ml)

4. The following day, pour the whole culture in a 500 ml flask of pre-warmed LB containing antibiotic (ampicillin 50 µg/ml)

5. Grow bacteria until OD_{595nm} ~0.4-0.5 and add 1 mM IPTG

6. Incubate for 3 h at 37 ºC (or RT for 5 h, or O/N at 18 ºC)

II. Purification (WORK ON ICE)

1. Spin the bacterial culture by centrifuging at 1400 xg for 20 min at 4 ºC

2. Resuspend the bacterial pellet in buffer B (see "Materials") so that the final volume is 32 ml

3. Add lysozyme 1 mg/ml final concentration (32 mg) and keep on ice for 10 - 15 min

4. Freeze in liquid N_2 and keep at -80 ºC for up to two weeks (optional)

5. Next day, sonicate the lysates and pour them into ultracentrifuge tubes

6. Add 4 ml of 10% Triton X-100 and 4 ml of 5 M NaCl (final concentrations: 1% Triton and 0.5 M NaCl)

7. Centrifuge at 17400 xg for 20 min at 4 ºC

8. Pre-wash Glutathione Sepharose beads: put 700 µl of beads in a conical tube and add buffer H up to 14 ml. Centrifuge at 400 xg for 2 min 4 ºC

9. Incubate the supernatant (from the ultracentrifugation) with the pre-washed beads in a conical tube for 1 h at 4 ºC

10. Wash (4x) in buffer H (400 xg for 3 min at 4 ºC)

11. Wash (4x) in buffer L (400 xg for 3 min at 4 ºC)

12. Elute the protein: add to the beads 200 µl buffer L and 500 µl 200 mM glutathione (dissolve 1.228 µg of glutathione in 18 ml of 50 mM Tris pH 8.0, adjust pH to 7 – 8 and the final volume to 20 ml)

13. Incubate on ice for 15 min, with gently mixing every 2 – 3 min

14. Centrifuge at 400 xg for 10 min at 4ºC

15. Take the supernatant and perform a second round of elution

16. Once eluted, centrifuge both supernatants at 16000 xg for 5 min at 4 ºC

17. Check if there is any detectable protein amount in the supernatants (see "Protein extraction and quantification" section)

18. Dialyze O/N in 2 l of buffer D. (Incubate the dialyzing membrane in buffer D for few minutes, take out the air with a syringe, inject the protein and then remove a little bit more air).

Flow cytometry assays

Cell cycle profiles

This is a method to stain DNA using ethanol to fix the cells and permeabilize the membrane, which allows the dye, propidium iodide (PI), to enter the cells. PI is a DNA-binding fluorochrome that gets intercalated into the double helix. Ribonuclease A is used to eliminate the staining of the double-stranded RNA.

1. Wash the cells once with PBS (400 xg for 5 min)

2. Place 330 µl of cell suspension (without cell clumps!) in a conical tube and add 600 µl ice-cold 100% ethanol drop-wise to the tube walls. Leave at least for 30 min at 4 ºC (may be left at this stage for a week).

3. Centrifuge at 400 xg for 5 min at 4 ºC to remove ethanol

4. Add 5 ml of cold PBS and wash by centrifuging at 400 xg for 5 min at 4 ºC and remove the supernatant

5. Resuspend in DNA staining solution and incubate (covered with aluminum foil) at 30 ºC for 30 min in a waterbath. Volumes per tube:

500 µl PBS

0.2 mg/ml RNase A

20 µg/ml PI

6. Acquire on an EPICS XL flow cytometer (collect 10000 events)

γ-H2AX staining

Histone H2AX is recruited to DNA double strand breaks and phosphorylated (γ-H2AX). This form can be detected by antibodies to quantify DNA damage.

1. Collect by trypsinization (see "Mammalian cell culture") sub-confluent cells grown in 60 mm ∅ dishes and wash them (2x) with PBS by centrifuging at 200 xg for 5 min at RT

2. Resuspend the cell pellets (without clumps!) in 330 µl of PBS and add 660 µl of ice-cold 100% ethanol drop-wise to the tube walls. Incubate at 4 ºC at least for 30 min (cells remain stable at this stage for a week)

3. Centrifuge at 400 xg for 5 min at 4 ºC to remove ethanol

4. Wash (1x) with PBS-T by centrifugation at 400 xg for 5 min at 4 ºC

5. Wash (1x) with 5 ml of 3% BSA in PBS-T (400 xg for 5 min at 4 ºC)

6. Incubate γ-H2AX antibody diluted 1:200 in 3% BSA in PBS-Tween 0.05% for 2 h at RT with gentle shaking

7. Wash (1x) with 10 ml of PBS-T (400 xg for 5 min at 4 ºC)

8. Incubate the Alexa Fluor-488 conjugated secondary antibody diluted 1:200 in PBS-T for 1 h at RT

9. Wash (2x) with 10 ml of PBS-T (400 xg for 5 min at 4 ºC)

10.Resuspend in DNA staining solution and incubate (covered with aluminum foil) at 30 ºC for 30 min in a waterbath. Volumes per tube:

500 µl PBS

0.2 mg/ml RNase A (5 µl from 20 mg/ml stock)

20 µg/ml PI (10 µl from 1 mg/ml stock)

11. Acquire on an FC500 flow cytometer (collect 10000 events)

Gene expression array

The RT^2 Profiler PCR Array System brings together the quantitative performance of real-time PCR and the multiple gene profiling capability of microarrays. The Human Oxidative Stress and Antioxidant Defense PCR Array profiles the expression of 84 genes involved in ROS regulation. Manufacturer's instructions were followed exactly (**Fig. 14**). Briefly, DNase-treated total RNA from MCF7 cells, either control or treated with 10 µM SB203580, was purified with the RNeasy minikit (Qiagen). cDNA was generated by reverse transcription from 4 µg of total RNA from each sample using the RT^2 First Strand Kit, then combined with the RT^2 qPCR Master Mix and added to lyophilized primer pairs in the 96 well plate arrays. Thermal cycling was performed in a CFX96™ Real Time System (Bio-Rad) and relative gene expression levels were calculated using the ΔΔC(t) method with normalization to the average expression of three housekeeping genes (GAPDH, HPRT1 and RPL13A).

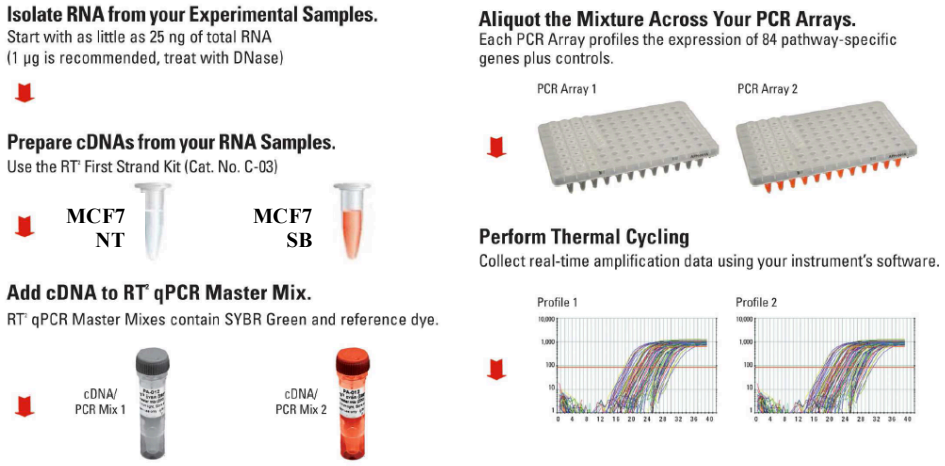

Figure 14. Overview of the PCR Array procedure. Isolated RNA from cell lysates is converted to cDNA and the expression of 84 genes involved in ROS regulation is quantified by qRT-PCR.

Gene knockdown by shRNA

I. $CaCl_2$-mediated transfection of packaging cells

1. Prepare 2.5 M $CaCl_2$ and 2x HBS buffer pH 7.12 and keep them at RT

2. Take 9 µg of DNA for a 100 mm ∅ dish (4.5 µg of shRNA + 4 µg of Δ89 + 0.5 µg VSVG), 50 µl of 2.5 M $CaCl_2$ and make this mix up to 500 µl by diluting it with H_2O in a 1.5 ml tube (first add DNA, then H_2O and finally $CaCl_2$ drop by drop, allowing it to slide down the walls of the tube). Incubate for 5 min at RT and then transfer the mix to a 15 ml tube

3. Add 500 µl of 2x HBS (drop by drop and simultaneous bubbling by air injection), vortex for 5 s and incubate the mix for 20 min at RT

4. Add the mix to the 293T cells in a drop-wise manner

5. About 6 h later, wash with PBS and add fresh growth medium

6. Collect the medium containing viral particles 48 h later and add fresh medium again to generate new viruses for a second infection

7. Collect again the medium 24 h later and perform a second round of infection. Discard 293T cells

II. Infection with generated viruses

1. Filter through a 0.45 μm PVDF filter (highly hydrophilic, low retention of viral particles) 4 ml of medium collected from 293T cells and mix it with other 4 ml of fresh growth medium

2. Add polybrene to the medium containing viral particles so it reaches a final concentration of 8 μg/ml and incubate the mixture for 5 min at RT

3. Remove media from the plates that will be infected and add the media containing the viral particles. If a second round of infection is needed, 24 h later repeat steps 1-2

4. Begin selection with 1 μg/ml puromycin 48 h after the last round of infection and keep it for 1 week

Gene knockdown by siRNA

Cancer cells grown up to 60% confluency in 60 mm ∅ dishes (and a final volume of 3 ml) were transfected with 50 nM siRNA following the protocol below:

1. Mix in tube 1 a 300 μl volume containing 6 μl of 25 μM siRNA + 294 μl of serum-free medium

2. Mix in tube 2 a 300 μl volume containing 6 μl of Dharmafect 1 reagent + 294 μl of serum-free medium

3. Gently mix the contents of each tube by pipetting carefully up and down and incubate for 5 min at RT

4. Add the content of tube 1 to tube 2 for a total volume of 600 μl. Mix by pipetting carefully up and down

5. Incubate for 20 min at RT

6. Remove culture medium from the cells and wash them once with antibiotic-free complete medium

7. Add 2400 μl of fresh antibiotic-free complete medium to the cells

8. Add the transfection mix from step 4 to the cells drop wise and incubate cells O/N at 37 ºC and 5% CO_2

9. 24 h later replace the transfection medium by complete growth medium

GST pull down of JNK-binding proteins

I. GST-JNK1 binding to beads

1. Prewash (2x) 50 µl of Glutathione Sepharose beads with 500 µl PBS contining protein inhibitors (PBS-PI) at 500 xg for 1 min at 4 ºC

2. Incubate the beads and GST-JNK1 for 1.5 h at 4 ºC and rotating with 500 µl PBS-PI (50 µl beads + 23 µl GST-JNK1 (~100 µg) + 427 µl PBS-PI)

3. Recover the protein bound to the beads by centrifuging at 500 xg for 6 min at 4 ºC. Take the supernatant with a 0.3 mm needle

4. Wash (1x) with 500 µl PBS-PI at 500 xg for 1 min at 4 ºC

5. Wash (1x) with 500 µl kinase buffer at 500 xg for 1 min at 4 ºC

6. Resuspend in 40 µl of kinase buffer

II. Cold phosphorylation of GST-JNK1

1. Prepare the kinase buffer

2. Prepare protein mixtures with a ratio 1:10 (kinase:substrate) in a V_f = 50 µl

40 µl beads·GST-JNK1 (~10 µg)
2 µl GST-MKK7 (0.5 µg/µl)
3 µl KiB
5 µl ATP (3 µl 10 mM + 6 µl KiB)

3. Incubate for 1 h at 30 ºC with light shaking

4. Stop the reaction by putting the samples on ice

III. Pull down of GST-P-JNK1

1. Collect and quantify the human cancer cells (treated or not with 10 µM SB203580) in phosphatase buffer

2. Pre-incubate 2 mg of cell lysates with 10 µg of GST protein for 30 min rotating at 4 ºC. Put the samples on ice to stop the reaction.

Vf ~500 µl	**SW620**	**SW620 SB**
µl lysate (2 mg)	303.48	284.52
µl GST (10 µg)	1.25	1.25

3. Prewash (2x) 50 µl beads with 500 µl phosphatase buffer at 500 xg for 1 min at 4 ºC

4. Incubate rotating the pre-washed beads and the cell lysates with GST protein for 30 min at 4 ºC

5. Recover the GST protein bound to the beads by centrifuging at 500 xg for 6 min at 4 ºC. Take the supernatant with a 0.3 mm needle

6. Mix 2 mg of the pre-cleared cell lysates with 10 µg of GST-P-JNK1 (from the cold kinase assay) and incubate them for 30 min at 37 ºC with light shaking. Put the samples on ice to stop the reaction

Vf ~300 µl	**SW620**	**SW620 SB**
µl lysate (2 mg)	–300	~300
µl GST-P-JNK1 (10 µg)	50	50

7. Recover the protein bound to the beads by centrifuging at 500 xg for 4 min at 4 ºC. Take the supernatant with a 0.3 mm needle

8. Wash with phosphatase buffer, up to 500 µl, at 500 xg for 3 min at 4 ºC

9. Resuspend in 40 µl of phosphatase buffer and add 10 µl of LSB5x to run in a gel and analyze by mass spectrometry

Histology and immunohistochemistry

For histological analysis, resected breast tumors were sliced, fixed in 10%-buffered formalin and embedded in paraffin wax. Sections of 3 µm were stained with hematoxylin and eosin (H-E) and analyzed in blinded fashion by two independent observers at the microscope. For each mouse, at least ten high power fields (200x) from two tissue slides of two different tumors were analyzed. The malignancy was determined based on the microscopic appearance of the tissues (degree of filled tubules, rate of cell division, cell size and uniformity) and classified into 4 stages: normal tissue, hyperplasia, adenocarcinoma and carcinoma. Hyperplasic tissue resembles normal cells, arranged around tubules, well differentiated and with a low proliferation rate. Adenoma showed moderately differentiated cells, which still retain the glandular-related tissue cytology and architecture, with clear tumor margins. Carcinoma showed very abnormal and poorly differentiated cells with no significant resemblance to the corresponding parent cells and tissue.

Additional immunohistochemical examination of the tumors was done to assess cell proliferation by Ki67 staining. Briefly, deparaffinated sections were treated with 10 mM citrate pH 6.0 for antigen retrieval, peroxidase was used for blocking and after incubation of primary the antibody (Ki67, see "Materials" for timing and dilution), BrightVision Poly-HRP-Anti Ms/Rb/Rt IgG and DAB were used for signal development. All sections were counterstained with hematoxylin.

Immunoblotting

1. Separate 50 µg of protein lysates by SDS-PAGE on 10% or 12% Laemmli gels, depending on the molecular weight of the protein of interest

2. After electrophoresis, transfer the proteins in the gel to a nitrocellulose membrane using a wet-blotting system (Bio Rad)

3. Stain with 0.1% Ponceau (in 5% acetic acid) for 2 min to evaluate the efficiency of transfer and then wash out the staining with PBS

4. Block the nitrocellulose membrane incubating for 1 h at RT (or O/N at 4 ºC) with 4% non-fatty milk (in PBS) and gently shaking

5. Rinse the membrane with PBS and incubate the primary antibodies diluted in 5% BSA in PBS-T (see "Materials" for specific timing and dilutions)

6. Wash (3x) with PBS-T for 5 min at RT

7. Incubate for 1 h at RT with the Alexa Fluor-conjugated secondary antibodies diluted 1:5000 in 1% non-fatty milk (diluted in PBS-T)

8. Wash (3x) with PBS-T for 5 min at RT

9. Scan the membranes in an Odyssey Infrared Imaging System (Li-Cor, Biosciences)

Immunofluorescence

1. Culture adherent cells on coverslides

2. Place the coverslides on a multi-well plate and fix the cells in 4% PFA for 10 min

3. Wash (x3) in TBS for 5 min

4. Incubate the cells with 0.5% Triton X-100 in TBS for 10 min to permeabilize them

5. Wash (x3) in TBS for 5 min

6. Incubate the cells with TNB shaking at RT for 1 h for the blocking

7. Remove the excess of TNB by touching some dry paper, place the slides face-up in a humid chamber and incubate a 60 µl drop of the primary phospho-antibody diluted 1/25 in TNB for 1 h at 37 ºC

8. Wash (3x) in TBS for 5 min

9. Remove the excess of TBS, place the slides face-up in a humid chamber and incubate a 60 µl drop of the secondary antibody diluted 1/250 in TNB for 30 min at 37 ºC

10. Wash (3x) in TBS for 5 min

11. For nuclear staining, incubate with DAPI at RT for 2 min

12. Wash (3x) in TBS for 5 min

13. Mounting in Mowiol:

- 30 min before mounting, incubate Mowiol at 55 ºC
- Immerse the coverslide for few seconds in water to avoid crystal precipitation from the buffer salts
- Remove the excess of water, add 10 µl of Mowiol on a slide and place the coverslide face-down carefully onto the Mowiol drop
- Keep the slides at 4 ºC O/N to allow Mowiol to dry

Mammalian cell culture

I. Maintenance and cell subculturing

All the cell lines were maintained in DMEM supplemented with 10% heat-inactivated FBS, 1% L-glutamine and 1% penicillin/streptomycin at 37 ºC and 5% CO_2.

Cells were washed once with PBS and incubated with 0.05% trypsin for 3 min at 37 ºC to detach and subculture them. Then, they were subsequently diluted in fresh medium (from 1/4 to 1/12, depending on the proliferation rate), resuspended and plated into a new culture dish.

II. Cell harvesting

Subconfluent cell cultures were washed twice with ice-cold PBS and immediately frozen on dry ice to keep stored at -80 ºC until further processed.

For apoptosis quantification, media from the cell cultures were collected on ice, together with PBS washings (1x) and the cells resuspended after trypsin detachment (see previous section). Cells were pelleted by centrifugation at 200 xg for 5 min at 4 ºC. Cell pellets were resuspended in ice-cold PBS and centrifuged again at 200 xg for 5 min at 4 ºC for washing. Supernatants were discarded and cell pellets were frozen at -80 ºC for further processing.

III. Cell freezing and thawing

To freeze the cells, subconfluent cell cultures grown on 10 cm ∅ dishes were harvested by trypsinization (see section I), resuspended in 2 ml of freezing medium (90% FBS + 10% DMSO) and divided into two cryo-tubes. These were stored in a Mr. Frosty (see "Materials") at -80 ºC for up to 48 h and then transferred to liquid nitrogen for long-term storage.

To thaw the cells, cryo-tubes were placed in a waterbath at 37 ºC. In order to minimize their exposure to the DMSO present in the freezing medium, cell suspensions were quickly transferred to conical tubes containing 5 ml of pre-warmed growth medium and pelleted by centrifuging at 200 xg for 5 min. Supernatants were discarded and cell pellets were resuspended in fresh growing medium and plated into new culture dishes.

IV. Cell treatments

Antioxidants

100 mM GSH and NAC (see "Materials") were directly diluted in the media of growing cells to reach a final concentration of 5 mM. Cells were preincubated for 1 h with a mixture of both before the final treatments.

Chemical inhibitors

Cells were preincubated for the times indicated in the figures with the following inhibitors, which were stored in aliquots at -20 ºC:

Inhibitor	Target pathway	Stock concentration	Final concentration
ASK1 inhibitor	ASK1	10 mM (in DMSO)	10 μM
DPI	NADPH oxidases	10 mM (in DMSO)	2.5 μM
LY294002	PI3K	20 mM (in DMSO)	20 μM
Rapamycin	p70 S6 kinase	100 μM (in ethanol)	50 nM
Rotenone	m.r.c.* complex I	5 mg/ml (in DMSO)	0.25 μg/ml
SB203580	p38 α/β MAPK	10 mM (in DMSO)	10 μM
SP600126	JNK	20 mM (in DMSO)	20 μM
U0126	MEK1/2	10 mM (in DMSO)	10 μM

**m.r.c.: mitochondrial respiratory chain*

Cisplatin

This is a small-molecule platinum compound that exerts its anti-tumoral properties by creating platinum-DNA adducts, which primarily form intra-strand cross-links that activate the apoptotic pathway, resulting in cell death. Treatments were done for the indicated times with the concentrations specified below. The stock was 1.66 mM in physiological saline and it was stored at RT:

· For apoptosis assays, cells were treated with 100 μM cisplatin.

· For clonogenic assays, cells were treated with 10 μM (SW620) or 50 μM (MCF7 and HT-29) cisplatin.

Doxorubicin

This is an anthracycline antibiotic used in cancer chemotherapy that works by intercalating DNA. Cells were treated with 1 μM doxorubicin (from a 10 mM stock in PBS stored at 4 ºC).

Etoposide

This drug is a topoisomerase inhibitor that forms a ternary complex with DNA and the topoisomerase II enzyme, preventing re-ligation of the DNA strands and therefore inducing their breakage. In the end it induces apoptosis of the cancer cell and therefore it is used as a cytotoxic agent. Cells were treated with 100 μM etoposide (from a 100 mM stock in DMSO stored at -20 ºC).

Hydrogen peroxide

This is a strong oxidizer used as a positive control for the generation of ROS. Cells were treated for the indicated times with 5 mM from an 8.8 M stock stored at 4 ºC.

Neocarzinostatin

This is a genotoxic drug that induces single and double strand breaks in DNA. It can be used as a positive control to induce histone H2AX phosphorylation. Cells were treated with 40 nM NCS for 1 h from a 20 mM stock stored at 4 ºC.

Ultraviolet radiation

This type of light induces thymine dimers as well as DNA double strand breaks. Cells were washed with PBS, covered with a thin PBS layer (1 ml every 60 mm ∅ dish), irradiated with 400 J/m^2 of UV light and incubated at 37 ºC for the indicated times.

Mice treatments

MMTV-PyMT mice (Guy et al., 1992) were provided by William Muller (McGill University, Canada). Female mice expressing MMTV-PyMT spontaneously develop breast tumors with 100% penetrance. When breast tumors reached a size of 200 mm^3 [$V=(\pi*l)*w^2$], mice were given a single injection of 6 mg/Kg cisplatin or vehicle (physiological saline) in the tail vein. The p38 MAPK inhibitor PH797804 (Hope et al., 2009) was prepared at 1 mg/ml in 0.5% methyl cellulose (in PBS) and 0.025% Tween-20 and administered to the mice by oral gavage (10 mg/Kg) every 24 h. Groups of at least four mice (each of them developing from two to four tumors) were used per condition in every experiment.

mRNA processing and PCR analysis

I. RNA isolation and purification

Total RNA was extracted from cells using the RNA Mini Kit from Ambion and was digested with DNase I as follows:

1. Add 1 µl of DNase I to the RNA and incubate for 1 h at 37 ºC (50 µl RNA + 40 µl RNase-free water + 10 µl buffer 10x + 1 µl DNase I)

2. Add, in the hood, 100 µl of phenol:chloroform and mix by vortexing

3. Centrifuge at 16000 xg for 5 min at 4 ºC

4. Take the upper phase (colorless, ~70 µl) and add 1/10 of sodium acetate 3 M (7 µl) and 1 µl of glycogen

5. Add 2.5 volumes of ice-cold 100% ethanol (195 µl)

6. Keep for 1 h at -80 ºC

7. Centrifuge at 16000 xg for 10 min at 4 ºC and remove the supernatant

8. Wash with 1 ml of 70% ethanol (vortex)

9. Centrifuge at 16000 xg for 5 min at 4 ºC

10. Discard the supernatants and leave the tubes opened for 10 min so ethanol can evaporate

11. Resuspend in 30 µl RNase-free water

12. Determine the RNA concentration by measuring the absorbance at 260 nm and its quality by monitoring the ratio of absorbance 260/280

II. Reverse transcription PCR

cDNA was obtained from 1 µg of the purified RNA following exactly the SuperScript II Reverse Transcriptase protocol from Invitrogen in a final volume of 20 µl.

III. Semi-quantitative PCR

The mix for one reaction of 50 µl was prepared as follows:

32 µl H_2O	2.5 µl 10 µM primer 3'
5 µl buffer 10x	1 µl 10 mM dNTPs
1.5 µl 50 mM $MgCl_2$	5 µl cDNA (diluted 1/5)
2.5 µl 10 µM primer 5'	0.5 µl 500U Taq polymerase

The program (denaturation at 94 ºC for 5 min, 20 - 30 cycles of denaturation at 94 ºC for 30 s, annealing at 55 ºC for 30 s, elongation at 72 ºC for 60 s and a final step of elongation at 72 ºC for 10 min) was run. *GAPDH* gene expression was used as a reference and the PCR products were analyzed by 2.5% agarose gel electrophoresis.

IV. qRT-PCR

The mix for one reaction of 10 µl was prepared as follows:

0.25 µl 10 µM primer 5′

0.25 µl 10 µM primer 3′

0.5 µl H_2O

5 µl Sybr Green Supermix

4 µl of cDNA (diluted 1/12) were loaded in triplicates in a 96-well plate and 6 µl of the mix reaction were added. The plate was sealed and centrifuged for 1 min at 200 xg and run as follows: 50 ºC for 2 min, 95 ºC for 10 min, 40 cycles of denaturation at 95 ºC for 15 s, annealing at 56 ºC for 15 s, elongation at 72 ºC for 60 s, and three final steps of 95 ºC for 15 s, 60 ºC for 2 min and 95 ºC for 15 s. *GAPDH* and *HMBS* were used as reference genes and the ΔΔC(t) method was used to quantify gene expression.

MTT assay

This assay is based on the cleavage of the yellow tetrazolium salt MTT to purple formazan crystals by metabolic active cells. These crystals are solubilized and the resulting colored solution is quantified using a 96 well plate spectrophotometer-reader. The intensity of absorbance is directly proportional to the number of metabolic active cells. Therefore, it can be used either to monitor the proliferation of cells or to measure the number of viable cells after a cytotoxic insult. For proliferation assays, 2000 cells/well were plated and different time points were measured up to 6 days. For viability assays, 10000 cells/well were plated and the percentage of viable cells was determined at the end of the experiment. In both cases, the metabolic active cells were measured as follows:

1. Add 10 µl of MTT reagent to cells growing in triplicates in 96-well plates with 100 µl of medium and incubate for 1 h at 37 ºC

2. Remove the medium, add 200 µl of DMSO and incubate shaking at RT for 15 min so the crystals are completely solubilized

3. Read the absorbance between 550 and 600 nm setting a reference wavelength above 650 nm

Oxyblot analysis

As a consequence of the oxidative modifications, carbonyl groups are introduced into protein side chains by a site-specific mechanism. This kit provides reagents for immunodetection of these carbonyl groups (after a derivatization reaction with DNPH), which is a hallmark of the oxidation status of proteins.

1. Transfer 10 µg of protein sample contained in a volume of 5 µl into each two 1.5 ml tubes (one of the aliquots will be subjected to the derivatization reaction and the other will serve as a negative control).

2. Denature each 5 µl aliquot of protein by adding 5 µl of 12% SDS for a final concentration of 6% SDS

3. Derivatize the sample by adding 10 µl of 1x DNPH solution to one of the tubes. To the aliquot designated as the negative control, add 10 µl of 1x Derivatization-Control solution instead of the DNPH solution

4. Incubate both tubes at RT for 15 min

5. Add 7.5 µl of Neutralization Solution to both tubes and add 1 µl of ß-mercaptoethanol to the sample mix.

Both the treated sample and the negative control are now ready to load into a polyacrylamide gel and be transferred to a membrane for further immunodetection, following manufacturer's instructions.

Phosphatase assays:

- JNK targeted-phosphatases activity

I. Hot phosphorylation of GST-JNK1

1. Prepare the kinase buffer

2. Prepare protein mixes with a ratio 1:10 (kinase:substrate) in a V_f = 144 µl

26.8 µl GST-JNK1 (4.5 µg/µl)

24.0 µl GST-MKK7 (0.5 µg/µl)

9.2 µl KiB

84.0 µl ATP (2.4 µl 10 mM + 2 µl ^{32}P-γ-ATP (10 µCi/µl, Perkin Elmer) + 79.6 µl KiB)

3. Incubate for 1 h at 30 ºC with light shaking

4. Stop the reaction by freezing the samples

II. GST-^{32}P-JNK1 pull down

1. Prewash (2x) 100 µl Glutathione Sepharose beads with 1 ml PBS containing protease inhibitors (PBS-PI) at 500 xg for 2 min at 4 ºC

2. Incubate the prewashed beads and the protein with PBS-PI for 2 h at 4 ºC and rotating (up to 500 µl) 100 µl beads + 144 µl GST-JNK1 (i.e. 120 µg) + 256 µl

3. Recover the protein bound to the beads by centrifuging at 200 xg for 6 min at 4 ºC. Take the supernatant with a 0.3 mm needle

4. Wash (2x) with PBS-PI: up to 1 ml, at 200 xg for 3 min at 4 ºC

5. Wash (1x) with phosphatase buffer, up to 1ml, at 200 xg for 3 min at 4 ºC

6. Resuspend in 240 µl of phosphatase buffer (~0.05 µg/µl of GST-JNK1)

III. Phosphatase assay

1. Collect and quantify the human cancer cells (treated or not with 10 µM SB203580) in phosphatase buffer. For the negative control, add phosphatase inhibitors to the phosphatase buffer (20 mM NaF, 10.4 mM NaVO, 1 µM microcystine)

2. Mix 100 µg of cell lysates with ~0.5 µg of GST-^{32}P-JNK1 (from the previous pull down) and incubate them at 37 ºC for the desired time points (5 - 30 min) with light shaking. Stop the reaction by adding LSB5x

Vf ~65 µl	**SW620**	**SW620 SB**
µl lysate (100 µg)	25.8	31.1
µl P-GST-JNK1 (0.5 µg)	10	10
µl PhB	16.2	10.9
µl LSB5x	13	13

- Ser/Thr or Tyr specific phosphatase activity

To measure these phosphatase activities, we used two different phosphatase assays from Promega. These systems determine the amount of free phosphate generated in a reaction by measuring the absorbance of a molybdate:malachite green:phosphate complex. They include chemically synthesized Ser/Thr- or Tyr-phosphorylated peptides that are dephosphorylated by cell lysates. Generic Tyr

and Ser/Thr phosphatase activity was measured following manufacturer's instructions (Fig. 15). Briefly, reactions were performed in 50 µl of volume containing 5 µg of phospho-peptide and 750 µg of cell lysate in 50 mM Tris pH 7.5, 250 mM NaCl and 0.1 mM DTT buffer. After incubation at 30ºC for the indicated times, the reaction was stopped by addition of 50 µl molybdate dye and absorbance was measured at 630 nm.

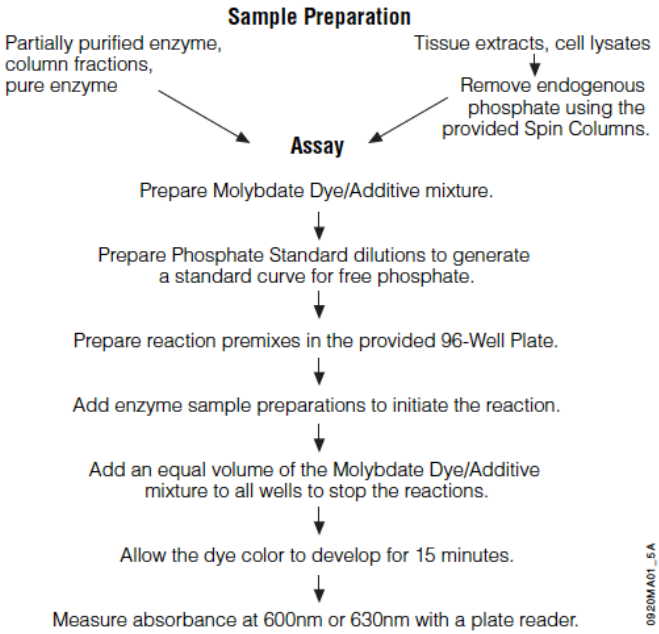

Figure 15. Overview of the phosphatase assays from Promega. The protocol was used to measure phosphatase activity from cell lysates.

Protein extraction and quantification

I. Protein extraction from cell lines

1. Frozen dishes containing sub-confluent grown cells are thawed on ice, scrapped in ~100 µl of lysis buffer and transferred to a 1.5 ml tube. (If cells are already pelleted, directly add the lysis buffer onto the pellets).

2. Vortex the cell lysates and keep on ice for 15 min (vortex every 5 min). To detect γ-H2AX, it is necessary to sonicate the cell lysates

3. Centrifuge at 16000 xg for 15 min at 4 ºC

4. Quantify the supernatants

II. Protein extraction from mouse tissues

1. Immerse breast tumors resected from mice in a suitable volume (~500 – 1500 µl) of ice-cold tissue lysis buffer

2. Mechanically disrupt the tumors in a Precellys apparatus (Bertin Technologies)

3. Vortex the tissue lysates and keep on ice for 15 min (vortex every 5 min)

4. Centrifuge at 16000 xg for 15 min at 4 ºC

5. Quantify the supernatants

III. Determination of protein concentration

The BioRad DC Protein Assay Reagents (based on the method of Lowry) were used as follows to measure protein concentrations:

1. Place 2 µl of every lysate into a 96-well plate, in duplicates

2. Mix in a 1.5 ml tube 10 µl of Reagent S and 500 µl of Reagent A

3. Add 25 µl of the previous mixture to every 2 µl of lysate

4. Add 200 µl of reagent B

5. Read absorbance at 750 nm and compare to a BSA calibration curve

Resazurin assays

Resazurin is a blue non-fluorescent dye until it is reduced to the highly red fluorescent product resofurin. It is used as an oxidation-reduction indicator in cell viability assays. At the end of the treatments, media from cells was replaced by fresh media containing 10 mg/l Resazurin (from a 1 g/l stock in PBS) and incubated for 4 h at 37 ºC. Fluorescence was measured using 530 nm excitation and 590 nm emission wavelengths.

ROS detection

DCFDA is a cell permeable nonfluorescent probe until its oxidation occurs within the cell. Esterase cleavage of the lipophilic blocking groups yields a charged form of the dye that is much better retained by cells than the parent compound. Oxidation of this probe was detected by monitoring the increase in fluorescence with a flow cytometer using excitation filters appropriate for fluorescein (FITC).

To visualize intracellular ROS levels, subconfluent cells were incubated for 30 min

at 37ºC with 10 µM DCFDA. Then cells were trypsinized with the minimum possible amount of trypsin and resuspended in 1 ml PBS with 1.4 µg/ml aprotinin. Cells were counter-stained using propidium iodide and analyzed by flow cytometry using the FlowJo software.

Statistical analysis

For ROS measurements, *p*-values were calculated using an unpaired two-tailed Student's *t*-test, under the null hypothesis that the mean is equal to zero. For mouse tumor sizes, we compared each treatment (p38 inh. and CDPP) with the double therapy (p38 inh. + CDPP) using a two-way ANOVA and applied the Bonferroni correction. $p<0.05$ was considered statistically significant.

TUNEL

This kit identifies DNA strand breaks generated during the apoptotic process by terminal deoxynucleotidyl transferase (TdT), which catalyzes polymerization of labeled nucleotides to free 3'-OH termini with modified nucleotides in an enzymatic reaction. Manufacturer's instructions (Roche) were followed exactly.

Results

To determine whether p38α could be considered as a therapeutic target in cancer, we followed two different approaches: (i) to look for synthetic lethal partners of p38 MAPK and (ii) to study whether its inhibition could synergize with chemotherapeutic agents to induce cancer cell death.

(i) Synthetic lethal partners of p38 MAPK in cancer cell viability

Two genes are considered to be synthetically lethal if mutation of either alone is compatible with cell viability but mutation of both leads to cell death (Kaelin, 2005). The concept of synthetic lethality applied to cancer therapy was proposed as a promising alternative to the unspecific and aggressive chemotherapeutic treatments in some types of cancer. There are already remarkable results using this approach, such as the use of poly(ADP-ribose) polymerase (PARP) inhibitors to treat BRCA-mutated breast tumors (Fong et al., 2009).

1. p38 MAPK is not a synthetic lethal partner of ERK1/2, mTOR or PI3K pathways

With the aim of finding synthetic lethal partners of p38 MAPK, we started by combining its inhibition with that of other relevant pathways for cancer cell survival, such as ERK1/2 and mTOR. We measured apoptosis by detecting the released DNA oligonucleosomes in U2OS cancer cells and found that there was an additive effect in the induction of programmed cell death when combining the inhibition of p38 MAPK and ERK1/2 pathways, but the effect was modest compared with a positive control provided by the kit (**Fig. 16A**). We then thought we might be able to see a bigger effect after cytotoxic challenging of the cells, so we treated them with cisplatin and doxorubicin, which are two chemotherapeutic agents used in the clinic for cancer treatment. A synergistic effect was not observed in any of the cases, but the differences in apoptosis among the various treatments became more apparent, maintaining the previously observed additive effect of inhibiting both p38 MAPK and ERK1/2 pathways (**Fig. 16B**).

Besides apoptosis, we decided to check the viability of the cancer cells using resazurin, a compound that becomes fluorescent when the cells metabolize it, indicating the number of alive cells. We also checked the effect of inhibiting the

PI3K pathway in both U2OS and HeLa cancer cells. As expected, cell viability was not significantly reduced in basal conditions after inhibition of the kinase pathways (**Fig. 17A**), and after treatment with cisplatin or doxorubicin these differences were increased, although never reached a synergizing effect (**Fig. 17B**).

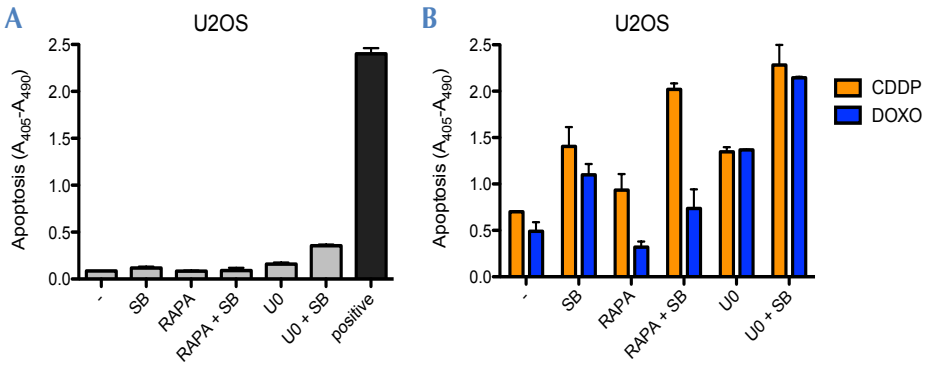

Figure 16. Inhibition of p38 MAPK together with the ERK1/2 pathway has additive effects inducing apoptosis in U2OS cancer cells. Apoptosis was measured with the Cell Death Detection ELISA kit from Roche. **(A)** U2OS cells were incubated with SB203580 (SB), rapamycin (RAPA) and U0126 (U0), alone or in combination with SB203580, overnight. "Positive" is an internal positive control of the kit. **(B)** U2OS cells were incubated with SB203580, rapamycin, U0126, alone or in combination with SB203580, overnight followed by cisplatin (CDDP) or doxorubicin (DOXO) treatment for 8 h.

It was really striking that inhibition of only the p38 MAPK pathway sufficed to reduce viability of the cancer cells after the cytotoxic treatments, so we decided to further characterize this observation, which will be addressed in the second part of the "Results" section.

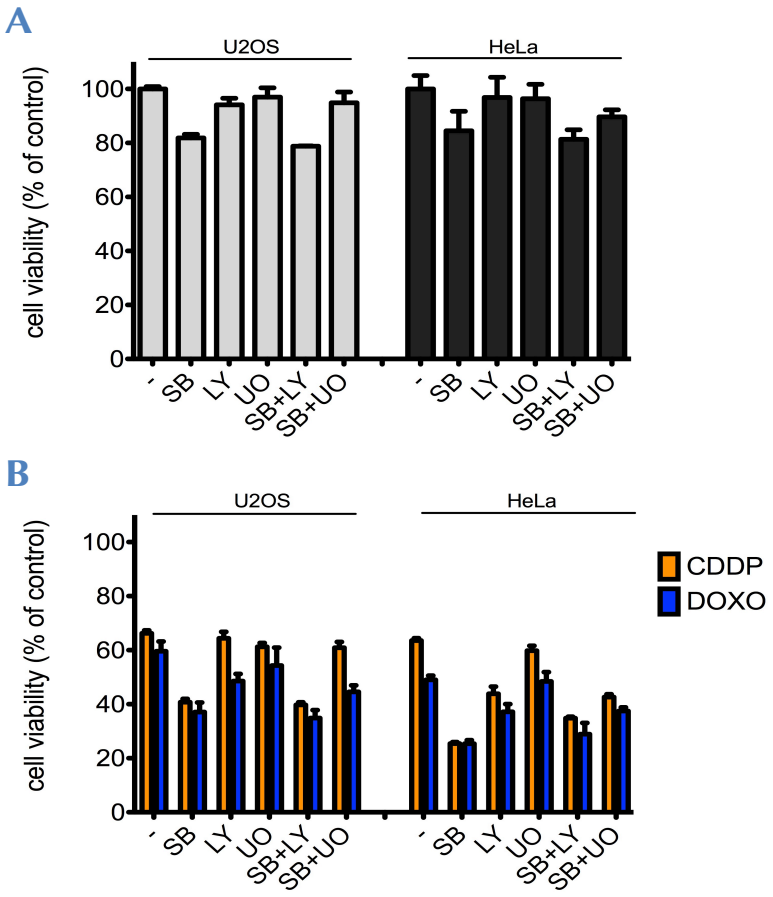

Figure 17. The combined inhibition of p38 MAPK and ERK1/2 or PI3K pathways do not synergize to reduce cancer cell viability. **(A)** U2OS and HeLa cancer cells were incubated with SB203580 (SB), LY294002 (LY) and U0126 (U0), alone or in combination with SB203580, overnight. **(B)** U2OS and HeLa cancer cells were incubated with SB203580, LY294002, U0126 (alone or in combination with SB203580) overnight followed by cisplatin (CDDP) or doxorubicin (DOXO) treatment for 8 h. Cell viability was measured with the resazurin assay.

2. Potential synthetic lethal interactions between eEF2 kinase and p38 MAPK in response to cisplatin treatment

Since the previously tested kinase pathways were not synthetic lethal partners of p38 MAPK, we performed a screening to analyze 84 chemical inhibitors that target 36 different cell signaling pathways (**Suppl. Fig. 1** and **Suppl. Table 1**). Based on experiments from **figures 16-17**, we anticipated that we would see bigger changes in cell survival under cytotoxic conditions, so we decided to compare control cells

with cells incubated with SB203580, both treated with cisplatin. We also decided to take into account the possible role of p53, so we used for the screening both the HCT116 colon cancer cell line and its derivative that lacks p53 expression (p53 KO). First, we confirmed that both cell lines responded to the chemotherapeutic agents cisplatin, doxorubicin and etoposide, and also observed that inhibition of p38 MAPK further reduced cell viability (**Fig. 18**).

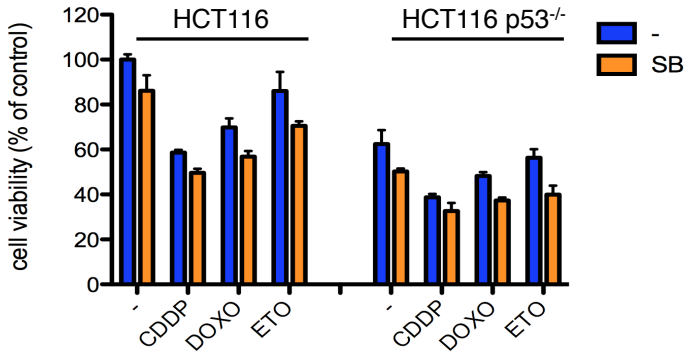

Figure 18. p38 MAPK inhibition reduces the viability of HCT116 WT and p53 KO cancer cells upon cytotoxic insults. HCT116 and HCT116 p53 KO cells were pre-incubated with SB203580 (SB) for 2 h followed by treatment with cisplatin (CDDP), doxorubicin (DOXO) or etoposide (ETO) for 15 h. Cell viability was measured with the resazurin assay.

Therefore, we performed the screening in both p53 WT and KO HCT116 cell lines measuring cell viability with resazurin after cisplatin treatment, in the presence or absence of SB203580, as explained above. We did the screening twice, plating either 10000 or 20000 cells per well, and after calculating the fold changes of cell viability relative to the cells where p38 MAPK was inhibited (primary data are provided in **Suppl. Figures 2-3**), we observed that the combined inhibition of the eEF2 kinase pathway together with that of p38 MAPK, reduced around two fold the cell viability in p53 WT cells (**Fig. 19**). Based on these data, although further characterization of this observation needs to be done, the eEF2 kinase can be considered as a putative synthetic lethal partner of p38 MAPK.

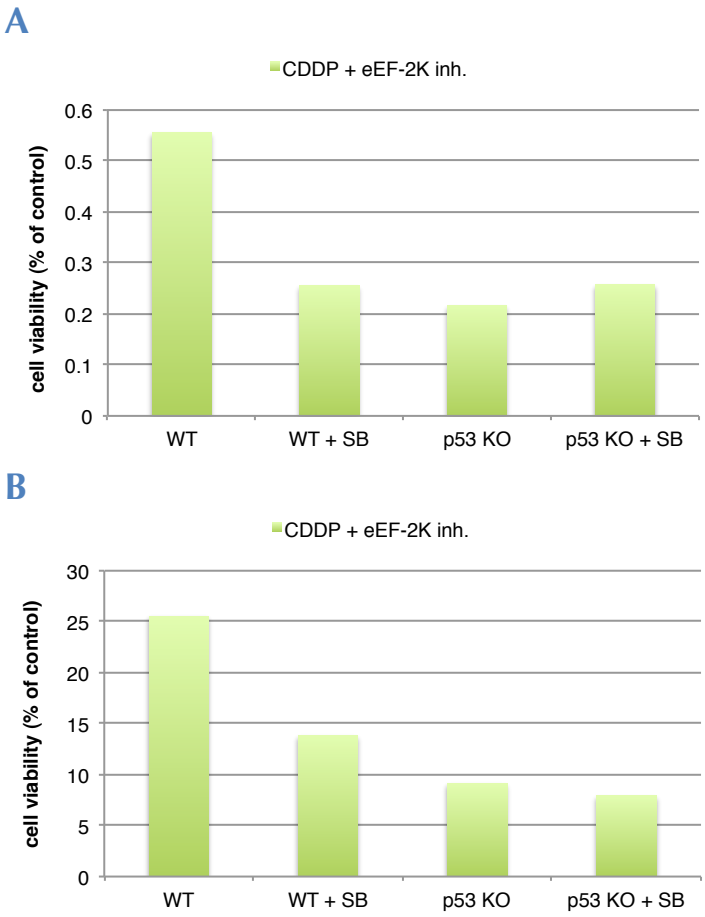

Figure 19. Inhibition of eEF2-kinase signaling cooperates with the inhibition of p38 MAPK to reduce cancer cell viability. Fold survival relative to untreated cells is represented. 10000 **(A)** or 20000 **(B)** HCT116 p53 WT (WT) and p53 KO (KO) cells per well were plated in the presence or absence of SB203580 (SB).

Ours results indicate that the eEF2 kinase pathway might function as a synthetic lethal partner of p38 MAPK only in p53 WT cells, since there was not a significant change in cell viability in HCT116 p53 KO cells. Nonetheless, we still need to properly characterize the role of eEF2 kinase as a putative synthetic lethal partner of p38 MAPK in response to cisplatin treatment. It is necessary to use genetic tools to specifically deplete both kinases and make sure the inhibitors are not affecting other related pathways. Furthermore, it would be interesting to know whether all p38α is the main isoform involved or whether others have a role as well.

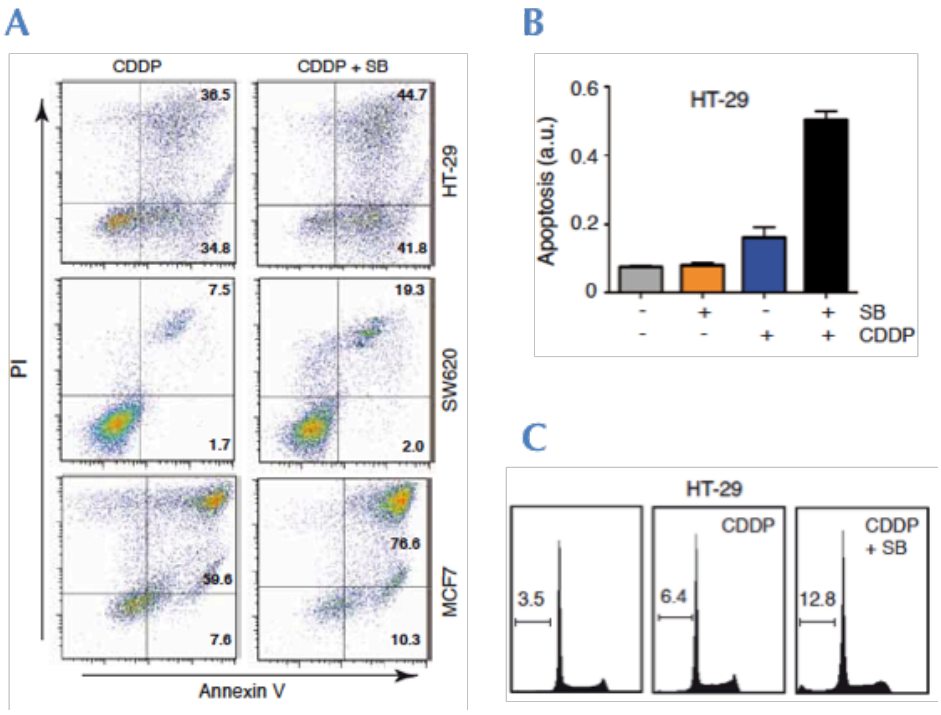

Figure 20. Inhibition of p38 MAPK sensitizes cancer cells to apoptosis upon cytotoxic insults. (A) HT-29, SW620 and MCF7 cells were incubated with SB203580 (SB) for 2 h followed by treatment with cisplatin (CDDP) for 24 h, and then they were stained with PI and Annexin V. The percentages of apoptotic cells are indicated. **(B)** HT-29 cells were incubated with SB203580 O/N followed by cisplatin for 8 h, as indicated. Apoptosis was measured with the Cell Death Detection kit ELISA PLUS. **(C)** HT-29 cells were treated as in (A) and the apoptotic sub-G0/G1 population was quantified by flow cytometry.

(ii) Sensitization to chemotherapy by p38α inhibition

1. Inhibition of p38 MAPK signaling sensitizes cancer cells to apoptosis

While looking for synthetic lethal partners of p38 MAPK, we realized that inhibition of this pathway reduced human cancer cell viability when combined with a chemotherapeutic agent (**Figs. 16-18**). To determine the role of p38 MAPK signaling in the survival of cancer cells exposed to chemotherapeutic agents, we treated human breast and colon cancer cells with cisplatin together with SB203580. Then we monitored apoptosis by different techniques. Annexin V staining revealed that the combination of cisplatin with SB203580 significantly potentiated the induction of apoptosis in both colon and breast cancer cells when

compared with the treatment of cisplatin alone (**Fig. 20A**). We confirmed this finding in HT-29 colon cancer cells by measuring the release of DNA oligonucleosomes (**Fig. 20B**) or by quantifying the percentage of cells that were in the subG0/G1 phase of the cell cycle (**Fig. 20C**).

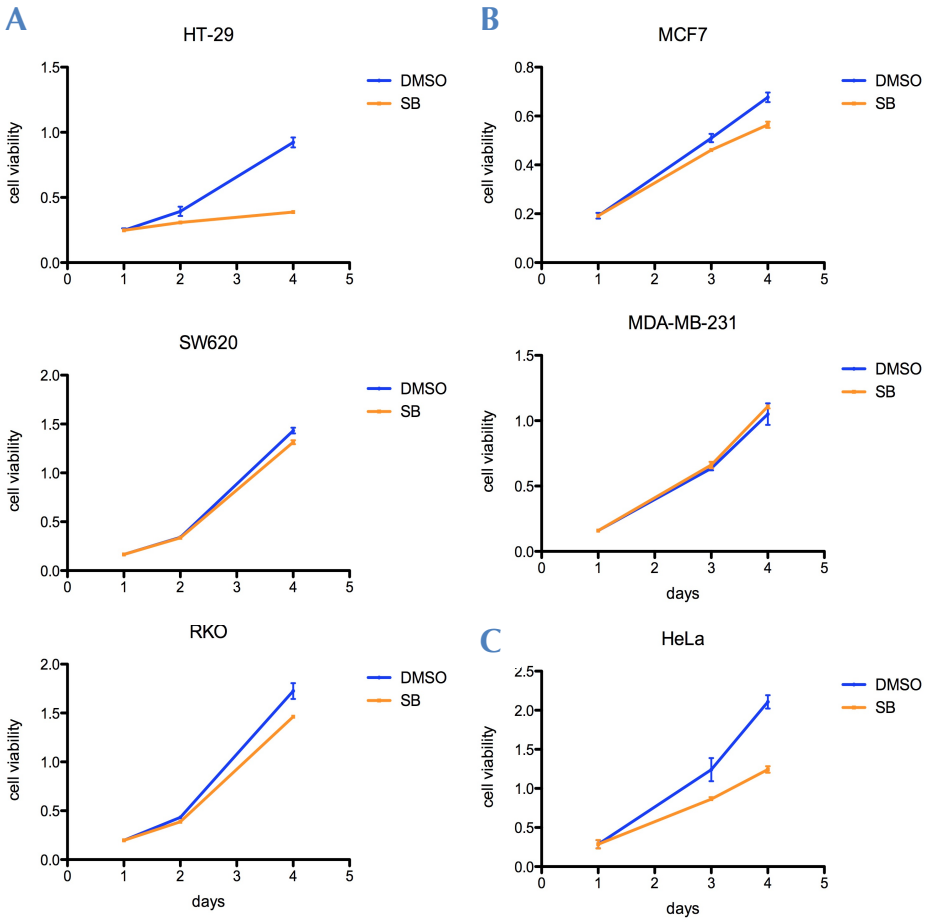

Figure 21. p38 MAPK might be necessary for the basal proliferation of some cancer cells. A panel of human colon **(A)**, breast **(B)** or cervix **(C)** cancer cell lines was grown in the presence of absence of the p38 MAPK inhibitor SB203580 and monitored for four days. Cell viability was assed by the MTT assay.

2. Regulation of apoptosis by p38 MAPK does not correlate with its role in cancer cell proliferation

p38 MAPK might have a role in the proliferation of some human cancer cells, such as HT-29, RKO, MCF7 and HeLa cells (**Fig. 21**). We have shown that some of these cancer cells (HT-29, SW620, MCF7, HeLa) are sensitized to apoptosis after p38 MAPK inhibition. Interestingly, sensitization to apoptosis seems to be independent of the implication of p38 MAPK in cell proliferation as shown in **figure 21** or of the p53 status in the cels (**Table 2**).

Table 2. Molecular features of selected human cancer cell lines

Cell line	Organ	Disease	p53 status	ER
HeLa	Cervix	Adenocarcinoma	Low expression	N/A
HT-29	Colon	Adenocarcinoma	Mutated	N/A
MCF7	Breast	Adenocarcinoma	WT	Expressed
MDA-MB-231	Breast	Adenocarcinoma	Mutated	Not expressed
RKO	Colon	Carcinoma	WT	N/A
SW620	Colon	Adenocarcinoma	Mutated	N/A

Moreover, incubation with SB203580 for up to four days did not induce DNA damage, as measured by γ-H2AX staining in both colon and breast by immunoblotting (**Fig. 22**).

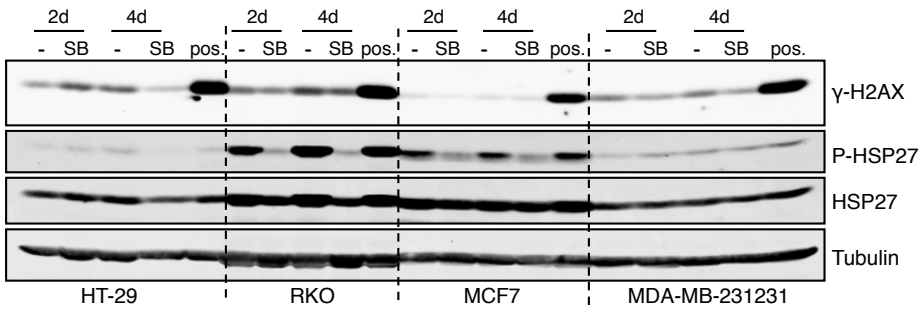

Figure 22. Inhibition of p38 MAPK does not cause DNA damage. Cancer cells were incubated with SB203580 (SB) for 2 or 4 days ("2d" and "4d", respectively) and treatment with neocarcinostatin was used as a positive control ("pos."). The indicated antibodies were detected in total cell lysates by immunoblotting.

3. Inhibition of p38 MAPK upregulates the JNK pathway, which sensitizes to apoptosis

Several studies indicate that p38 MAPK signaling can negatively regulate the JNK pathway in different cell contexts, mainly in non-transformed cells (Perdiguero et al., 2007b; Wagner and Nebreda, 2009). Since JNK signaling plays an important role in apoptosis induction (Davis, 2000), we investigated whether the JNK pathway was implicated in the enhanced apoptosis observed in cisplatin-treated cancer cells upon p38 MAPK inhibition. We found that inhibition of p38 MAPK signaling with SB203580, as shown by the reduced phosphorylation of its downstream target Hsp27, resulted in enhanced phosphorylation of the JNK substrate c-Jun in three different human cancer cell lines from breast or colon origin (**Fig. 23A**). It has been reported that the JNK pathway is an important mediator of cisplatin effects (Brozovic and Osmak, 2007). Accordingly, the JNK chemical inhibitor SP600125 impaired the enhanced apoptosis observed in cisplatin-treated cancer cells when p38 MAPK was inhibited, as determined by the reduced levels of processed p85PARP, which is one of the fragments released when PARP is cleaved by caspases during programmed cell death. (**Fig. 23B**). These results indicate a functional interplay between both signaling cascades in cancer cells, with the JNK pathway mediating the enhanced apoptosis induced by cisplatin upon p38 MAPK inhibition.

To exclude possible off-target effects of the chemical inhibitors, we used RNAi to downregulate the expression of p38α. We confirmed that siRNA-mediated depletion of p38α mimicked the effect of the SB203580 inhibitor and enhanced JNK phosphorylation (**Fig. 24A**). Moreover, siRNA or shRNA-mediated downregulation of p38α increased the levels of cisplatin-induced apoptosis in both breast and colon cancer cells (**Figs. 24B-C**). Processed p85PARP was increased when MCF7 cells were incubated with siRNA of p38α compared with the scrambled siRNA (control) and this correlated with higher phosphorylation of JNK (**Fig. 24B**). Moreover, the subG0/G1 population of SW620 was increased when p38α was depleated by shRNA compared to the non-targeting shRNA used in control cells (**Fig. 24C**). Recapitulation of the effects observed with SB203580 by

genetic downregulation of p38α indicates that this p38 MAPK family member is a major contributor to the observed functional interplay.

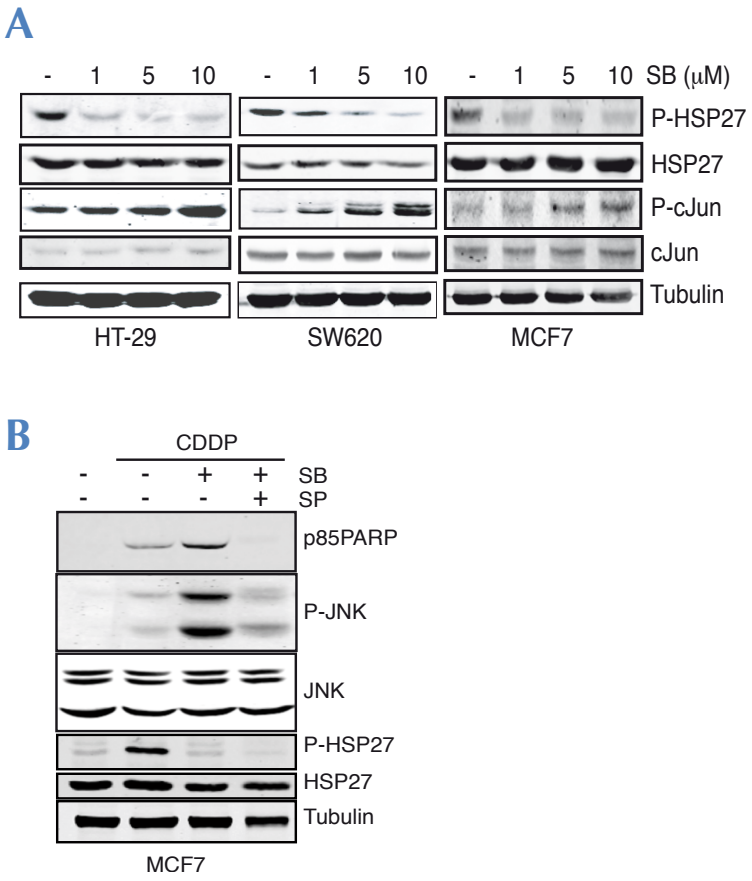

Figure 23. p38 MAPK inhibition in cancer cells upregulates the JNK pathway and sensitizes to apoptosis. Total cell lysates were analyzed by immunoblotting with the indicated antibodies. **(A)** HT-29, SW620 and MCF7 cells were treated with increasing concentrations (1-10 μM) of SB203580 (SB) for 6 h. **(B)** MCF7 cells were incubated O/N with 10 μM SB203580, alone or in combination with 20 μM SP600125 (SP) for 1 h, followed by 8 h treatment with cisplatin (CDDP).

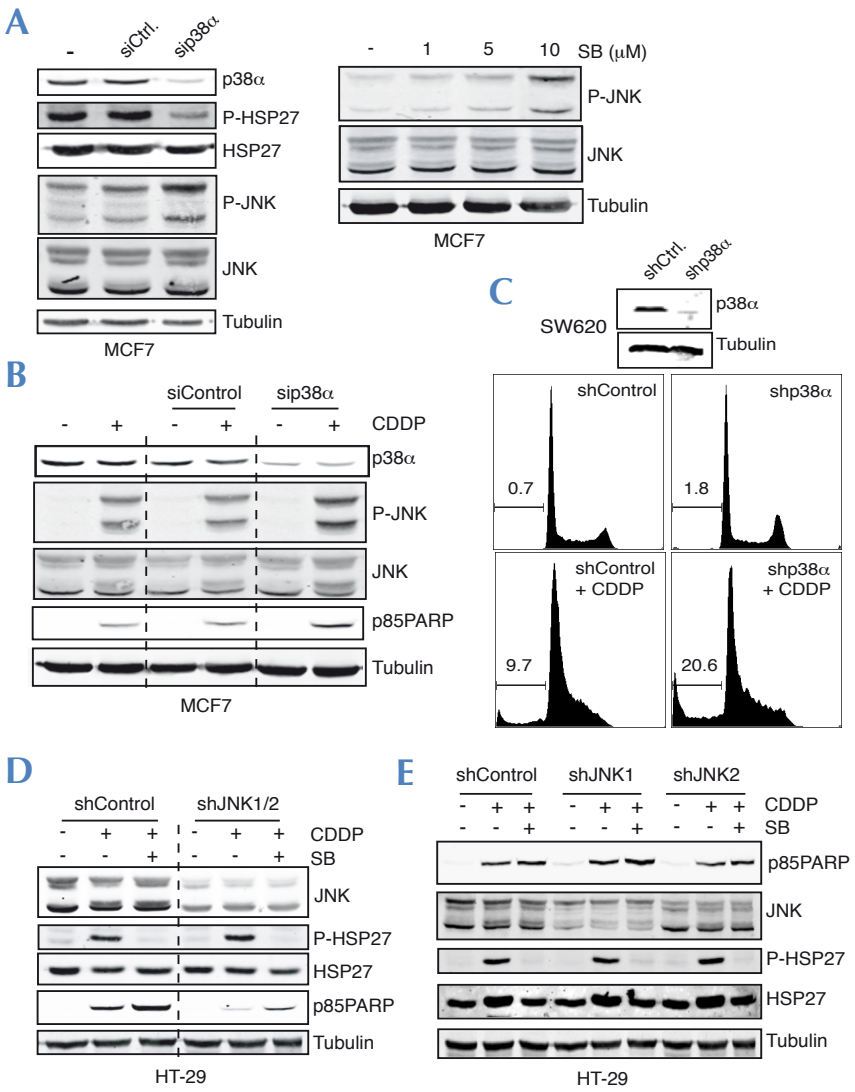

Figure 24. p38α downregulation activates JNK and increases apoptosis in cancer cells treated with cisplatin. Total cell lysates were analyzed by immunoblotting with the indicated antibodies. **(A)** MCF7 cells were incubated with p38α siRNA (sip38α, 50 nM for 48 h) or treated with increasing concentrations of SB203580 (1-10 μM). A scrambled siRNA (siCtrl.) was used as a negative control. **(B)** MCF7 cells were incubated with p38α siRNA or siControl as in (A) and then treated for 8 h with cisplatin. **(C)** SW620 cells were infected with lentiviruses expressing shRNAs against p38α (shp38α) or a non-targeting control (shControl). After one week of puromycin selection, pools of cells were treated for 24 h with cisplatin and the apoptotic subG0/G1 population was quantified by flow cytometry and indicated by a solid line. **(D)** HT-29 cells were infected with shRNAs against JNK1 and JNK2 (shJNK1/2) or a non-targeting control (shControl). After one week of puromycin selection, pools of cells were incubated overnight in the presence or absence of SB203580

and then treated for 8 h with cisplatin. **(E)** HT-29 cells were infected with lentiviruses expressing shRNAs against JNK1 (shJNK1) and JNK2 (shJNK2) or a non-targeting control (shControl), as indicated. After one week of puromycin selection, pools of cells were treated as in (D).

Next, we used shRNAs to downregulate JNK1 and JNK2, which confirmed a key role for this signaling pathway as a mediator of the apoptosis induced by cisplatin in cancer cells. Interestingly, the downregulation of JNK1 and JNK2 also decreased the enhanced apoptosis induced by cisplatin when p38 MAPK signaling was inhibited in HT-29 colon cancer cells (**Fig. 24D**). In contrast, the independent downregulation of only JNK1 or JNK2 did not significantly affect cisplatin-induced apoptosis in cancer cells (**Fig. 24E**). These results indicate that JNK1 and JNK2 are both involved in the sensitization to cisplatin-induced cell death upon p38α inhibition.

4. Increased ROS levels mediate JNK activation and apoptosis sensitization

It has been reported that JNK signaling can be activated by ROS (Shen and Liu, 2006) and high endogenous ROS levels have been correlated with activation of the JNK pathway in human cancer cells (Dolado et al., 2007). There is also evidence that p38 MAPK signaling can sometimes impair ROS accumulation (Gutierrez-Uzquiza et al., 2012) and p38α downregulation has been associated with an oxidative stress gene expression signature (Mateescu et al., 2011). We therefore hypothesized that inhibition of p38 MAPK signaling might result in increased ROS levels, which in turn would activate the JNK pathway. We found that inhibition of p38 MAPK signaling with SB203580 produced a modest but consistent increase in the endogenous ROS levels of different human cancer cell lines (**Fig. 25A**). Similar results were observed upon shRNA-mediated downregulation of p38α (**Fig. 25B**), suggesting that this is a key family member to drive the observed effects.

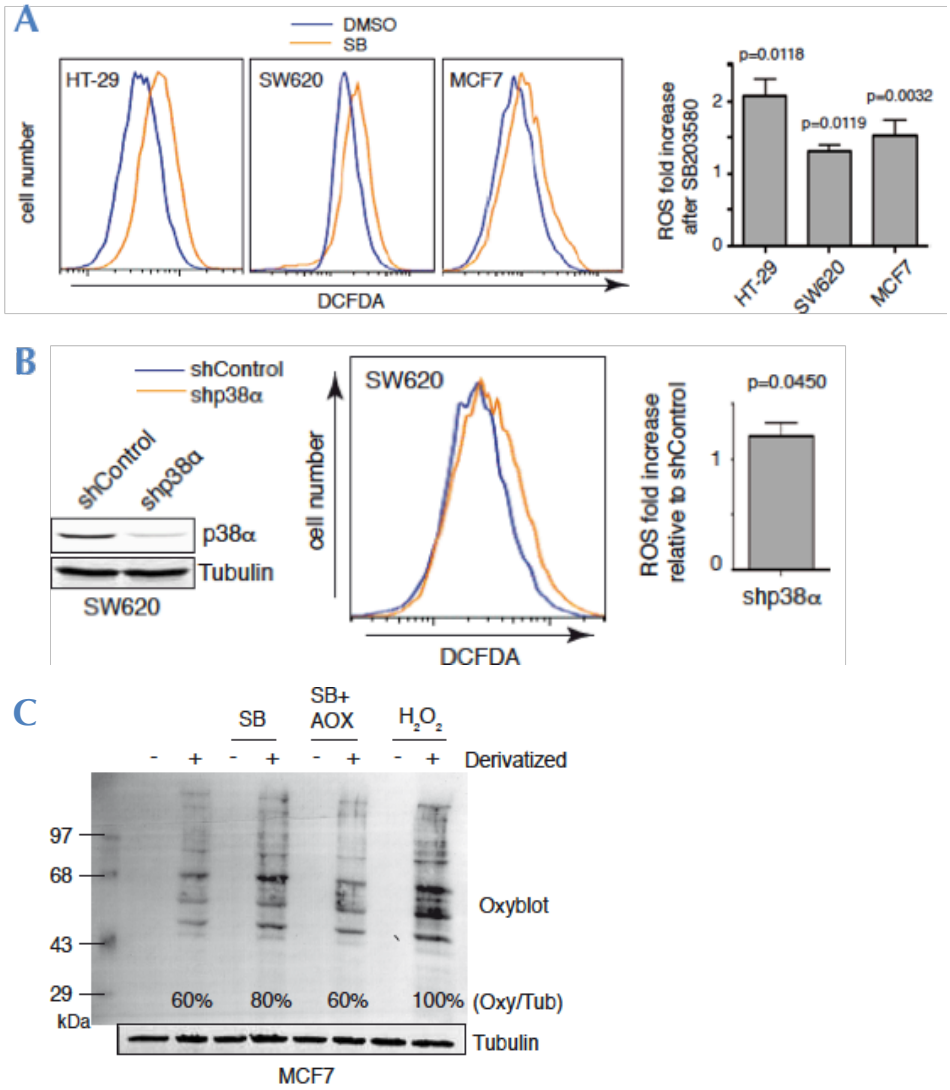

Figure 25. p38 MAPK inhibition increases ROS levels. **(A)** The indicated cancer cells were incubated overnight either with DMSO or SB203580 (SB) and ROS levels were measured with the DCFDA probe by flow cytometry. Fold increase of ROS compared to the control cells is indicated in the bars diagram. **(B)** SW620 cells were infected with lentiviruses expressing shRNAs against p38α (shp38α) or a non-targeting control (shControl). Pools of cells were selected with puromycin for one week and basal ROS levels were measured with DCFDA by flow cytometry. Total cell lysates were analysed with the indicated antibodies. **(C)** MCF7 cells were incubated overnight with SB203580 and pre-treated for 1 h with a mixture of GSH and NAC antioxidants (AOX), or treated with 5 mM H_2O_2 for 1 h, as indicated. Cell lysates were analyzed by immunoblotting using Oxyblot and the total protein oxidation signal per lane was quantified using tubulin as a reference (Oxy/Tub).

To confirm the significance of the observed changes in ROS, we measured the effect of p38 MAPK inhibition on the overall oxidation state of cellular proteins using a chemical derivatization protocol. These experiments showed that the enhanced ROS levels induced by incubation with SB203580 resulted in higher levels of protein oxidation in the cancer cells (**Fig. 25C**).

We then investigated if the enhanced ROS production was linked to cisplatin-induced apoptosis. Certainly, we found that the sensitization to apoptosis produced by p38 MAPK inhibition and JNK upregulation, was rescued by incubation with antioxidants to scavenge ROS (**Fig. 26A**). Importantly, this reduced levels of p85PARP correlated with lower phosphorylation of JNK, confirming that JNK is a main inducer of apoptosis after cisplatin treatment and suggesting that its activation might be related to ROS production. This is also consistent with the observed increased viability of human cancer cells after cytotoxic treatments if they were previously incubated with antioxidants (**Fig. 26B**). The ROS scavengers were able to rescue cell viability almost to the levels of untreated cells. Of note, clonogenic assays confirmed that the reduced apoptosis observed with antioxidants correlated with higher overall survival of the cancer cell population (**Fig. 26C**). Taken together, our results indicate that ROS induced upon p38 MAPK inhibition are responsible for the upregulation of the JNK pathway, which in turn induces apoptosis.

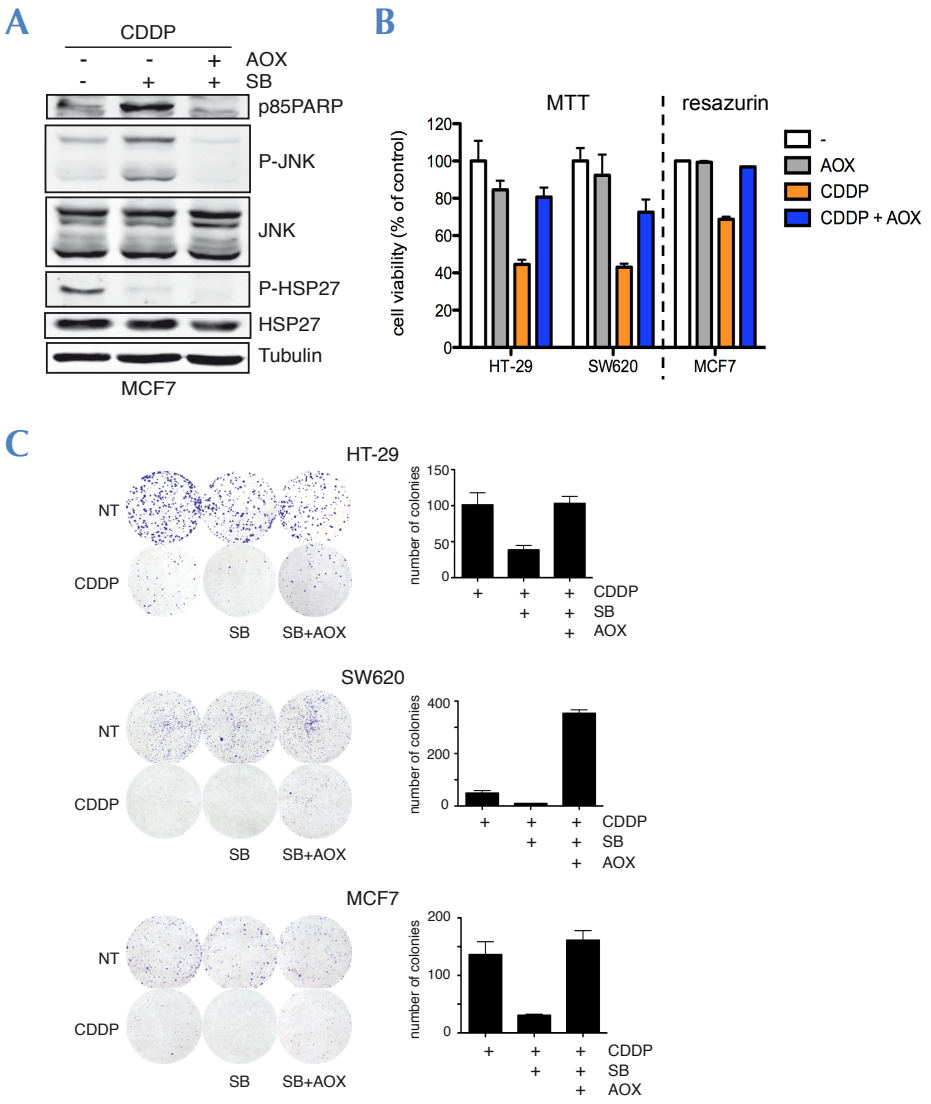

Figure 26. Increased ROS are involved in the sensitization to apoptosis through JNK. (A) MCF7 cells were pre-treated for 1 h with antioxidants (AOX), followed by incubation overnight with SB203580 (SB) and then treated with cisplatin (CDDP) for 8 h. Total cell lysates were analyzed by immunoblotting with the indicated antibodies. **(B)** The indicated human cancer cells were pre-treated for 1 h with AOX followed by 15 h incubation with cisplatin. Resazurin or MTT reagents were used to determine the remaining viable cells. **(C)** Clonogenic assays after O/N incubation with SB203580 followed by 1 h treatment with 50 μM cisplatin for MCF7 and HT-29 cells, or 10 μM cisplatin for SW620 cells. The bars diagrams represent number of colonies.

Since ROS upregulation potentiated cisplatin-induced apoptosis, we wondered whether cancer cells that have high basal levels of ROS would be also sensitized to apoptosis upon p38 MAPK inhibition. To address this question, we selected the breast cancer cell line MDA-MB-231, which has higher levels of basal ROS than MCF7 cells (**Fig. 27A**). We found that MDA-MB-231 cells also showed JNK hyper-activation in response to p38 MAPK inhibition, and this effect was impaired by treatment with antioxidants (**Fig. 27B**). Consistently, basal levels of JNK activation was higher in MDA-MB-231 cells than in MCF7 cells, directly correlating with their endogenous ROS levels. Moreover, inhibition of p38 MAPK signaling induced a time-dependent accumulation of ROS in MDA-MB-231 cells (**Fig. 27C**). In agreement with these observations, p38 MAPK inhibition further activated JNK signaling enhancing apoptosis in cisplatin-treated MDA-MB-231 cells, and incubation with antioxidants reduced JNK activation and the consequent apoptotic response (**Fig. 27D**), and therefore increased cell viability (**Fig. 27E**). These results indicate that the mechanism linking the inhibition of p38 MAPK with ROS accumulation, JNK activation and apoptosis induction is probably relevant to different types of cancer cells, regardless of their basal ROS content.

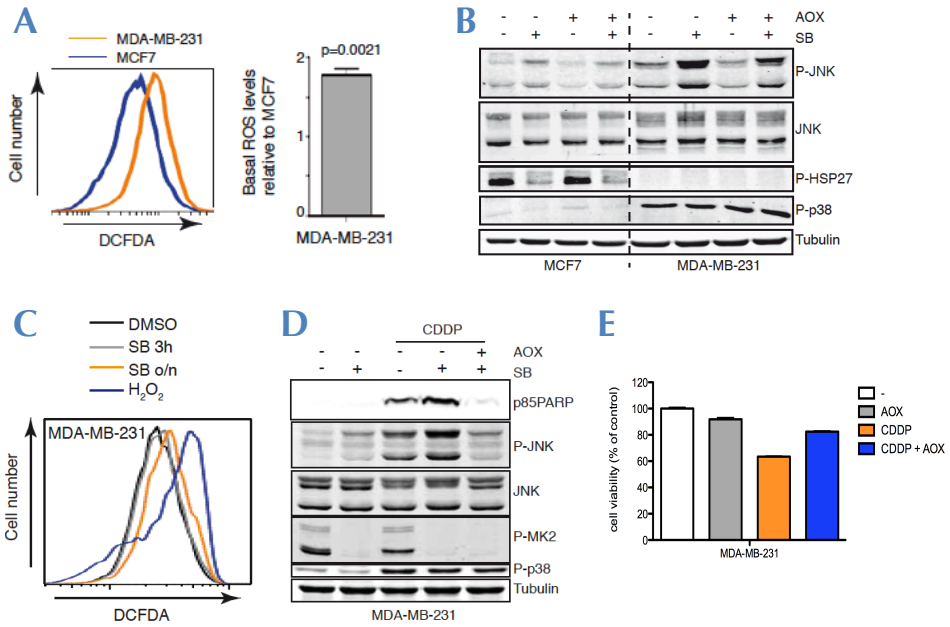

Figure 27. p38 MAPK inhibition sensitizes cancer cells that bear high ROS to apoptosis. Total cell lysates were analyzed by immunoblotting with the indicated antibodies. **(A)** Endogenous ROS levels of MCF7 and MDA-MB-231 cancer cells were measured with the DCFDA probe by flow cytometry. Fold increase of ROS levels compared to MCF7 cells is represented. **(B)** Cells were incubated O/N in the presence or absence of SB203580 (SB), and pre-treated for 1 h with a mixture of GSH and NAC antioxidants (AOX). **(C)** MDA-MB-231 cells were incubated for the indicated times with DMSO, SB203580 or 5 mM H_2O_2 for 10 min. ROS levels were measured with DCFDA by flow cytometry. **(D)** MDA-MB-231 cells were pre-treated for 1 h with AOX, followed by 16 h incubation with SB203580 and then treated for 8 h with cisplatin (CDDP). **(E)** MDA-MB-231 cells were pre-treated for 1 h with AOX followed by 15 h incubation with cisplatin. Resazurin was used to determine the percentage of viable cells.

5. Inhibition of p38 MAPK downregulates antioxidant enzymes

To characterize the mechanism by which inhibition of p38 MAPK increases the levels of ROS, we investigated how SB203580 affects the expression of genes associated with the regulation of oxidative stress. We analyzed a gene expression array of 84 genes looking for changes after p38 MAPK inhibition in MCF7 cells (see "Methods"). The analysis (**Suppl. Fig. 4**) revealed eight genes encoding proteins with antioxidant activity whose expression was downregulated more than 1.5 fold in response to p38 MAPK inhibition. Re-examination of the expression of these candidate genes with custom primers showed that three genes were significantly downregulated upon p38 MAPK inhibition both in breast and in colon cancer cells (**Table 3**). One of the genes was *PTGS2*, which encodes the anti-inflammatory protein cyclooxygenase 2 (COX-2). This was described as an anti-oxidant gene in the array but we were not aware of clear evidence linking COX-2 to antioxidant activity. We used shRNAs to downregulate COX-2 in SW620 colon cancer cells but found no evidence that this protein had a major anti-oxidant role; if anything there was a slight decrease in ROS levels upon COX-2 downregulation. As a control, shRNA-mediated downregulation of p38α in the same cells showed the expected increase in ROS production (**Fig. 28A**). Therefore, the regulation of COX-2 expression by p38 MAPK does not seem to impinge on the ROS levels of cancer cells and we decided not to further characterize this candidate.

Table 3. Antioxidant enzyme-encoding genes regulated by p38 MAPK in cancer cells

RefSeq	Name	Array	MCF7	HT-29
NM_002083	GPX2	-1.91	-1.38	1.83
NM_002084	GPX3	-1.49	-1.07	-1.31
NM_001509	**GPX5**	**-1.96**	**-2.16**	**-1.50**
NM_000637	GSR	-1.70	-1.17	1.09
NM_006151	LPO	-1.88	1.50	-5.56
NM_000963	**PTGS2**	**-5.87**	**-4.09**	**-1.53**
NM_144651	PXDNL	-1.86	-9.52	-1.45
NM_032243	**TXNDC2**	**-3.15**	**-1.91**	**-2.35**

The expression of eight candidate genes identified in the array was validated by qRT-PCR in breast MCF7 and colon HT-29 cancer cells. Numbers indicate fold changes in the expression of genes upon incubation of the cells with SB203580 to inhibit p38 MAPK signaling. Genes downregulated at least 1.5 fold in both cell lines are in bold.

The other two genes regulated by p38 MAPK were *GPX5* and *TXNDC2*, which encode a glutathione peroxidase and a thioredoxin, respectively, two well-known enzymes with antioxidant activity. Interestingly, we found that siRNA mediated downregulation of *GPX5* or *TXNDC2* sufficed to enhance the basal JNK activity levels in MCF7 cells (**Fig. 28B**). This indicates that GPX5 and TXNDC2 are both good candidates to mediate the upregulation of ROS observed upon p38 MAPK inhibition in cancer cells. Thus, we hypothesized that reduced expression of these antioxidant enzymes after inhibition of p38 MAPK would induce ROS upregulation and activation of the JNK pathway.

Since mitochondria are one of the main sources of ROS in the cell, we also investigated the possibility that p38 MAPK could regulate the mitochondrial production of ROS. In the same line, we also wondered about the possible contribution of NADPH oxidase (Nox) enzymes to ROS generation after p38 MAPK inhibition. We observed that the Nox inhibitor DPI did not affect the production of ROS after p38 MAPK inhibition but rotenone, an inhibitor of the mitochondrial respiratory chain, was able to block it (**Fig. 28C**). This indicates that regulation of mitochondrial activity might also contribute to the production of ROS upon p38 MAPK inhibition.

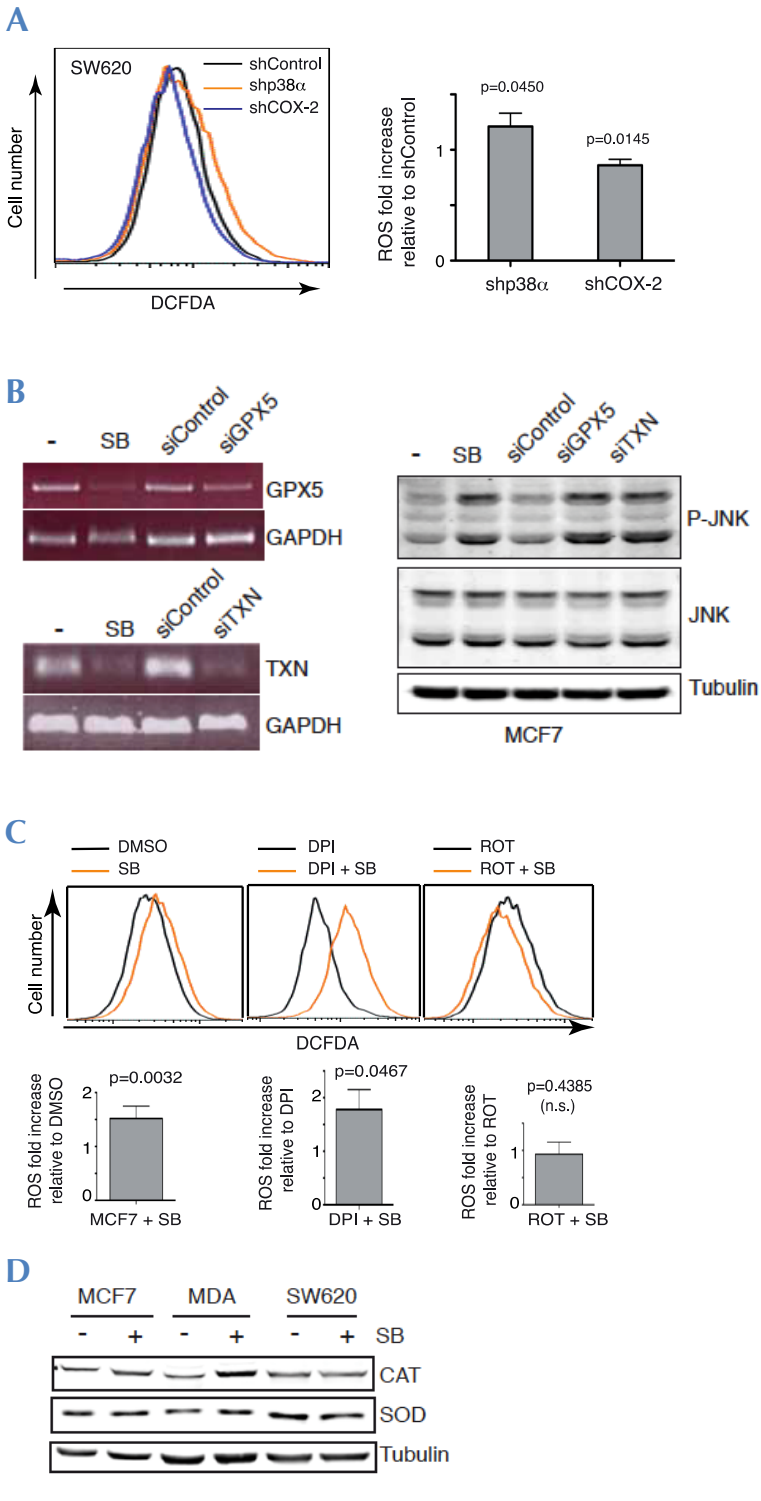
A
SW620
shControl
shp38α
shCOX-2
Cell number
DCFDA
ROS fold increase relative to shControl
p=0.0450
p=0.0145
shp38α
shCOX-2
B
-
SB
siControl
siGPX5
GPX5
GAPDH
siTXN
TXN
P-JNK
JNK
Tubulin
MCF7
C
DMSO
SB
DPI
DPI + SB
ROT
ROT + SB
Cell number
DCFDA
ROS fold increase relative to DMSO
p=0.0032
MCF7 + SB
ROS fold increase relative to DPI
p=0.0467
DPI + SB
ROS fold increase relative to ROT
p=0.4385 (n.s.)
ROT + SB
D
MCF7
MDA
SW620
SB
CAT
SOD
Tubulin

Figure 28. Downregulation of antioxidant enzymes induces JNK activation. (A) SW620 cells were infected with lentiviruses expressing shRNAs against PTGS2 (shCOX-2) and p38α (shp38α) or a non-targeting control (shControl). Pools of cells were selected with puromycin for one week and levels of ROS were measured with DCFDA by flow cytometry. **(B)** MCF7 breast cancer cells were transfected with siRNAs against GPX5 (siGPX5), TXNDC2 (siTXN) or scramble (siControl). The expression levels of the indicated mRNAs were determined by semi-quantitative RT-PCR (left panel). Total cell lysates were analyzed by immunoblotting with the indicated antibodies (right panel). **(C)** MCF7 cells were pretreated for 1 h with 2.5 μM DPI or 0.25 μg/ml rotenone (ROT), incubated for 6 h with DMSO or SB203580, and ROS levels were measured with DCFDA by flow cytometry. **(D)** Different breast (MCF7, MDA-MB-231) and colon (SW620) cancer cells were treated O/N with SB203580 (SB). Total cell lysates were analyzed by immunoblotting with the indicated antibodies.

A recent report (Gutierrez-Uzquiza et al., 2012) has proposed that p38α regulates ROS production in MEFs through the antioxidant enzymes catalase and SOD. However, inhibition of p38α did not affect the protein levels of these enzymes in the cancer cells we analyzed (**Fig. 28D**), suggesting that regulation of ROS production by p38α may involve different mechanisms in non-transformed and tumor cells.

6. Inactivation of JNK phosphatases by increased ROS levels

Previous reports have shown that ROS can lead to the inhibition of phosphatases, since their catalytic cysteine is susceptible to inactivation by oxidation (Kamata et al., 2005; Teng et al., 2007). Thus, we investigated whether the activation of JNK signaling observed upon p38 MAPK inhibition was due to the ROS-mediated inactivation of JNK phosphatases. With that aim, we expressed and purified recombinant GST-JNK1 and GST-MKK7 proteins and performed an *in vitro* kinase assay (see "Methods"). Then, we purified the *in vitro*-phosphorylated JNK1 protein and incubated it with lysates of cancer cells, which had been treated or not with SB203580 (**Fig. 29A**). We observed that the lysates of SB203580-treated cells were less efficient at dephosphorylating JNK1, suggesting that JNK phosphatases were less active in cells where p38 MAPK was inhibited, probably due to their higher levels of ROS. As a control, we confirmed that treatment with phosphatase inhibitors impaired JNK1 dephosphorylation by the cell lysates (**Fig. 29B**).

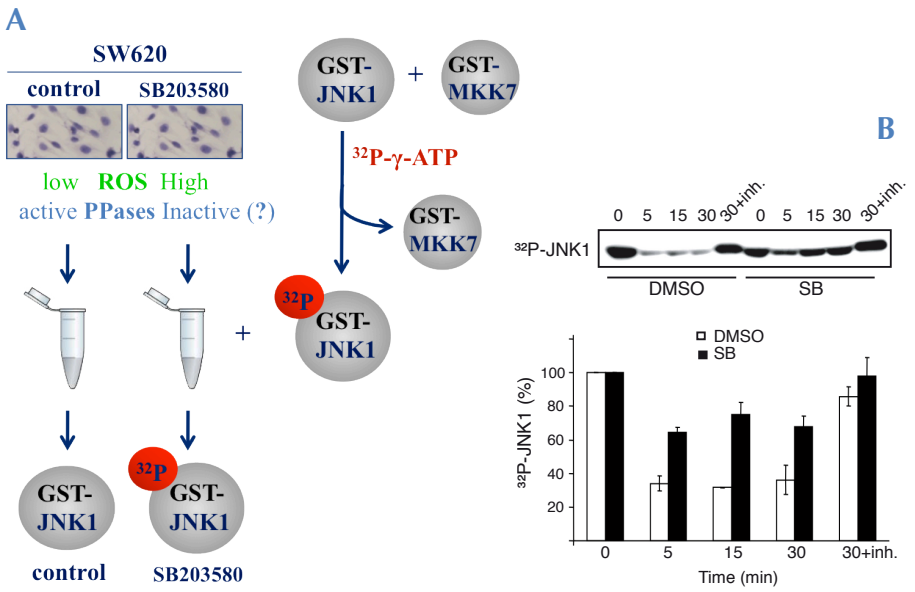

Figure 29. Increased ROS levels inactivate JNK phosphatases. (A) Schematic representation of the phosphatase assay. **(B)** Recombinant GST-JNK1 protein was incubated with MKK7 and ^{32}P-γ-ATP, affinity purified and then incubated for the indicated times (0-30 min) with total cell lysates obtained from SW620 cells treated or not with SB203580. As a control, phosphatase inhibitors were added to the SW620 cell lysates (30+inh). The amount of phosphorylated JNK1 was visualized by autoradiography and was quantified relative to the amount initially present at time 0.

We took advantage of the fact that we could purify the *in vitro*-phosphorylated recombinant JNK1, to check what phosphatases could be bound to it. For this experiment, we first incubated the GST-JNK1 protein to the beads and then we proceed with the phosphorylation by MKK7. The phosphorylated GST-JNK1 bound to the beads was incubated with lysates from SW620 cancer cells either treated or not with SB203580. The beads were then recovered, washed and analyzed by SDS-PAGE. We selected for mass spectrometry (MS) analysis three areas of the gel where different patterns of proteins could be observed between lysates of cells, treated or not with S203580 (**Fig. 30**). The proteins identified in bands 1, 2 and 3 are listed in **Supplementary Tables 2, 3** and **4**, respectively.

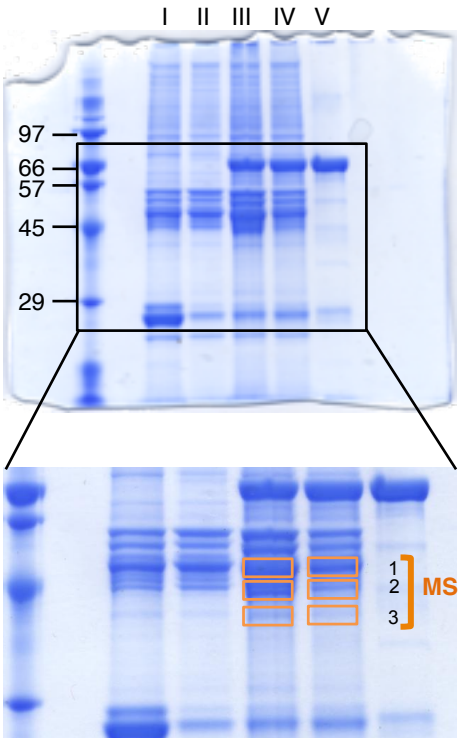

Figure 30. SDS-PAGE from GST-JNK1 incubated with cancer cell lysates. Laemmli gel stained with coomassie. I: GST+lysate, II: MKK7+lysate, III: JNK1 + control lysate, IV: JNK1 + SB lysate, V: JNK1. Bands 1, 2 and 3 were sent for mass spectrometry (MS) analyses.

Most of the pulled down proteins that were identified either in the control lysates or in the SB203580-treated ones, were cytoskeletal keratins. Since we did not pull down any phosphatase, we decided to follow another approach to identify what type of phosphatases was affected by the ROS produced upon p38 MAPK inhibition. First, we measured either the Tyr or Ser/Thr phosphatase activity of human cancer cells that were incubated or not with SB203580. We observed that in lysates of cells where p38 MAPK was inhibited, the rate of dephosphorylation of Tyr phosphopeptides was significantly reduced in comparison with control lysates (not treated with SB203580). In contrast, dephosphorylation of Ser/Thr phosphopeptides was less affected by p38 MAPK inhibition. As a control, treatment with H_2O_2 significantly reduced both types of phosphatase activities (**Fig. 31A**). To follow up on these results, we focused on Tyr phosphatases that are susceptible to ROS inactivation and that have been reported to negatively regulate JNK activity, such as PTP1B, PTP-PEST, DUSP8, DUSP10 and DUSP16 (Keyse, 2008; Wu et al., 2008). Furthermore, these phosphatases have been shown to be

dysregulated in breast and colon cancer cells (Labbe et al., 2012). We used siRNAs to downregulate each of these five phosphatases and found that DUSP8 downregulation sufficed to enhance the basal phosphorylation of JNK in MCF7 cells (**Fig. 31B**). The result with DUSP16 was not reproducible. This identifies DUSP8 as a phosphatase that controls the basal activity of JNK, and whose inactivation due to increased ROS levels could explain the observed activation of JNK induced by p38 MAPK inhibition in MCF7 cells. However, DUSP8 did not seem to play a major role in the regulation of basal JNK phosphorylation in other cancer cells (**Fig. 31C**), suggesting that different ROS-regulatable phosphatases might control the basal levels of JNK phosphorylation in different types of tumor cells.

A

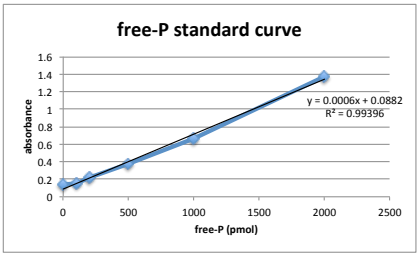

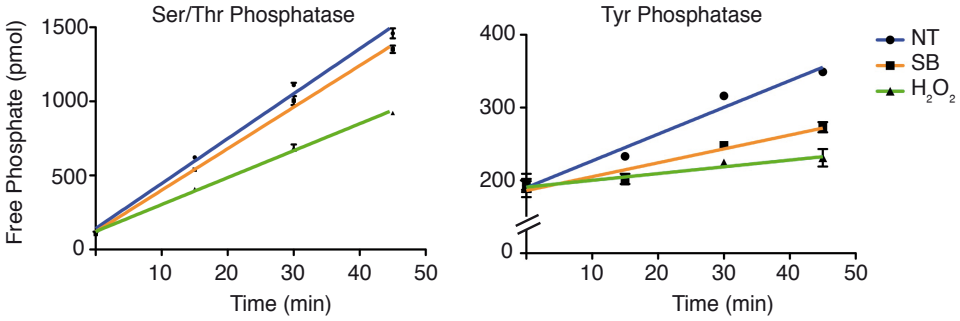

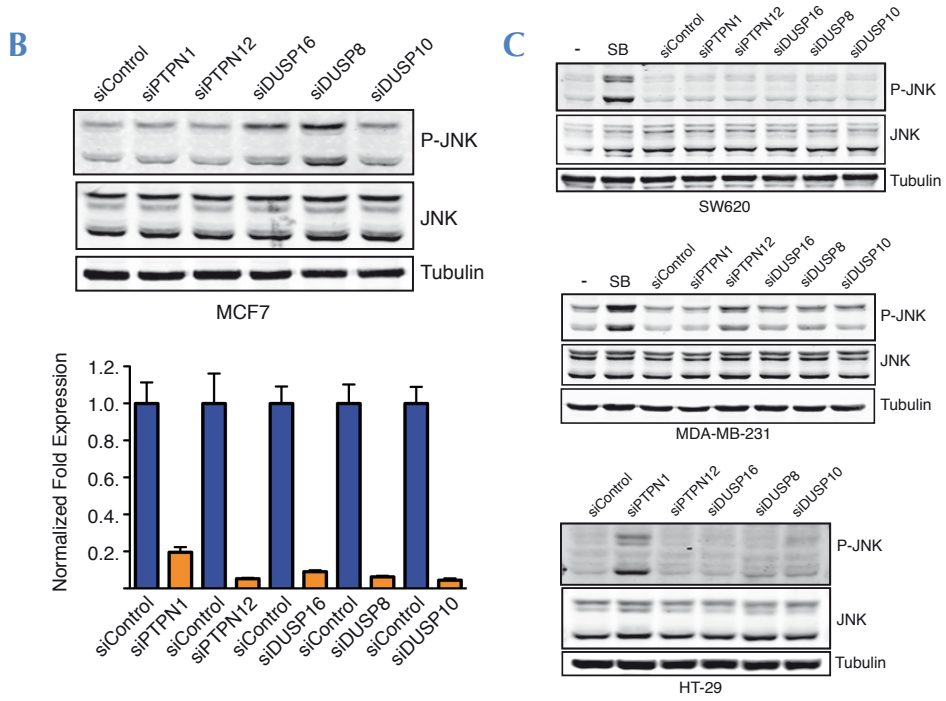

Figure 31. Increased ROS levels inactivate JNK phosphatases. **(A)** SW620 cells were incubated with SB203580 (SB) O/N or with 5 mM H_2O_2 for 1 h and the Ser/Thr or Tyr phosphatase activities were measured in total cell lysates with the kits from Promega. **(B)** MCF7 cells were transfected with siRNAs against PTPN1, PTPN12, DUSP16, DUSP8 or DUSP10, or with a scramble control, and 48 h later total cell lysates were analyzed by immunoblotting with the indicated antibodies. Downregulation of the target genes was confirmed by qRT-PCR, as shown in the histogram. **(C)** The indicated cancer cell lines were transfected with siRNAs against PTPN1, PTPN12, DUSP16, DUSP8 and DUSP10, or with a scramble control, and 48 h later total cell lysates were analyzed by immunoblotting with the indicated antibodies. As a positive control, some cells were incubated O/N with SB203580 before immunoblotting.

We also considered the possibility that inhibition of p38 MAPK could impinge on upstream activators of the JNK pathway, but we were not able to detect the phosphorylation levels of endogenous MKK4 and MKK7 in these cancer cells. Thus, we used an inhibitor of ASK1, a MAP3K that can mediate oxidative stress-induced phosphorylation of JNK activators. We used UV radiation to fully stimulate JNK activation through ASK1, together with increasing concentrations of the ASK1 inhibitor (0-10 μM), and we confirmed that ASK1 inhibition blocked the activation of JNK induced by UV (**Fig. 32A**). However, neither JNK activation nor

the enhanced apoptosis induced by cisplatin upon p38α inhibition were affected by ASK1 inhibition (**Fig. 32B**). Taken together, our results indicate that phosphatase inhibition plays a key role in the ROS-induced upregulation of JNK activity triggered by p38 MAPK inhibition.

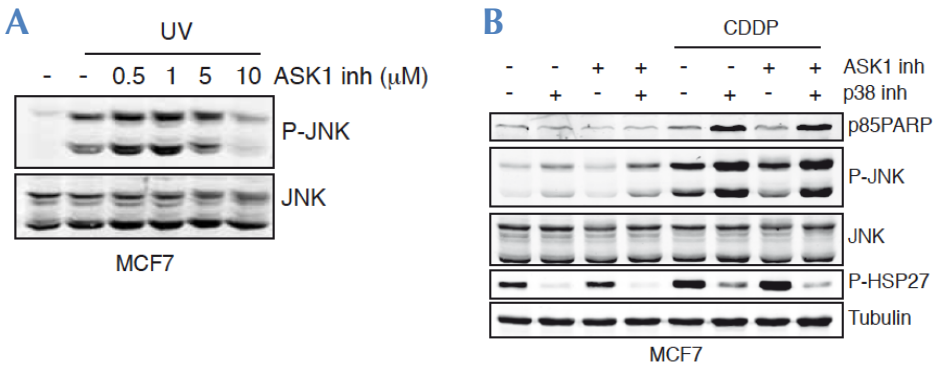

Figure 32. ASK1 inhibition does not affect cisplatin-induced apoptosis upon p38 MAPK inhibition. In both panels, total cell lysates were analyzed by immunoblotting with the indicated antibodies. **(A)** MCF7 cells were treated with the indicated concentrations of ASK1 inhibitor O/N and then irradiated with 50 J/m2 UV followed by 30 min incubation. **(B)** MCF7 cells were incubated O/N with SB203580 and/or 10 μM ASK1 inhibitor followed by cisplatin treatment for 8 h.

7. Inhibition of p38 MAPK cooperates with cisplatin to reduce breast tumorigenesis in mice

To obtain *in vivo* evidence for the implication of p38 MAPK signaling in the response of cancer cells to cisplatin, we used the MMTV-PyMT mouse model of breast cancer. These mice develop spontaneous tumors in the mammary glands that become palpable when females are around 2.5 months old. Tumors were allowed to grow until they reached 200 mm^3 and then four different treatments were applied.

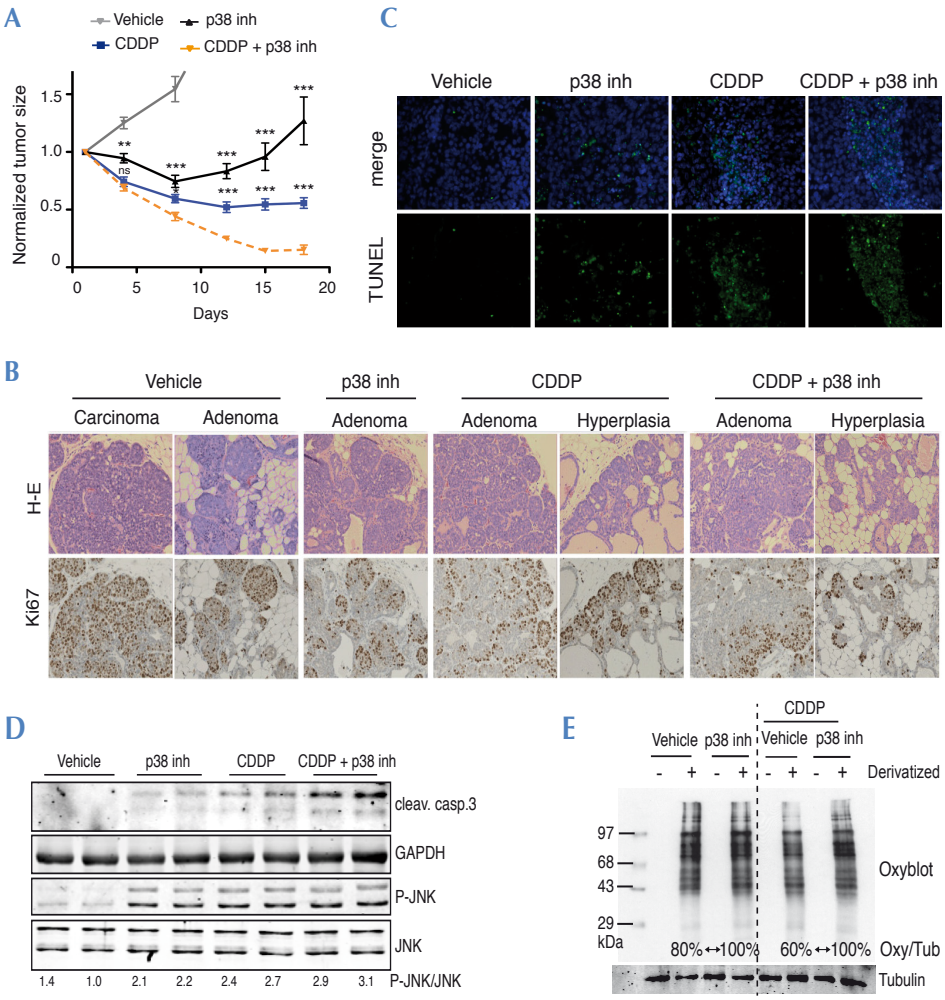

Figure 33. Cisplatin cooperates with p38 MAPK inhibition to reduce breast tumors in mice. (A) MMTV-PyMT female mice with breast tumors of 200 mm^3 in volume were treated with a single-dose of cisplatin followed by daily administration of the p38 MAPK inhibitor PH-797804 (10 mg/Kg) for 18 days. Tumor size was measured at the indicated times and normalized relative to the original size of each tumor when the treatment began. The graph compiles the results of two independent experiments, in which a minimum of four mice was used per condition. *** = $p<0.0001$, ** = $p<0.001$, * = $p<0.05$, ns = $p>0.05$. **(B)** H-E and Ki67 staining of breast tumors analyzed at day 7. Images are 20x. **(C)** TUNEL staining of breast tumors analyzed at day 7. **(D)** Total cell lysates obtained from two representative mice of each condition were analyzed by immunoblotting with the indicated antibodies. **(E)** Protein oxidation in tumor samples was analyzed by immunoblotting using Oxyblot, and the total protein oxidation signal per lane was quantified with tubulin as a reference. Results were confirmed using three mice per condition.

In the first experiment, female mice were treated either with a single dose of cisplatin (Evers et al., 2010), with daily administration of the p38 MAPK inhibitor PH-797804 (Xing et al., 2009), with the combination of both, or only with vehicle of the inhibitor and physiological saline (control animals). We monitored tumor evolution for 18 days (except for the control animals, which had to be sacrificed before due to the size of their tumors). As shown in **figure 33A**, tumors from control mice ("Vehicle") increased their size over time; tumors from mice treated with PH-797804 slightly decreased during the first 10 days, but then they started to grow again; tumors from mice treated with cisplatin decreased almost to a 50% of their initial size; and tumors from the double treatment were reduced about 90%. Thus, in agreement with our observations in human cancer cells, we found that the combination of cisplatin treatment with p38 MAPK inhibition showed a clear additive effect and reduced the size of breast tumors in mice more than treatment with cisplatin alone.

Immunohistochemical (IHC) analysis based on Ki67 staining confirmed reduced levels of tumor cell proliferation in the single treatments, and to a greater extent in the double treatment at day 7 (**Fig. 33B**). At this point of the experiment, all three treatments induced a decrease in tumor size but they were all within the same range, so we decided to compare tumors at the molecular level. Apoptotic events, as determined by TUNEL staining (**Fig. 33C**) or by cleaved caspase-3 detection by immunoblotting (**Fig. 33D**), were higher in the tumors from mice subjected to the double treatment. The fact that at an early time point (day 7), when tumors have more or less the same size, we already saw higher apoptosis and lower proliferation in the case of the combined therapy, could explain its additive effect, consistent with what we observed in the human cancer cell lines.

We also investigated whether p38 MAPK inhibition in mice would induce activation of JNK in the breast tumors as well. Indeed, we confirmed that JNK was activated in tumors of mice treated with the p38 MAPK inhibitor, and this was further enhanced in tumors of mice subjected to the double treatment (**Fig. 33D**). To correlate the results *in vivo* with those obtained in cancer cell lines, we

analyzed the general oxidation state in the breast tumor proteins by Oxyblot, which revealed higher levels of oxidation in mice treated with the p38 MAPK inhibitor and cisplatin (**Fig. 33E**). These results indicate that the inhibition of p38 MAPK combined with cisplatin treatment cooperate to induce tumor cell apoptosis, which correlates with increased ROS and JNK pathway activation in the breast tumor cells.

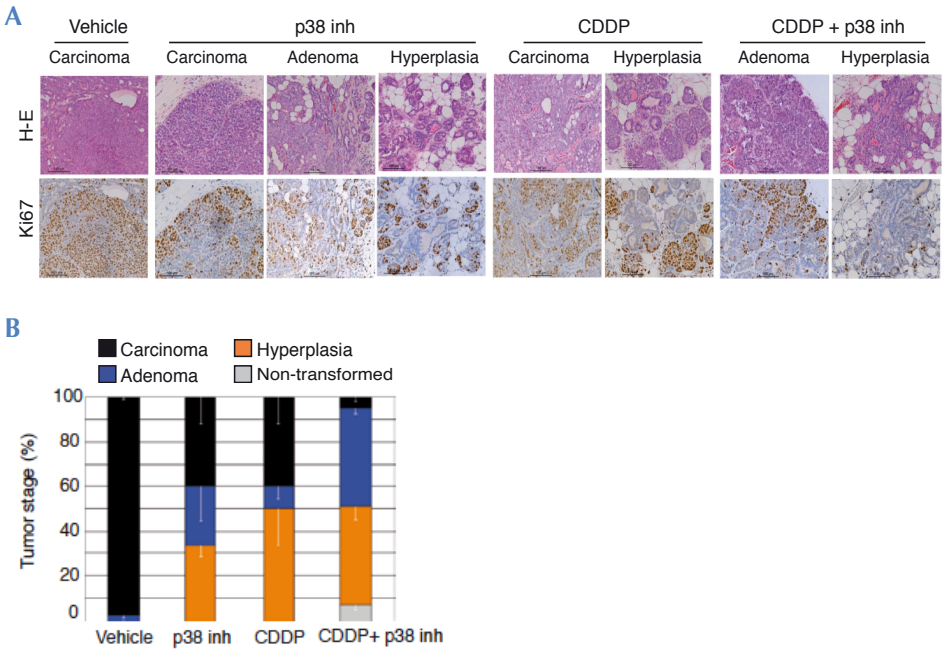

Figure 34. p38 MAPK inhibition reduces tumor malignancy in a mouse model of breast cancer. (A) H-E and Ki67 staining of breast tumors analyzed at day 18. Images are 20x. **(B)** H-E stained sections of breast tumors were analyzed in blinded fashion at day 18. Samples were classified as carcinoma, adenoma, hyperplasia and normal tissue based on the microscopic analysis of the tissue.

Importantly, IHC analysis of the tumors at the end of the experiment showed that the double treatment kept on reducing the proliferative capacity of the tumor cells (**Fig. 34A**). Moreover, evaluation of the tumor grade showed that tumors were in a less advanced stage (**Fig. 34B**). Considering that the size of the tumors is also strongly reduced by the combined treatment, a better prognosis could be expected in the event of a possible relapse after therapy termination.

To test this hypothesis, we repeated the experiment under the same conditions described above, but we stopped treatment with the p38 MAPK inhibitor after 15 days and then monitored the evolution of each group of tumors up to 24 days (**Fig. 35**). We found that the rate of growth of the tumors coming from mice that were treated with the double therapy was slower than with the individual therapy, indicating that new tumors would probably appear later after the combined treatment.

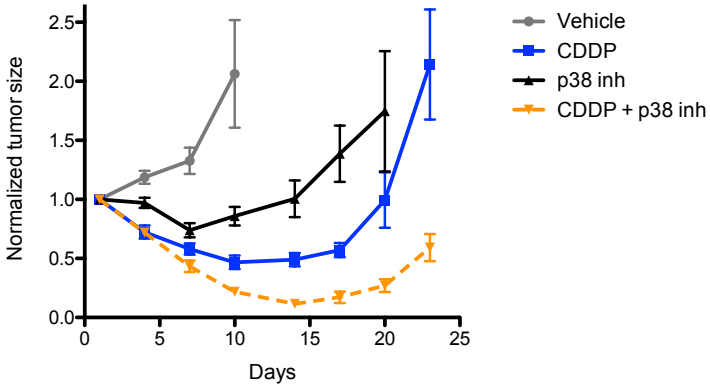

Figure 35. After therapy termination, relapse in the double treatment is slower. MMTV-PyMT female mice with breast tumors of 200 mm^3 in volume were treated with a single-dose of cisplatin followed by daily administration of PH797804 (10 mg/Kg) up to 15 days, when the therapy was stopped. Tumor size was measured at the indicated times and normalized relative to the original size of each tumor when the treatment began.

8. Different types of transformed cells are sensitized to apoptosis after p38 MAPK inhibition

Other types of human epithelial cancer cells might also rely on this mechanism of response to cytotoxic treatments, as we have observed enhanced JNK activation upon p38 MAPK inhibition, both with chemical compounds (**Fig. 36A-B**) and by genetic downregulation (**Fig. 36C-D**) of p38α. We confirmed that combination of cytotoxic treatments, either cisplatin or doxorubicin, with the inhibition of p38 MAPK sensitized to apoptosis. (**Fig.37A**). Besides, ROS was implicated as well in the sensitization of RKO cancer cells to death after cisplatin incubation and UV

radiation (Fig. 37B), as we demonstrated for other breast and colon cancer cell lines.

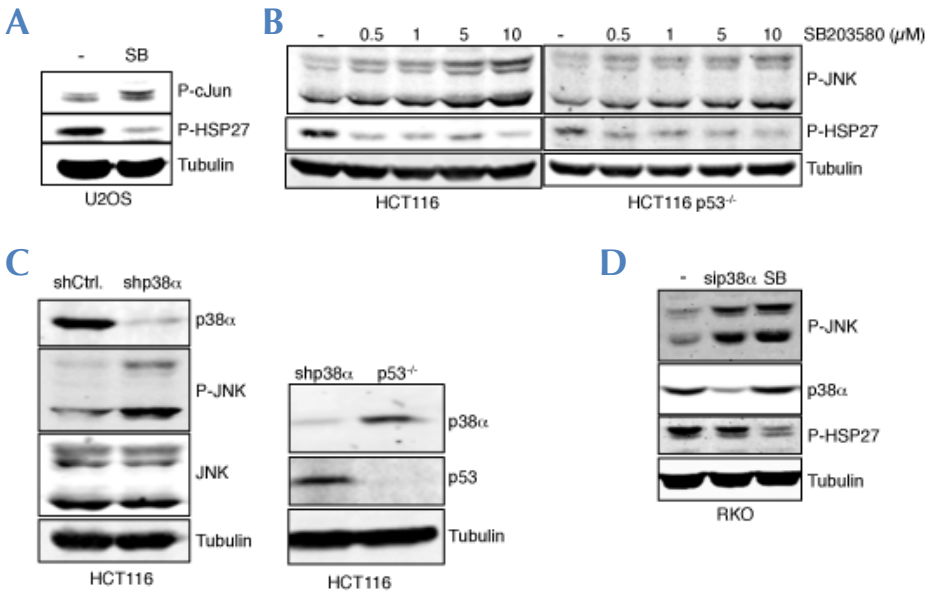

Figure 36. Impairment of p38 MAPK activates the JNK pathway in epithelial cancer cells. Total cell lysates were analyzed by immunoblotting with the indicated antibodies. **(A)** U2OS cancer cells were incubated with SB203580 for 24h. **(B)** HCT116 and HCT116 p53^{-} colon cancer cells were treated with increasing concentrations of SB203580 (0.5 – 10 μM) for 24 h. **(C)** HCT116 cells were infected with shRNA against p38α (shp38α) or a non-targeting control (shCtrl.). After one week of puromycin selection, pools of cells were collected for their analysis. **(D)** RKO colon cancer cells were incubated with p38α siRNA (sip38α, 50 nM for 48 h) or treated with SB203580.

Interestingly, when analizing by immunofluorescence U2OS cells, we observed that SB203580 mainly induced JNK activation in the cytoplasm, in contrast with the nuclear localization of active JNK observed after UV radiation (Fig. 38).

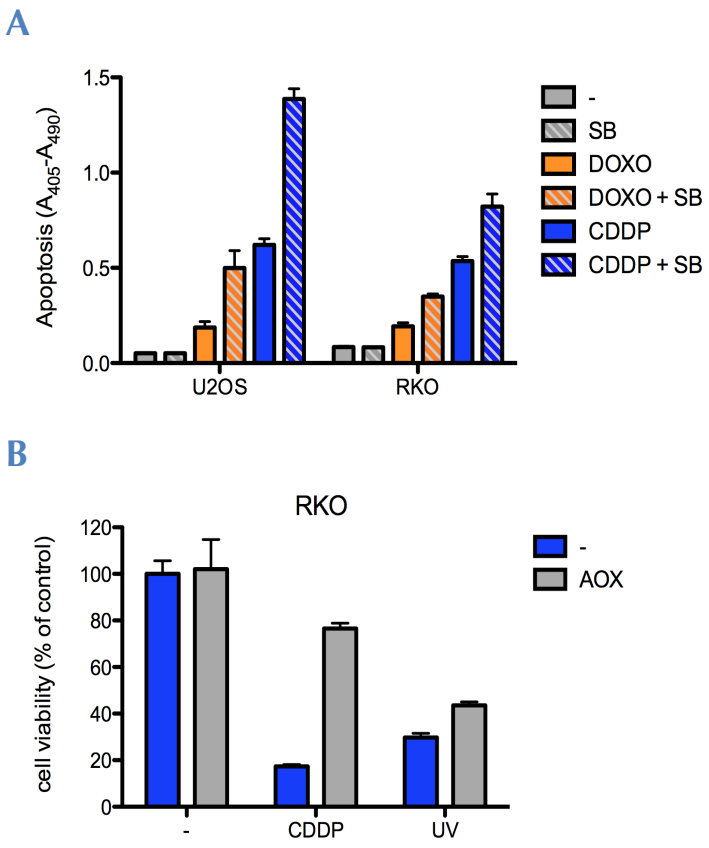

Figure 37. p38 MAPK inhibition sensitizes some epithelial cancer cells to cell death. (A) U2OS and RKO cells were pre-incubated with SB203580 for 2 h followed by treatment with cisplatin (CDDP) or doxorubicin (DOXO) for 15 h. Apoptosis was measured with the Cell Death Detection ELISA kit. **(B)** RKO cells were pre-incubated for 1 h with a mixture of antioxidants (AOX) followed by treatment with cisplatin or UV radiation for 15 h. Cell viability was measured by MTT.

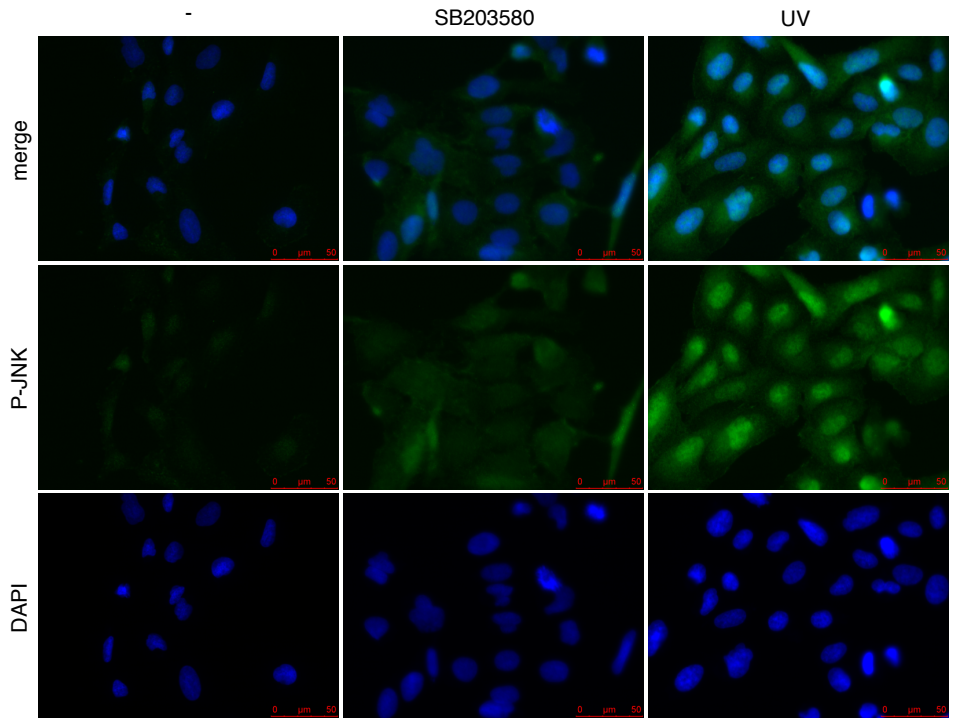

Figure 38. p38 MAPK inhibition induces JNK activation mainly in the cytoplasm. U2OS cells were incubated with SB203580 for 6 h or 400 J/m² UV for 1 h. Phosphorylated JNK was detected by immunofluorescence.

We also investigated the effect of depleting p38α in H-Ras transformed MEFs. We found that H-Ras p38α WT MEFs beared much lower basal ROS levels than H-Ras p38α KO, even after treatment with H_2O_2 (**Fig. 39**). Also, JNK signaling was more efficiently activated in challenged H-Ras p38α KO MEFs than in WT ones (**Fig. 40A**), in agreement with previous observations where high ROS levels induced JNK activation. We then postulated that transformed MEFs deficient in p38α should be more sensitized to apoptosis after cisplatin treatment. Therefore, we incubated them with this drug and measured the apoptotic subG0/G1 population by flow cytometry (**Fig. 40B**). We found that, not only H-Ras transformed p38α KO MEFs were more susceptible to cisplatin-induced apoptosis than WT, but also that pre-incubation with antioxidants strongly reduced the apoptotic population.

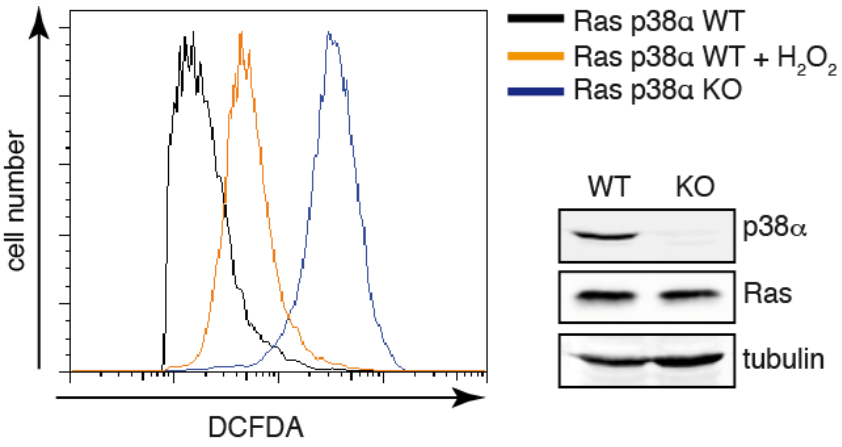

Figure 39. H-Ras transformed p38α WT MEFs bear lower levels of ROS than p38α KO ones. Basal levels of ROS were measured with the DCFDA probe. Transformed p38α WT MEFs were also incubated for 1 h with H_2O_2 prior to ROS measurement. Total cell lysates were analyzed by immunoblotting with the indicated antibodies.

Taken together, these results indicate that the p38 MAPK pathway negatively regulates cisplatin-induced apoptosis in transformed fibroblasts as in epithelial cancer cells. It should be noted that p38α negatively regulates the onset of Ras-induced MEF transformation (Dolado et al., 2007), but it is apparently required for survival in cisplatin-treated transformed MEFs, suggesting differential roles of p38α signaling depending on the stage of cell transformation.

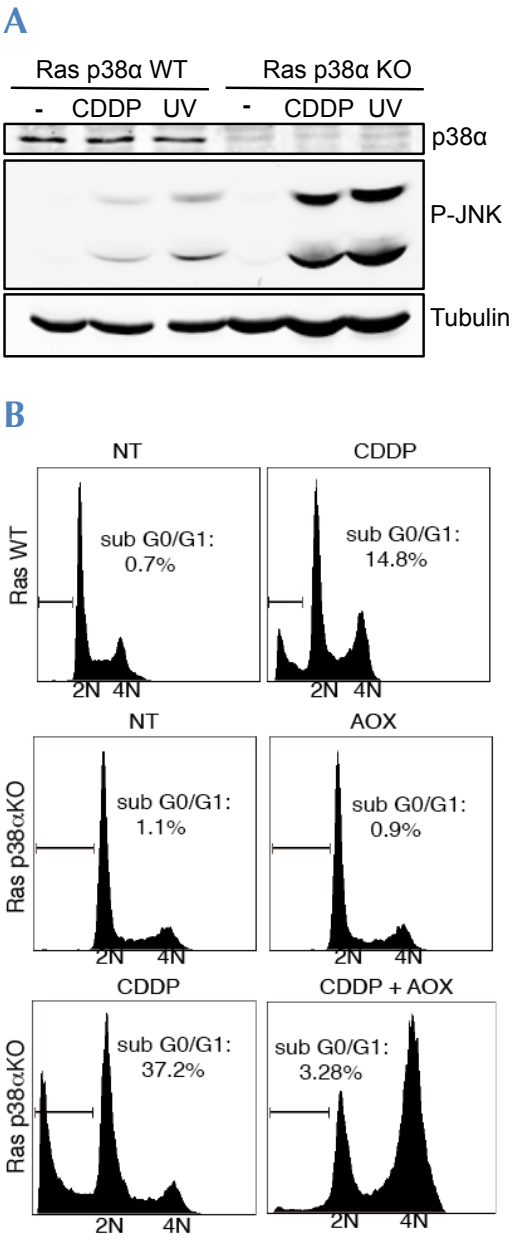

Figure 40. Transformed p38α KO MEFs activate JNK signaling more efficiently than WT and they are more sensitized to cisplatin-induced apoptosis. (A) After 8 h incubation with cisplatin (CDDP) or UV radiation, total cell lysates were analyzed by immunoblotting with the indicated antibodies. **(B)** The apoptotic subG0/G1 population (indicated by a solid line) was analyzed by flow cytometry, either in basal conditions (NT), after 1 h incubation with antioxidants (AOX), 24 h treatment with 100 μM cisplatin (CDDP), or with the indicated combinations (CDDP+AOX).

Discussion

Reactive oxygen species (ROS) might function as a double-edged sword. A moderate increase of ROS may promote cell proliferation and survival. However, when the increase of ROS reaches a certain level (the toxic threshold), it may overwhelm the antioxidant capacity of the cell and trigger cell death (**Fig. 41**).

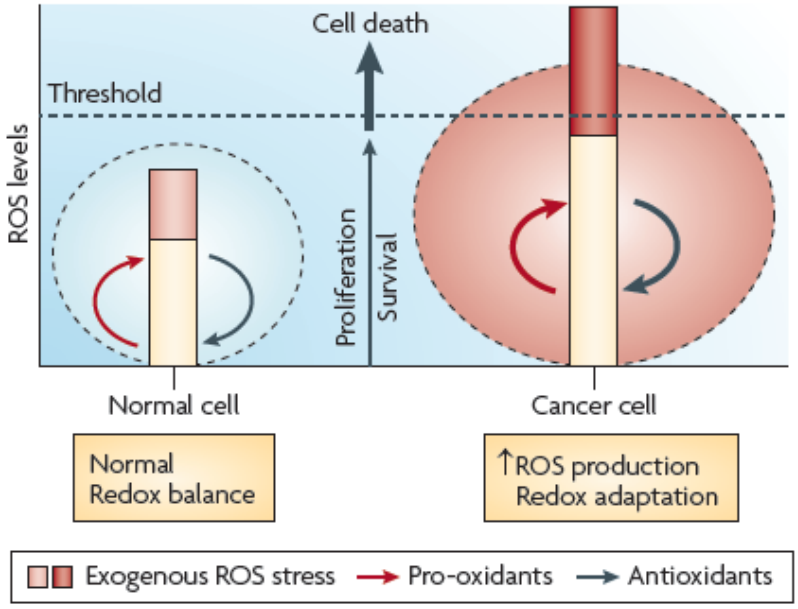

Figure 41. Normal versus cancer redox biology. Cancer cells typically bear higher endogenous ROS levels than normal cells due to their increased metabolism and oncogenic signaling. This reduces their tolerance to exogenous ROS stress reaching more easily the cell-death threshold (horizontal dotted line). (Trachootham et al., 2009).

Under physiological conditions, normal cells maintain redox homeostasis with low levels of basal ROS by controlling the balance between ROS generation (pro-oxidants) and elimination (antioxidant capacity). Normal cells can tolerate a certain level of exogenous ROS stress owing to their antioxidant capacity, which can be mobilized to prevent the ROS level from reaching the cell-death threshold.

In cancer cells, the increase in ROS generation from metabolic abnormalities and oncogenic signaling may trigger a redox adaptation response, leading to an upregulation of antioxidant capacity and a shift of redox dynamics with high ROS generation and elimination to maintain the ROS levels below the toxic threshold. As such, cancer cells would be more dependent on the antioxidant system and more vulnerable to further oxidative stress induced by exogenous ROS-generating agents or compounds that inhibit the antioxidant system. A further increase of oxidative stress in cancer cells is likely to cause elevation of ROS above the threshold level, leading to cell death.

This idea puts into perspective the biological relevance of our work. We show that the inhibition of p38α signaling in cancer cells suffices to increase ROS levels (by downregulating antioxidant enzymes), which in turn inactivate JNK phosphatases. The JNK pathway is an important mediator of apoptosis induction in response to different chemotherapeutic agents, in particular cisplatin (Bae et al., 2006; Sanchez-Perez et al., 2000). Therefore, p38α-mediated ROS increase in cancer cells inactivates JNK phosphatases, which stimulates JNK-induced apoptosis in response to cisplatin. Although we have robust data supporting these findings, there are still some points that are worth discussing.

p38α negatively regulates JNK in cancer cells through ROS downregulation

1. Interplays between JNK and p38 MAPK

The JNK and p38 MAPK pathways can cooperate in the response to certain stimuli as they share several upstream activators (Cuevas et al., 2007). For instance, they

synergize in murine fibroblasts to induce AP1 transcriptional activity in response to UV and anisomycin insults, as p38α can sometimes mediate the expression of both Jun and its partner Fos (Hazzalin et al., 1996).

Nevertheless, the most frequent scenario is that they display opposite effects. There are a number of reports illustrating this interplay both in basal or under stress conditions (Wagner and Nebreda, 2009), which mainly focus on non-transformed cells, like cardiomyocytes (Nemoto et al., 1998), mouse embryonic fibroblasts (Wada et al., 2008) or myoblasts (Perdiguero et al., 2007a). In all the cases, p38α exerts an inhibitory role on the JNK pathway. The mechanisms described involve both upstream and downstream levels of regulation, as p38α negatively regulates the JNK activator MLK3 (Muniyappa and Das, 2008) and changes in expression of the JNK-activating adaptor proteins Grsp2 and HPK1 (Hui et al., 2007).

Much less literature describing the antagonistic roles of both MAPKs in cancer is available, and in none of them describes an interplay mediated by ROS. Here, we show a novel mechanism of regulation of the JNK pathway activity by p38α through ROS downregulation.

It is not so clear whether JNK has could have an inhibitory role on the p38 MAPK cascade, with the exception of a report showing that Jun-deficient hepatocytes have increased p38α phosphorylation (Stepniak et al., 2006). Nevertheless, it is not known until what extent this is a general mechanism. We did not address this possibility but it would be interesting to know whether there can be a bidirectional

regulation. Nonetheless, as p38α maintains the levels of ROS low, we would not expect a sensitization of the cancer cells to apoptosis if inhibition of JNK would upregulate p38α, and this is not biologically interesting.

2. Regulation of ROS by p38 MAPK

p38α is a stress-activated protein kinase, so it is not surprising that it has been reported to be activated by ROS. What is interesting is the fact that p38α itself can regulate ROS levels in cancer cells. We have addressed how the inhibition of p38α increases ROS levels in cancer cells. Experiments using rotenone suggests that electron transport through the mitochondrial respiratory chain may contribute to ROS generation after p38α inhibition. Furthermore, we also identified two antioxidant genes in an array, *GPX5* and *TXNDC2*, which are positively regulated by p38α signaling in cancer cells. Thus, p38α may negatively regulate ROS accumulation at different levels. Of note, p38α signaling has been reported to negatively regulate ROS accumulation in MEFs through the upregulation of the antioxidant enzymes catalase and superoxide dismutase (Gutierrez-Uzquiza et al., 2012), but we found no evidence for the regulation of these two enzymes by p38α in human cancer cells. This indicates that p38α signaling can probably regulate ROS accumulation by different mechanisms in transformed cells. In fact, the different sensitivity of transformed and non-transformed cells to ROS has been proposed to be therapeutically useful (Mateescu et al., 2011; Raj et al., 2011; Shaw et al., 2011).

3. Activation of JNK by ROS

ASK1 has been proposed as a key regulator of apoptosis in response to oxidative stress through the activation of MKK4 and MKK7 (Takeda et al., 2008). Nevertheless, these JNK upstream activators are unlikely to be implicated in the JNK activation process that we describe here. Instead, our results indicate that the inhibition of JNK phosphatases by the accumulation of intracellular ROS (a mechanism that has been suggested in other cellular contexts (Karisch et al., 2011; Ostman et al., 2011)) may account for the hyperactivation of the JNK pathway upon p38α impairment.

We have found no evidence that p38α inhibition affects the expression of the inducible nuclear phosphatase MKP1 (Keyse, 2008), which based on overexpression experiments was proposed to regulate cisplatin-induced JNK activation (Sanchez-Perez et al., 2000). However, by analyzing cytoplasmic phosphatases that have been reported to target JNK phosphorylation (Dickinson and Keyse, 2006), we show that DUSP8 controls the basal levels of JNK phosphorylation in MCF7 breast cancer cells. DUSP8 has been shown to interact with JNK in non-stimulated cells (Sanchez-Perez et al., 2000). Curiously, we provide evidence that DUSP8 is unlikely to play a major role regulating the basal levels of JNK phosphorylation in other human cancer cells. Taken together, our results indicate that different cysteine-based phosphatases might be involved in the regulation of basal JNK activity depending on the cancer cell type.

Sustained JNK activation sensitizes cancer cells to apoptosis

We have previously reported that p38α activation in non-transformed cells induces apoptosis in response to the expression of some oncogenes, whereas the JNK pathway does not seem to be involved in this process (Dolado et al., 2007). Contrary to the above scenario at the onset of cell transformation, we now show that enhanced JNK activity sensitizes cancer cells to apoptosis induced by chemotherapeutic drugs. This response seems to be conserved in different types of tumor cells, suggesting that it could be potentially exploited for cancer therapy in combination with oxidative stress-inducing agents (Engel and Evens, 2006). Our results imply that whereas p38α plays a key role inducing apoptosis in response to ROS accumulation during tumor initiation (Dolado et al., 2007), this function seems to have been taken over by JNK in advanced tumor stages, where JNK hyperactivation sensitizes to apoptosis induced by chemotherapeutic agents. Thus, inhibition of p38α may sensitize tumor cells to these treatments by increasing the basal levels of ROS through downregulation of antioxidant enzymes and generating higher levels of activated JNK that will potentiate the induction of apoptosis in response to genotoxic insults.

We provide evidence for the biological relevance of this mechanism in the response of cancer cells to chemotherapeutic treatments, extending previous reports on the implication of ROS in JNK-mediated apoptosis (Hou et al., 2008; Kamata et al., 2005).

p38α inhibition sensitizes to chemotherapy

1. *In vitro* evidence

Previous reports have suggested that inhibition of the p38 MAPK signaling pathway may help chemotherapeutic agents to kill cancer cells. This is the case for myeloma cell lines treated with bortezomib (Navas et al., 2006), lymphoma cell lines treated with etoposide (Kurosu et al., 2005), or glioma cell lines treated with temozolomide (Demuth et al., 2007). Moreover, the downregulation of MK2, a downstream effector of p38α, sensitizes p53-deficient mouse embryionic fibroblasts (MEFs) transformed with oncogenic Ras to doxorubicin or cisplatin treatment (Reinhardt et al., 2007). In these cases, the enhanced cytotoxic effect observed upon p38 MAPK inhibition has been associated with defective G2 cell cycle arrest. Recent work has also proposed that p38α signaling may play an important role regulating the expression of pro-survival proteins in the G2-arrested cells (Phong et al., 2010). Independently of a putative role of p38α in the regulation of cell cycle checkpoints in human cancer cells, we show that p38α inhibition results in ROS upregulation and JNK activation sensitizing to cisplatin-induced tumor cell death. It seems unlikely that cell cycle arrest would be required for ROS upregulation in response to p38α inhibition, although we cannot rule out that G2 arrest might contribute to the reduced tumor cell proliferation observed upon treatment with the p38 MAPK inhibitor.

Our results also indicate that the additive effect of p38α inhibition and cisplatin treatment is probably independent of p53, as we have observed this pro-apoptotic effect in cancer cells with different p53 status. Of note, p38α inhibitors could also

potentially ameliorate cisplatin-resistance, which has been proposed to rely on p38 MAPK activity (Galan-Moya et al., 2011). Altogether, our results illustrate a new mechanism by which p38a contributes to tumor cell survival, and suggest that the combination of p38a inhibitors with chemotherapeutic agents should be considered for cancer therapy.

2. *In vivo* evidence

Using the MMTV-PyMT mouse model for breast cancer and a p38α inhibitor that is in Phase II clinical trials for antiinflamatory processes (Goldstein et al., 2010; Hope et al., 2009), we confirmed that inhibition of p38α cooperates with cisplatin to kill tumor cells *in vivo*. Importantly, upon treatment with cisplatin and a p38 MAPK inhibitor, not only breast tumors are smaller, but they also look histologically less malignant and tumor cell proliferation is significantly reduced. Altogether, these results may explain the slower growth of relapsed tumors grow slower when they have been treated with the combined therapy.

Comparative gene expression analyses of the MMTV-PyMT tumors along with different types of human breast tumors suggest the placement of PyMT tumors in a luminal group (Fluck and Schaffhausen, 2009), which are less sensitive to chemotherapy (Turner and Jones, 2008). This provides a potential therapeutic advantage for our suggested combined therapy with a p38 MAPK inhibitor, as we have shown that it sensitizes tumors to cisplatin treatment.

Nonetheless, it appears that even though cisplatin is widely used for the treatment of solid tumors like those from colon or ovary, in the case of breast cancer is only

applicable to the basal (or triple negative) subtype. Instead, doxorubicin derivatives are more widely used as chemotherapeutic agents to treat luminal breast cancers. It would be interesting to check whether the additive effect that we have reported with cisplatin also takes place with doxorubicin treatment *in vivo*. In principle, we would anticipate that this should be the case, since we already showed *in vitro* sensitization of some human cancer cell lines to doxorubicin treatment after p38 MAPK inhibition.

Proposed model

Based on the data presented, we propose a model were p38α contributes to cancer cell survival by keeping ROS levels low through, at least, two different mechanisms: (i) inducing the expression of antioxidant enzymes and (ii) regulating mitochondrial function. Therefore, upon treatment with cisplatin, cancer cells undergo apoptosis (**Fig. 42A**), which is increased when p38α is inhibited (**Fig. 42B**). In this situation, ROS are increased and inhibit phosphatases that target JNK, further activating this pathway and therefore sensitizing to apoptosis.

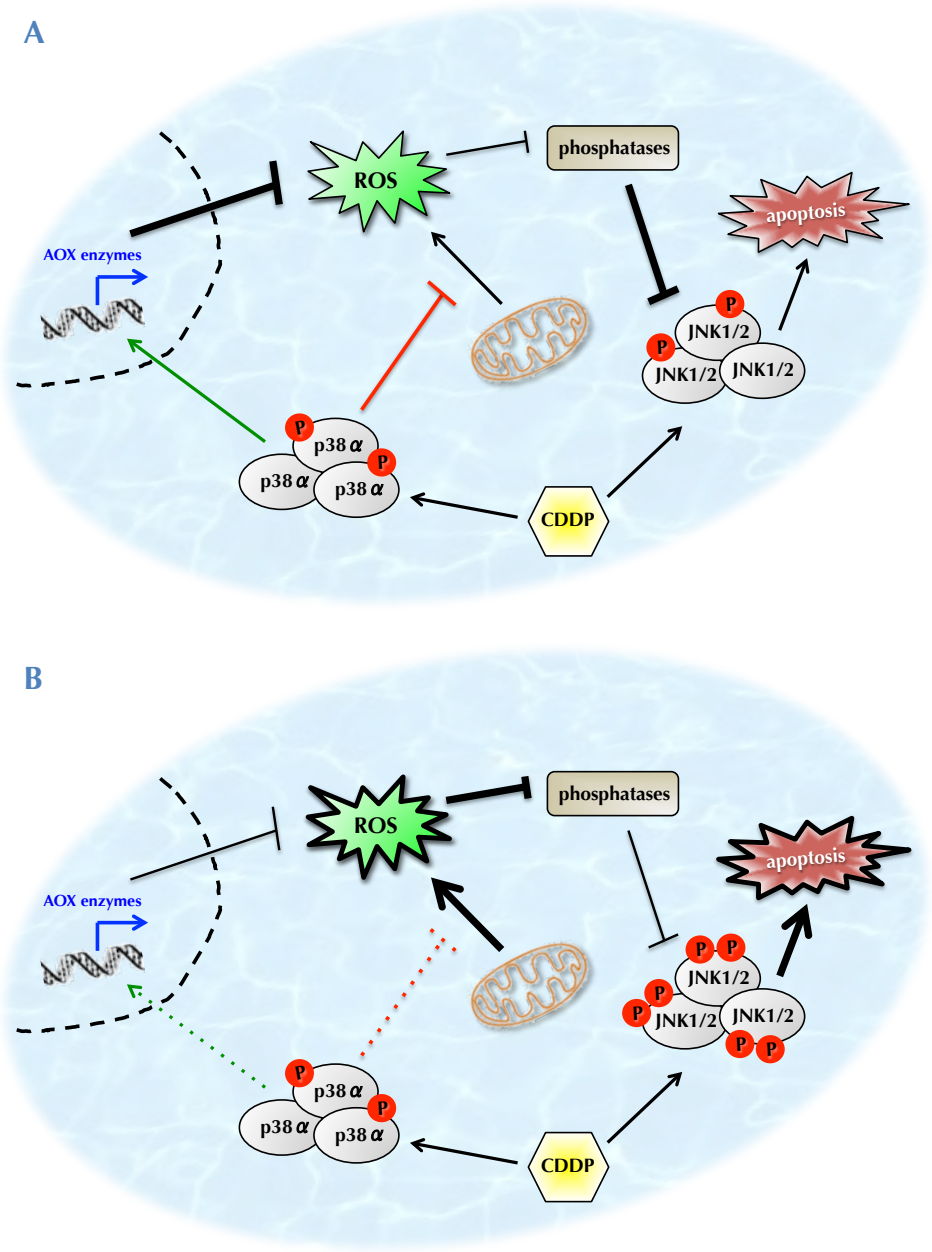

Figure 42. Proposed model. **(A)** p38α prevents the accumulation of ROS by inducing the expression of antioxidant enzymes and by regulating the mitochondrial function. JNK induces apoptosis after cisplatin treatment. **(B)** When p38α is not active, intracellular ROS levels increase, inactivating JNK-targeted phosphatases and inducing the hyperactivation of JNK in response to cisplatin treatment, which further sensitizes cancer cells to apoptosis.

Conclusions

1. eEF2 kinase might be a synthetic lethal partner of p38 MAPK in p53 wild-type cancer cells treated with cisplatin.

2. p38 MAPK is not essential for the proliferation of all cancer cells.

3. Impairment of p38α upregulates the JNK pathway in basal conditions and sensitizes cancer cells to apoptosis, independently of their p53 status.

4. Inhibition of p38 MAPK increases ROS levels, which lead to the inactivation of JNK phosphatases in cancer cells.

5. Inhibition of p38 MAPK cooperates with cisplatin to reduce the size and malignancy of tumors in a mouse model of breast cancer.

Bibliography

(2001). Common Stock Solutions, Buffers, and Media. In Current Protocols in Cell Biology, (John Wiley & Sons, Inc.).

Alonso, A., Sasin, J., Bottini, N., Friedberg, I., Friedberg, I., Osterman, A., Godzik, A., Hunter, T., Dixon, J., and Mustelin, T. (2004). Protein tyrosine phosphatases in the human genome. Cell *117*, 699-711.

Ambrosino, C., and Nebreda, A. R. (2001). Cell cycle regulation by p38 MAP kinases. Biology of the cell / under the auspices of the European Cell Biology Organization *93*, 47-51.

Andersen, J. K. (2004). Oxidative stress in neurodegeneration: cause or consequence? Nature medicine *10 Suppl*, S18-25.

Arner, E. S., and Holmgren, A. (2000). Physiological functions of thioredoxin and thioredoxin reductase. European journal of biochemistry / FEBS *267*, 6102-6109.

Aunoble, B., Sanches, R., Didier, E., and Bignon, Y. J. (2000). Major oncogenes and tumor suppressor genes involved in epithelial ovarian cancer (review). International journal of oncology *16*, 567-576.

Avruch, J. (2007). MAP kinase pathways: the first twenty years. Biochimica et biophysica acta *1773*, 1150-1160.

Bae, I. H., Kang, S. W., Yoon, S. H., and Um, H. D. (2006). Cellular components involved in the cell death induced by cisplatin in the absence of p53 activation. Oncology reports *15*, 1175-1180.

Bae, Y. S., Sung, J. Y., Kim, O. S., Kim, Y. J., Hur, K. C., Kazlauskas, A., and Rhee, S. G. (2000). Platelet-derived growth factor-induced H(2)O(2) production requires the activation of phosphatidylinositol 3-kinase. J Biol Chem *275*, 10527-10531.

Bendayan, M., and Reddy, J. K. (1982). Immunocytochemical localization of catalase and heat-labile enoyl-CoA hydratase in the livers of normal and peroxisome proliferator-treated rats. Laboratory investigation; a journal of technical methods and pathology *47*, 364-369.

Beutler, E. (1969). Effect of flavin compounds on glutathione reductase activity: in vivo and in vitro studies. The Journal of clinical investigation *48*, 1957-1966.

Bienert, G. P., Moller, A. L., Kristiansen, K. A., Schulz, A., Moller, I. M., Schjoerring, J. K., and Jahn, T. P. (2007). Specific aquaporins facilitate the diffusion of hydrogen peroxide across membranes. J Biol Chem *282*, 1183-1192.

Bode, A. M., and Dong, Z. (2007). The functional contrariety of JNK. Molecular carcinogenesis *46*, 591-598.

Boulikas, T., and Vougiouka, M. (2003). Cisplatin and platinum drugs at the molecular level. (Review). Oncology reports *10*, 1663-1682.

Boulton, T. G., Nye, S. H., Robbins, D. J., Ip, N. Y., Radziejewska, E., Morgenbesser, S. D., DePinho, R. A., Panayotatos, N., Cobb, M. H., and Yancopoulos, G. D. (1991). ERKs: a family of protein-serine/threonine kinases that are activated and tyrosine phosphorylated in response to insulin and NGF. Cell *65*, 663-675.

Brabec, V., and Balcarova, Z. (1993). Restriction-enzyme cleavage of DNA modified by platinum(II) complexes. European journal of biochemistry / FEBS *216*, 183-187.

Brigelius-Flohe, R. (1999). Tissue-specific functions of individual glutathione peroxidases. Free Radic Biol Med *27*, 951-965.

Brondello, J. M., Brunet, A., Pouyssegur, J., and McKenzie, F. R. (1997). The dual specificity mitogen-activated protein kinase phosphatase-1 and -2 are induced by the p42/p44MAPK cascade. J Biol Chem *272*, 1368-1376.

Brozovic, A., and Osmak, M. (2007). Activation of mitogen-activated protein kinases by cisplatin and their role in cisplatin-resistance. Cancer Lett *251*, 1-16.

Bulavin, D. V., Demidov, O. N., Saito, S., Kauraniemi, P., Phillips, C., Amundson, S. A., Ambrosino, C., Sauter, G., Nebreda, A. R., Anderson, C. W., *et al.* (2002). Amplification of PPM1D in human tumors abrogates p53 tumor-suppressor activity. Nature genetics *31*, 210-215.

Bulavin, D. V., and Fornace, A. J., Jr. (2004). p38 MAP kinase's emerging role as a tumor suppressor. Advances in cancer research *92*, 95-118.

Carlberg, I., and Mannervik, B. (1975). Purification and characterization of the flavoenzyme glutathione reductase from rat liver. J Biol Chem *250*, 5475-5480.

Cecena, G., Wen, F., Cardiff, R. D., and Oshima, R. G. (2006). Differential sensitivity of mouse epithelial tissues to the polyomavirus middle T oncogene. The American journal of pathology *168*, 310-320.

Chen, L., Mayer, J. A., Krisko, T. I., Speers, C. W., Wang, T., Hilsenbeck, S. G., and Brown, P. H. (2009). Inhibition of the p38 kinase suppresses the proliferation of human ER-negative breast cancer cells. Cancer research *69*, 8853-8861.

Chen, Y. R., and Tan, T. H. (2000). The c-Jun N-terminal kinase pathway and apoptotic signaling (review). International journal of oncology *16*, 651-662.

Cheon, D. J., and Orsulic, S. (2011). Mouse models of cancer. Annual review of pathology *6*, 95-119.

Chiacchiera, F., Matrone, A., Ferrari, E., Ingravallo, G., Lo Sasso, G., Murzilli, S., Petruzzelli, M., Salvatore, L., Moschetta, A., and Simone, C. (2009). p38alpha blockade inhibits colorectal cancer growth in vivo by inducing a switch from HIF1alpha- to FoxO-dependent transcription. Cell death and differentiation *16*, 1203-1214.

Chiarugi, P., and Cirri, P. (2003). Redox regulation of protein tyrosine phosphatases during receptor tyrosine kinase signal transduction. Trends in biochemical sciences *28*, 509-514.

Chiarugi, P., and Fiaschi, T. (2007). Redox signalling in anchorage-dependent cell growth. Cellular signalling *19*, 672-682.

Cohen, P. (2009). Targeting protein kinases for the development of anti-inflammatory drugs. Current opinion in cell biology *21*, 317-324.

Copin, J. C., Gasche, Y., and Chan, P. H. (2000). Overexpression of copper/zinc superoxide dismutase does not prevent neonatal lethality in mutant mice that lack manganese superoxide dismutase. Free Radic Biol Med *28*, 1571-1576.

Coulthard, L. R., White, D. E., Jones, D. L., McDermott, M. F., and Burchill, S. A. (2009). p38(MAPK): stress responses from molecular mechanisms to therapeutics. Trends in molecular medicine *15*, 369-379.

Crompton, M. (1999). The mitochondrial permeability transition pore and its role in cell death. The Biochemical journal *341 (Pt 2)*, 233-249.

Cuadrado, A., and Nebreda, A. R. (2010). Mechanisms and functions of p38 MAPK signalling. The Biochemical journal *429*, 403-417.

Cuenda, A., Cohen, P., Buee-Scherrer, V., and Goedert, M. (1997). Activation of stress-activated protein kinase-3 (SAPK3) by cytokines and cellular stresses is mediated via SAPKK3 (MKK6); comparison of the specificities of SAPK3 and SAPK2 (RK/p38). The EMBO journal *16*, 295-305.

Cuenda, A., and Rousseau, S. (2007). p38 MAP-kinases pathway regulation, function and role in human diseases. Biochimica et biophysica acta *1773*, 1358-1375.

Cuevas, B. D., Abell, A. N., and Johnson, G. L. (2007). Role of mitogen-activated protein kinase kinase kinases in signal integration. Oncogene *26*, 3159-3171.

Davis, R. J. (2000). Signal transduction by the JNK group of MAP kinases. Cell *103*, 239-252.

Dawe, C. J., Freund, R., Mandel, G., Ballmer-Hofer, K., Talmage, D. A., and Benjamin, T. L. (1987). Variations in polyoma virus genotype in relation to tumor

induction in mice. Characterization of wild type strains with widely differing tumor profiles. The American journal of pathology *127*, 243-261.

Demuth, T., Reavie, L. B., Rennert, J. L., Nakada, M., Nakada, S., Hoelzinger, D. B., Beaudry, C. E., Henrichs, A. N., Anderson, E. M., and Berens, M. E. (2007). MAP-ing glioma invasion: mitogen-activated protein kinase kinase 3 and p38 drive glioma invasion and progression and predict patient survival. Molecular cancer therapeutics *6*, 1212-1222.

den Hertog, J., Groen, A., and van der Wijk, T. (2005). Redox regulation of protein-tyrosine phosphatases. Archives of biochemistry and biophysics *434*, 11-15.

Derijard, B., Hibi, M., Wu, I. H., Barrett, T., Su, B., Deng, T., Karin, M., and Davis, R. J. (1994). JNK1: a protein kinase stimulated by UV light and Ha-Ras that binds and phosphorylates the c-Jun activation domain. Cell *76*, 1025-1037.

Desai, K. V., Xiao, N., Wang, W., Gangi, L., Greene, J., Powell, J. I., Dickson, R., Furth, P., Hunter, K., Kucherlapati, R., *et al.* (2002). Initiating oncogenic event determines gene-expression patterns of human breast cancer models. Proceedings of the National Academy of Sciences of the United States of America *99*, 6967-6972.

Dhillon, A. S., Hagan, S., Rath, O., and Kolch, W. (2007). MAP kinase signalling pathways in cancer. Oncogene *26*, 3279-3290.

Dickinson, R. J., and Keyse, S. M. (2006). Diverse physiological functions for dual-specificity MAP kinase phosphatases. Journal of cell science *119*, 4607-4615.

Dolado, I., Swat, A., Ajenjo, N., De Vita, G., Cuadrado, A., and Nebreda, A. R. (2007). p38alpha MAP kinase as a sensor of reactive oxygen species in tumorigenesis. Cancer cell *11*, 191-205.

Dreskin, S. C., Thomas, G. W., Dale, S. N., and Heasley, L. E. (2001). Isoforms of Jun kinase are differentially expressed and activated in human monocyte/macrophage (THP-1) cells. J Immunol *166*, 5646-5653.

Ekerot, M., Stavridis, M. P., Delavaine, L., Mitchell, M. P., Staples, C., Owens, D. M., Keenan, I. D., Dickinson, R. J., Storey, K. G., and Keyse, S. M. (2008). Negative-feedback regulation of FGF signalling by DUSP6/MKP-3 is driven by ERK1/2 and mediated by Ets factor binding to a conserved site within the DUSP6/MKP-3 gene promoter. The Biochemical journal *412*, 287-298.

el-Khateeb, M., Appleton, T. G., Gahan, L. R., Charles, B. G., Berners-Price, S. J., and Bolton, A. M. (1999). Reactions of cisplatin hydrolytes with methionine, cysteine, and plasma ultrafiltrate studied by a combination of HPLC and NMR techniques. Journal of inorganic biochemistry *77*, 13-21.

Elenitoba-Johnson, K. S., Jenson, S. D., Abbott, R. T., Palais, R. A., Bohling, S. D., Lin, Z., Tripp, S., Shami, P. J., Wang, L. Y., Coupland, R. W., *et al.* (2003). Involvement of multiple signaling pathways in follicular lymphoma transformation: p38-mitogen-activated protein kinase as a target for therapy. Proceedings of the National Academy of Sciences of the United States of America *100*, 7259-7264.

Engel, R. H., and Evens, A. M. (2006). Oxidative stress and apoptosis: a new treatment paradigm in cancer. Frontiers in bioscience : a journal and virtual library *11*, 300-312.

Enslen, H., Raingeaud, J., and Davis, R. J. (1998). Selective activation of p38 mitogen-activated protein (MAP) kinase isoforms by the MAP kinase kinases MKK3 and MKK6. J Biol Chem *273*, 1741-1748.

Esteva, F. J., Sahin, A. A., Smith, T. L., Yang, Y., Pusztai, L., Nahta, R., Buchholz, T. A., Buzdar, A. U., Hortobagyi, G. N., and Bacus, S. S. (2004). Prognostic significance of phosphorylated P38 mitogen-activated protein kinase and HER-2 expression in lymph node-positive breast carcinoma. Cancer *100*, 499-506.

Evers, B., Schut, E., van der Burg, E., Braumuller, T. M., Egan, D. A., Holstege, H., Edser, P., Adams, D. J., Wade-Martins, R., Bouwman, P., and Jonkers, J. (2010). A high-throughput pharmaceutical screen identifies compounds with specific toxicity against BRCA2-deficient tumors. Clinical cancer research : an official journal of the American Association for Cancer Research *16*, 99-108.

Ferraro, D., Corso, S., Fasano, E., Panieri, E., Santangelo, R., Borrello, S., Giordano, S., Pani, G., and Galeotti, T. (2006). Pro-metastatic signaling by c-Met through RAC-1 and reactive oxygen species (ROS). Oncogene *25*, 3689-3698.

Finkel, T. (2003). Oxidant signals and oxidative stress. Current opinion in cell biology *15*, 247-254.

Fluck, M. M., and Haslam, S. Z. (1996). Mammary tumors induced by polyomavirus. Breast cancer research and treatment *39*, 45-56.

Fluck, M. M., and Schaffhausen, B. S. (2009). Lessons in signaling and tumorigenesis from polyomavirus middle T antigen. Microbiology and molecular biology reviews : MMBR *73*, 542-563, Table of Contents.

Fong, P. C., Boss, D. S., Yap, T. A., Tutt, A., Wu, P., Mergui-Roelvink, M., Mortimer, P., Swaisland, H., Lau, A., O'Connor, M. J., *et al.* (2009). Inhibition of poly(ADP-ribose) polymerase in tumors from BRCA mutation carriers. The New England journal of medicine *361*, 123-134.

Frese, K. K., and Tuveson, D. A. (2007). Maximizing mouse cancer models. Nat Rev Cancer *7*, 645-658.

Freshney, N. W., Rawlinson, L., Guesdon, F., Jones, E., Cowley, S., Hsuan, J., and Saklatvala, J. (1994). Interleukin-1 activates a novel protein kinase cascade that results in the phosphorylation of Hsp27. Cell *78*, 1039-1049.

Fuertes, M. A., Alonso, C., and Perez, J. M. (2003). Biochemical modulation of Cisplatin mechanisms of action: enhancement of antitumor activity and circumvention of drug resistance. Chemical reviews *103*, 645-662.

Galan-Moya, E. M., de la Cruz-Morcillo, M. A., Llanos Valero, M., Callejas-Valera, J. L., Melgar-Rojas, P., Hernadez Losa, J., Salcedo, M., Fernandez-Aramburo, A., Ramon y Cajal, S., and Sanchez-Prieto, R. (2011). Balance between MKK6 and MKK3 mediates p38 MAPK associated resistance to cisplatin in NSCLC. PLoS One *6*, e28406.

Goedert, M., Cuenda, A., Craxton, M., Jakes, R., and Cohen, P. (1997). Activation of the novel stress-activated protein kinase SAPK4 by cytokines and cellular stresses is mediated by SKK3 (MKK6); comparison of its substrate specificity with that of other SAP kinases. The EMBO journal *16*, 3563-3571.

Gohla, A., Birkenfeld, J., and Bokoch, G. M. (2005). Chronophin, a novel HAD-type serine protein phosphatase, regulates cofilin-dependent actin dynamics. Nature cell biology *7*, 21-29.

Goldstein, B. J., Mahadev, K., Wu, X., Zhu, L., and Motoshima, H. (2005). Role of insulin-induced reactive oxygen species in the insulin signaling pathway. Antioxidants & redox signaling *7*, 1021-1031.

Goldstein, D. M., Kuglstatter, A., Lou, Y., and Soth, M. J. (2010). Selective p38alpha inhibitors clinically evaluated for the treatment of chronic inflammatory disorders. Journal of medicinal chemistry *53*, 2345-2353.

Goustin, A. S., Leof, E. B., Shipley, G. D., and Moses, H. L. (1986). Growth factors and cancer. Cancer research *46*, 1015-1029.

Griendling, K. K., Minieri, C. A., Ollerenshaw, J. D., and Alexander, R. W. (1994). Angiotensin II stimulates NADH and NADPH oxidase activity in cultured vascular smooth muscle cells. Circulation research *74*, 1141-1148.

Groen, A., Lemeer, S., van der Wijk, T., Overvoorde, J., Heck, A. J., Ostman, A., Barford, D., Slijper, M., and den Hertog, J. (2005). Differential oxidation of protein-tyrosine phosphatases. J Biol Chem *280*, 10298-10304.

Gupta, S., Barrett, T., Whitmarsh, A. J., Cavanagh, J., Sluss, H. K., Derijard, B., and Davis, R. J. (1996). Selective interaction of JNK protein kinase isoforms with transcription factors. The EMBO journal *15*, 2760-2770.

Gutierrez-Uzquiza, A., Arechederra, M., Bragado, P., Aguirre-Ghiso, J. A., and Porras, A. (2012). p38alpha mediates cell survival in response to oxidative stress

via induction of antioxidant genes: effect on the p70S6K pathway. J Biol Chem *287*, 2632-2642.

Guy, C. T., Cardiff, R. D., and Muller, W. J. (1992). Induction of mammary tumors by expression of polyomavirus middle T oncogene: a transgenic mouse model for metastatic disease. Molecular and cellular biology *12*, 954-961.

Haigis, M. C., and Yankner, B. A. (2010). The aging stress response. Molecular cell *40*, 333-344.

Han, D., Williams, E., and Cadenas, E. (2001). Mitochondrial respiratory chain-dependent generation of superoxide anion and its release into the intermembrane space. The Biochemical journal *353*, 411-416.

Han, J., Lee, J. D., Bibbs, L., and Ulevitch, R. J. (1994). A MAP kinase targeted by endotoxin and hyperosmolarity in mammalian cells. Science *265*, 808-811.

Hanahan, D., and Weinberg, R. A. (2000). The hallmarks of cancer. Cell *100*, 57-70.

Hanahan, D., and Weinberg, R. A. (2011). Hallmarks of cancer: the next generation. Cell *144*, 646-674.

Haq, R., Brenton, J. D., Takahashi, M., Finan, D., Finkielsztein, A., Damaraju, S., Rottapel, R., and Zanke, B. (2002). Constitutive p38HOG mitogen-activated protein kinase activation induces permanent cell cycle arrest and senescence. Cancer research *62*, 5076-5082.

Hashimoto, F., and Hayashi, H. (1990). Significance of catalase in peroxisomal fatty acyl-CoA beta-oxidation: NADH oxidation by acetoacetyl-CoA and H2O2. Journal of biochemistry *108*, 426-431.

Hayes, J. D., Flanagan, J. U., and Jowsey, I. R. (2005). Glutathione transferases. Annual review of pharmacology and toxicology *45*, 51-88.

Hazzalin, C. A., Cano, E., Cuenda, A., Barratt, M. J., Cohen, P., and Mahadevan, L. C. (1996). p38/RK is essential for stress-induced nuclear responses: JNK/SAPKs and c-Jun/ATF-2 phosphorylation are insufficient. Current biology : CB *6*, 1028-1031.

Hofmann, B., Hecht, H. J., and Flohe, L. (2002). Peroxiredoxins. Biological chemistry *383*, 347-364.

Hope, H. R., Anderson, G. D., Burnette, B. L., Compton, R. P., Devraj, R. V., Hirsch, J. L., Keith, R. H., Li, X., Mbalaviele, G., Messing, D. M., *et al.* (2009). Anti-inflammatory properties of a novel N-phenyl pyridinone inhibitor of p38 mitogen-activated protein kinase: preclinical-to-clinical translation. The Journal of pharmacology and experimental therapeutics *331*, 882-895.

Hou, N., Torii, S., Saito, N., Hosaka, M., and Takeuchi, T. (2008). Reactive oxygen species-mediated pancreatic beta-cell death is regulated by interactions between stress-activated protein kinases, p38 and c-Jun N-terminal kinase, and mitogen-activated protein kinase phosphatases. Endocrinology *149*, 1654-1665.

Hui, L., Bakiri, L., Mairhorfer, A., Schweifer, N., Haslinger, C., Kenner, L., Komnenovic, V., Scheuch, H., Beug, H., and Wagner, E. F. (2007). p38alpha suppresses normal and cancer cell proliferation by antagonizing the JNK-c-Jun pathway. Nature genetics *39*, 741-749.

Ip, Y. T., and Davis, R. J. (1998). Signal transduction by the c-Jun N-terminal kinase (JNK)--from inflammation to development. Current opinion in cell biology *10*, 205-219.

Irmak, M. B., Ince, G., Ozturk, M., and Cetin-Atalay, R. (2003). Acquired tolerance of hepatocellular carcinoma cells to selenium deficiency: a selective survival mechanism? Cancer research *63*, 6707-6715.

Jamieson, E. R., and Lippard, S. J. (1999). Structure, Recognition, and Processing of Cisplatin-DNA Adducts. Chemical reviews *99*, 2467-2498.

Jeffrey, K. L., Camps, M., Rommel, C., and Mackay, C. R. (2007). Targeting dual-specificity phosphatases: manipulating MAP kinase signalling and immune responses. Nature reviews Drug discovery *6*, 391-403.

Jiang, Y., Chen, C., Li, Z., Guo, W., Gegner, J. A., Lin, S., and Han, J. (1996). Characterization of the structure and function of a new mitogen-activated protein kinase (p38beta). J Biol Chem *271*, 17920-17926.

Jiang, Y., Gram, H., Zhao, M., New, L., Gu, J., Feng, L., Di Padova, F., Ulevitch, R. J., and Han, J. (1997). Characterization of the structure and function of the fourth member of p38 group mitogen-activated protein kinases, p38delta. J Biol Chem *272*, 30122-30128.

Jordan, P., and Carmo-Fonseca, M. (2000). Molecular mechanisms involved in cisplatin cytotoxicity. Cellular and molecular life sciences : CMLS *57*, 1229-1235.

Julien, S. G., Dube, N., Hardy, S., and Tremblay, M. L. (2011). Inside the human cancer tyrosine phosphatome. Nat Rev Cancer *11*, 35-49.

Kaelin, W. G., Jr. (2005). The concept of synthetic lethality in the context of anticancer therapy. Nat Rev Cancer *5*, 689-698.

Kamata, H., Honda, S., Maeda, S., Chang, L., Hirata, H., and Karin, M. (2005). Reactive oxygen species promote TNFalpha-induced death and sustained JNK activation by inhibiting MAP kinase phosphatases. Cell *120*, 649-661.

Karisch, R., Fernandez, M., Taylor, P., Virtanen, C., St-Germain, J. R., Jin, L. L., Harris, I. S., Mori, J., Mak, T. W., Senis, Y. A., *et al.* (2011). Global proteomic assessment of the classical protein-tyrosine phosphatome and "Redoxome". Cell *146*, 826-840.

Karlsson-Rosenthal, C., and Millar, J. B. (2006). Cdc25: mechanisms of checkpoint inhibition and recovery. Trends in cell biology *16*, 285-292.

Kelland, L. R. (2000). Preclinical perspectives on platinum resistance. Drugs *59 Suppl 4*, 1-8; discussion 37-38.

Keshet, Y., and Seger, R. (2010). The MAP kinase signaling cascades: a system of hundreds of components regulates a diverse array of physiological functions. Methods Mol Biol *661*, 3-38.

Keyse, S. M. (2000). Protein phosphatases and the regulation of mitogen-activated protein kinase signalling. Current opinion in cell biology *12*, 186-192.

Keyse, S. M. (2008). Dual-specificity MAP kinase phosphatases (MKPs) and cancer. Cancer Metastasis Rev *27*, 253-261.

Kim, G. J., Chandrasekaran, K., and Morgan, W. F. (2006). Mitochondrial dysfunction, persistently elevated levels of reactive oxygen species and radiation-induced genomic instability: a review. Mutagenesis *21*, 361-367.

Koyama, T., Mikami, T., Koyama, T., Imakiire, A., Yamamoto, K., Toyota, H., and Mizuguchi, J. (2006). Apoptosis induced by chemotherapeutic agents involves c-Jun N-terminal kinase activation in sarcoma cell lines. Journal of orthopaedic research : official publication of the Orthopaedic Research Society *24*, 1153-1162.

Krilleke, D., Ucur, E., Pulte, D., Schulze-Osthoff, K., Debatin, K. M., and Herr, I. (2003). Inhibition of JNK signaling diminishes early but not late cellular stress-induced apoptosis. International journal of cancer *107*, 520-527.

Krishna, M., and Narang, H. (2008). The complexity of mitogen-activated protein kinases (MAPKs) made simple. Cellular and molecular life sciences : CMLS *65*, 3525-3544.

Kummer, J. L., Rao, P. K., and Heidenreich, K. A. (1997). Apoptosis induced by withdrawal of trophic factors is mediated by p38 mitogen-activated protein kinase. J Biol Chem *272*, 20490-20494.

Kurosu, T., Takahashi, Y., Fukuda, T., Koyama, T., Miki, T., and Miura, O. (2005). p38 MAP kinase plays a role in G2 checkpoint activation and inhibits apoptosis of human B cell lymphoma cells treated with etoposide. Apoptosis : an international journal on programmed cell death *10*, 1111-1120.

Kyriakis, J. M., and Avruch, J. (2012). Mammalian MAPK signal transduction pathways activated by stress and inflammation: a 10-year update. Physiological reviews *92*, 689-737.

Kyriakis, J. M., Banerjee, P., Nikolakaki, E., Dai, T., Rubie, E. A., Ahmad, M. F., Avruch, J., and Woodgett, J. R. (1994). The stress-activated protein kinase subfamily of c-Jun kinases. Nature *369*, 156-160.

Labbe, D. P., Hardy, S., and Tremblay, M. L. (2012). Protein tyrosine phosphatases in cancer: friends and foes! Prog Mol Biol Transl Sci *106*, 253-306.

Lambeth, J. D. (2004). NOX enzymes and the biology of reactive oxygen. Nature reviews Immunology *4*, 181-189.

Lechner, C., Zahalka, M. A., Giot, J. F., Moller, N. P., and Ullrich, A. (1996). ERK6, a mitogen-activated protein kinase involved in C2C12 myoblast differentiation. Proceedings of the National Academy of Sciences of the United States of America *93*, 4355-4359.

Lee, J. D., Ulevitch, R. J., and Han, J. (1995). Primary structure of BMK1: a new mammalian map kinase. Biochemical and biophysical research communications *213*, 715-724.

Levresse, V., Marek, L., Blumberg, D., and Heasley, L. E. (2002). Regulation of platinum-compound cytotoxicity by the c-Jun N-terminal kinase and c-Jun signaling pathway in small-cell lung cancer cells. Molecular pharmacology *62*, 689-697.

Li, F., Meng, L., Zhou, J., Xing, H., Wang, S., Xu, G., Zhu, H., Wang, B., Chen, G., Lu, Y. P., and Ma, D. (2005). Reversing chemoresistance in cisplatin-resistant human ovarian cancer cells: a role of c-Jun NH2-terminal kinase 1. Biochemical and biophysical research communications *335*, 1070-1077.

Lin, E. Y., Jones, J. G., Li, P., Zhu, L., Whitney, K. D., Muller, W. J., and Pollard, J. W. (2003). Progression to malignancy in the polyoma middle T oncoprotein mouse breast cancer model provides a reliable model for human diseases. The American journal of pathology *163*, 2113-2126.

Liou, G. Y., and Storz, P. (2010). Reactive oxygen species in cancer. Free radical research *44*, 479-496.

Litwin, J. A., Volkl, A., Muller-Hocker, J., Hashimoto, T., and Fahimi, H. D. (1987). Immunocytochemical localization of peroxisomal enzymes in human liver biopsies. The American journal of pathology *128*, 141-150.

Lo, Y. Y., and Cruz, T. F. (1995). Involvement of reactive oxygen species in cytokine and growth factor induction of c-fos expression in chondrocytes. J Biol Chem *270*, 11727-11730.

Lunn, J. E., Ashton, A. R., Hatch, M. D., and Heldt, H. W. (2000). Purification, molecular cloning, and sequence analysis of sucrose-6F-phosphate phosphohydrolase from plants. Proceedings of the National Academy of Sciences of the United States of America *97*, 12914-12919.

Mansouri, A., Ridgway, L. D., Korapati, A. L., Zhang, Q., Tian, L., Wang, Y., Siddik, Z. H., Mills, G. B., and Claret, F. X. (2003). Sustained activation of JNK/p38 MAPK pathways in response to cisplatin leads to Fas ligand induction and cell death in ovarian carcinoma cells. J Biol Chem *278*, 19245-19256.

Martyn, K. D., Frederick, L. M., von Loehneysen, K., Dinauer, M. C., and Knaus, U. G. (2006). Functional analysis of Nox4 reveals unique characteristics compared to other NADPH oxidases. Cellular signalling *18*, 69-82.

Mateescu, B., Batista, L., Cardon, M., Gruosso, T., de Feraudy, Y., Mariani, O., Nicolas, A., Meyniel, J. P., Cottu, P., Sastre-Garau, X., and Mechta-Grigoriou, F. (2011). miR-141 and miR-200a act on ovarian tumorigenesis by controlling oxidative stress response. Nature medicine *17*, 1627-1635.

Mertens, S., Craxton, M., and Goedert, M. (1996). SAP kinase-3, a new member of the family of mammalian stress-activated protein kinases. FEBS letters *383*, 273-276.

Minamoto, T., Mai, M., and Ronai, Z. (2000). K-ras mutation: early detection in molecular diagnosis and risk assessment of colorectal, pancreas, and lung cancers--a review. Cancer detection and prevention *24*, 1-12.

Minamoto, T., Ougolkov, A. V., and Mai, M. (2002). Detection of oncogenes in the diagnosis of cancers with active oncogenic signaling. Expert review of molecular diagnostics *2*, 565-575.

Moorhead, G. B., Trinkle-Mulcahy, L., and Ulke-Lemee, A. (2007). Emerging roles of nuclear protein phosphatases. Nature reviews Molecular cell biology *8*, 234-244.

Muniyappa, H., and Das, K. C. (2008). Activation of c-Jun N-terminal kinase (JNK) by widely used specific p38 MAPK inhibitors SB202190 and SB203580: a MLK-3-MKK7-dependent mechanism. Cellular signalling *20*, 675-683.

Mustacich, D., and Powis, G. (2000). Thioredoxin reductase. The Biochemical journal *346 Pt 1*, 1-8.

Navas, T. A., Nguyen, A. N., Hideshima, T., Reddy, M., Ma, J. Y., Haghnazari, E., Henson, M., Stebbins, E. G., Kerr, I., O'Young, G., *et al.* (2006). Inhibition of p38alpha MAPK enhances proteasome inhibitor-induced apoptosis of myeloma cells by modulating Hsp27, Bcl-X(L), Mcl-1 and p53 levels in vitro and inhibits tumor growth in vivo. Leukemia *20*, 1017-1027.

Nehme, A., Baskaran, R., Aebi, S., Fink, D., Nebel, S., Cenni, B., Wang, J. Y., Howell, S. B., and Christen, R. D. (1997). Differential induction of c-Jun NH2-terminal kinase and c-Abl kinase in DNA mismatch repair-proficient and -deficient cells exposed to cisplatin. Cancer research *57*, 3253-3257.

Nemoto, S., Sheng, Z., and Lin, A. (1998). Opposing effects of Jun kinase and p38 mitogen-activated protein kinases on cardiomyocyte hypertrophy. Molecular and cellular biology *18*, 3518-3526.

Ostman, A., Frijhoff, J., Sandin, A., and Bohmer, F. D. (2011). Regulation of protein tyrosine phosphatases by reversible oxidation. Journal of biochemistry *150*, 345-356.

Paravicini, T. M., and Touyz, R. M. (2006). Redox signaling in hypertension. Cardiovascular research *71*, 247-258.

Patterson, K. I., Brummer, T., O'Brien, P. M., and Daly, R. J. (2009). Dual-specificity phosphatases: critical regulators with diverse cellular targets. The Biochemical journal *418*, 475-489.

Perdiguero, E., Ruiz-Bonilla, V., Gresh, L., Hui, L., Ballestar, E., Sousa-Victor, P., Baeza-Raja, B., Jardi, M., Bosch-Comas, A., Esteller, M.*, et al.* (2007a). Genetic analysis of p38 MAP kinases in myogenesis: fundamental role of p38alpha in abrogating myoblast proliferation. The EMBO journal *26*, 1245-1256.

Perdiguero, E., Ruiz-Bonilla, V., Serrano, A. L., and Muñoz-Cánoves, P. (2007b). Genetic deficiency of p38alpha reveals its critical role in myoblast cell cycle exit: the p38alpha-JNK connection. Cell Cycle *6*, 1298-1303.

Perou, C. M., Sorlie, T., Eisen, M. B., van de Rijn, M., Jeffrey, S. S., Rees, C. A., Pollack, J. R., Ross, D. T., Johnsen, H., Akslen, L. A.*, et al.* (2000). Molecular portraits of human breast tumours. Nature *406*, 747-752.

Persons, D. L., Yazlovitskaya, E. M., Cui, W., and Pelling, J. C. (1999). Cisplatin-induced activation of mitogen-activated protein kinases in ovarian carcinoma cells: inhibition of extracellular signal-regulated kinase activity increases sensitivity to cisplatin. Clinical cancer research : an official journal of the American Association for Cancer Research *5*, 1007-1014.

Phong, M. S., Van Horn, R. D., Li, S., Tucker-Kellogg, G., Surana, U., and Ye, X. S. (2010). p38 mitogen-activated protein kinase promotes cell survival in response to DNA damage but is not required for the G(2) DNA damage checkpoint in human cancer cells. Molecular and cellular biology *30*, 3816-3826.

Pomerance, M., Quillard, J., Chantoux, F., Young, J., and Blondeau, J. P. (2006). High-level expression, activation, and subcellular localization of p38-MAP kinase in thyroid neoplasms. The Journal of pathology *209*, 298-306.

Raj, L., Ide, T., Gurkar, A. U., Foley, M., Schenone, M., Li, X., Tolliday, N. J., Golub, T. R., Carr, S. A., Shamji, A. F., *et al.* (2011). Selective killing of cancer cells by a small molecule targeting the stress response to ROS. Nature *475*, 231-234.

Rakitina, T. V., Vasilevskaya, I. A., and O'Dwyer, P. J. (2003). Additive interaction of oxaliplatin and 17-allylamino-17-demethoxygeldanamycin in colon cancer cell lines results from inhibition of nuclear factor kappaB signaling. Cancer research *63*, 8600-8605.

Raman, M., Chen, W., and Cobb, M. H. (2007). Differential regulation and properties of MAPKs. Oncogene *26*, 3100-3112.

Rassoulzadegan, M., Courtneidge, S. A., Loubiere, R., el Baze, P., and Cuzin, F. (1990). A variety of tumours induced by the middle T antigen of polyoma virus in a transgenic mouse family. Oncogene *5*, 1507-1510.

Rebay, I., Silver, S. J., and Tootle, T. L. (2005). New vision from Eyes absent: transcription factors as enzymes. Trends in genetics : TIG *21*, 163-171.

Reinhardt, H. C., Aslanian, A. S., Lees, J. A., and Yaffe, M. B. (2007). p53-deficient cells rely on ATM- and ATR-mediated checkpoint signaling through the p38MAPK/MK2 pathway for survival after DNA damage. Cancer Cell *11*, 175-189.

Rhee, S. G., Kang, S. W., Jeong, W., Chang, T. S., Yang, K. S., and Woo, H. A. (2005). Intracellular messenger function of hydrogen peroxide and its regulation by peroxiredoxins. Current opinion in cell biology *17*, 183-189.

Rhee, S. G., Kang, S. W., Netto, L. E., Seo, M. S., and Stadtman, E. R. (1999). A family of novel peroxidases, peroxiredoxins. Biofactors *10*, 207-209.

Ricote, M., Garcia-Tunon, I., Bethencourt, F., Fraile, B., Onsurbe, P., Paniagua, R., and Royuela, M. (2006). The p38 transduction pathway in prostatic neoplasia. The Journal of pathology *208*, 401-407.

Roberts, S. J., Stewart, A. J., Sadler, P. J., and Farquharson, C. (2004). Human PHOSPHO1 exhibits high specific phosphoethanolamine and phosphocholine phosphatase activities. The Biochemical journal *382*, 59-65.

Rouse, J., Cohen, P., Trigon, S., Morange, M., Alonso-Llamazares, A., Zamanillo, D., Hunt, T., and Nebreda, A. R. (1994). A novel kinase cascade triggered by stress and heat shock that stimulates MAPKAP kinase-2 and phosphorylation of the small heat shock proteins. Cell *78*, 1027-1037.

Roy, D., Sarkar, S., and Felty, Q. (2006). Levels of IL-1 beta control stimulatory/inhibitory growth of cancer cells. Frontiers in bioscience : a journal and virtual library *11*, 889-898.

Russell, P., and Nurse, P. (1986). cdc25+ functions as an inducer in the mitotic control of fission yeast. Cell *45*, 145-153.

Salmeen, A., and Barford, D. (2005). Functions and mechanisms of redox regulation of cysteine-based phosphatases. Antioxidants & redox signaling *7*, 560-577.

Sanchez-Perez, I., Benitah, S. A., Martinez-Gomariz, M., Lacal, J. C., and Perona, R. (2002). Cell stress and MEKK1-mediated c-Jun activation modulate NFkappaB activity and cell viability. Molecular biology of the cell *13*, 2933-2945.

Sanchez-Perez, I., Martinez-Gomariz, M., Williams, D., Keyse, S. M., and Perona, R. (2000). CL100/MKP-1 modulates JNK activation and apoptosis in response to cisplatin. Oncogene *19*, 5142-5152.

Sanchez-Perez, I., Murguia, J. R., and Perona, R. (1998). Cisplatin induces a persistent activation of JNK that is related to cell death. Oncogene *16*, 533-540.

Sanchez-Perez, I., and Perona, R. (1999). Lack of c-Jun activity increases survival to cisplatin. FEBS letters *453*, 151-158.

Schindler, E. M., Hindes, A., Gribben, E. L., Burns, C. J., Yin, Y., Lin, M. H., Owen, R. J., Longmore, G. D., Kissling, G. E., Arthur, J. S., and Efimova, T. (2009). p38delta Mitogen-activated protein kinase is essential for skin tumor development in mice. Cancer research *69*, 4648-4655.

Schneider, B. L., and Kulesz-Martin, M. (2004). Destructive cycles: the role of genomic instability and adaptation in carcinogenesis. Carcinogenesis *25*, 2033-2044.

Sharma, R., Yang, Y., Sharma, A., Awasthi, S., and Awasthi, Y. C. (2004). Antioxidant role of glutathione S-transferases: protection against oxidant toxicity and regulation of stress-mediated apoptosis. Antioxidants & redox signaling *6*, 289-300.

Shaw, A. T., Winslow, M. M., Magendantz, M., Ouyang, C., Dowdle, J., Subramanian, A., Lewis, T. A., Maglathin, R. L., Tolliday, N., and Jacks, T. (2011). Selective killing of K-ras mutant cancer cells by small molecule inducers of oxidative stress. Proceedings of the National Academy of Sciences of the United States of America *108*, 8773-8778.

She, Q. B., Bode, A. M., Ma, W. Y., Chen, N. Y., and Dong, Z. (2001). Resveratrol-induced activation of p53 and apoptosis is mediated by extracellular-signal-regulated protein kinases and p38 kinase. Cancer research *61*, 1604-1610.

Shen, H. M., and Liu, Z. G. (2006). JNK signaling pathway is a key modulator in cell death mediated by reactive oxygen and nitrogen species. Free Radic Biol Med *40*, 928-939.

Shukla, V., Mishra, S. K., and Pant, H. C. (2011). Oxidative stress in neurodegeneration. Advances in pharmacological sciences *2011*, 572634.

Sorlie, T., Tibshirani, R., Parker, J., Hastie, T., Marron, J. S., Nobel, A., Deng, S., Johnsen, H., Pesich, R., Geisler, S., *et al.* (2003). Repeated observation of breast tumor subtypes in independent gene expression data sets. Proceedings of the National Academy of Sciences of the United States of America *100*, 8418-8423.

Stepniak, E., Ricci, R., Eferl, R., Sumara, G., Sumara, I., Rath, M., Hui, L., and Wagner, E. F. (2006). c-Jun/AP-1 controls liver regeneration by repressing p53/p21 and p38 MAPK activity. Genes & development *20*, 2306-2314.

Storz, P. (2005). Reactive oxygen species in tumor progression. Frontiers in bioscience : a journal and virtual library *10*, 1881-1896.

Storz, P. (2006). Reactive oxygen species-mediated mitochondria-to-nucleus signaling: a key to aging and radical-caused diseases. Science's STKE : signal transduction knowledge environment *2006*, re3.

Sundaresan, M., Yu, Z. X., Ferrans, V. J., Irani, K., and Finkel, T. (1995). Requirement for generation of H2O2 for platelet-derived growth factor signal transduction. Science *270*, 296-299.

Szatrowski, T. P., and Nathan, C. F. (1991). Production of large amounts of hydrogen peroxide by human tumor cells. Cancer research *51*, 794-798.

Takeda, K., Noguchi, T., Naguro, I., and Ichijo, H. (2008). Apoptosis signal-regulating kinase 1 in stress and immune response. Annual review of pharmacology and toxicology *48*, 199-225.

Tehranian, A., Morris, D. W., Min, B. H., Bird, D. J., Cardiff, R. D., and Barry, P. A. (1996). Neoplastic transformation of prostatic and urogenital epithelium by the polyoma virus middle T gene. The American journal of pathology *149*, 1177-1191.

Teng, C. H., Huang, W. N., and Meng, T. C. (2007). Several dual specificity phosphatases coordinate to control the magnitude and duration of JNK activation in signaling response to oxidative stress. J Biol Chem *282*, 28395-28407.

Tiku, M. L., Liesch, J. B., and Robertson, F. M. (1990). Production of hydrogen peroxide by rabbit articular chondrocytes. Enhancement by cytokines. J Immunol *145*, 690-696.

Toh, W. H., Siddique, M. M., Boominathan, L., Lin, K. W., and Sabapathy, K. (2004). c-Jun regulates the stability and activity of the p53 homologue, p73. J Biol Chem *279*, 44713-44722.

Tonks, N. K. (2005). Redox redux: revisiting PTPs and the control of cell signaling. Cell *121*, 667-670.

Tonks, N. K. (2006). Protein tyrosine phosphatases: from genes, to function, to disease. Nature reviews Molecular cell biology *7*, 833-846.

Tournier, C., Hess, P., Yang, D. D., Xu, J., Turner, T. K., Nimnual, A., Bar-Sagi, D., Jones, S. N., Flavell, R. A., and Davis, R. J. (2000). Requirement of JNK for stress-induced activation of the cytochrome c-mediated death pathway. Science *288*, 870-874.

Townsend, D. M., and Tew, K. D. (2003). The role of glutathione-S-transferase in anti-cancer drug resistance. Oncogene *22*, 7369-7375.

Trachootham, D., Alexandre, J., and Huang, P. (2009). Targeting cancer cells by ROS-mediated mechanisms: a radical therapeutic approach? Nature reviews Drug discovery *8*, 579-591.

Trachootham, D., Zhou, Y., Zhang, H., Demizu, Y., Chen, Z., Pelicano, H., Chiao, P. J., Achanta, G., Arlinghaus, R. B., Liu, J., and Huang, P. (2006). Selective killing of oncogenically transformed cells through a ROS-mediated mechanism by beta-phenylethyl isothiocyanate. Cancer Cell *10*, 241-252.

Turner, N. C., and Jones, A. L. (2008). Management of breast cancer--Part II. BMJ *337*, a540.

Ursini, F., Maiorino, M., Brigelius-Flohe, R., Aumann, K. D., Roveri, A., Schomburg, D., and Flohe, L. (1995). Diversity of glutathione peroxidases. Methods in enzymology *252*, 38-53.

Vargo-Gogola, T., and Rosen, J. M. (2007). Modelling breast cancer: one size does not fit all. Nat Rev Cancer *7*, 659-672.

Vasilevskaya, I. A., Rakitina, T. V., and O'Dwyer, P. J. (2004). Quantitative effects on c-Jun N-terminal protein kinase signaling determine synergistic interaction of cisplatin and 17-allylamino-17-demethoxygeldanamycin in colon cancer cell lines. Molecular pharmacology *65*, 235-243.

Ventura, J. J., Tenbaum, S., Perdiguero, E., Huth, M., Guerra, C., Barbacid, M., Pasparakis, M., and Nebreda, A. R. (2007). p38alpha MAP kinase is essential in lung stem and progenitor cell proliferation and differentiation. Nature genetics *39*, 750-758.

Wada, T., Stepniak, E., Hui, L., Leibbrandt, A., Katada, T., Nishina, H., Wagner, E. F., and Penninger, J. M. (2008). Antagonistic control of cell fates by JNK and p38-MAPK signaling. Cell death and differentiation *15*, 89-93.

Wagner, E. F., and Nebreda, A. R. (2009). Signal integration by JNK and p38 MAPK pathways in cancer development. Nat Rev Cancer *9*, 537-549.

Wang, S. N., Lee, K. T., Tsai, C. J., Chen, Y. J., and Yeh, Y. T. (2012). Phosphorylated p38 and JNK MAPK proteins in hepatocellular carcinoma. Eur J Clin Invest.

Wang, W., Chen, J. X., Liao, R., Deng, Q., Zhou, J. J., Huang, S., and Sun, P. (2002). Sequential activation of the MEK-extracellular signal-regulated kinase and MKK3/6-p38 mitogen-activated protein kinase pathways mediates oncogenic ras-induced premature senescence. Molecular and cellular biology *22*, 3389-3403.

Wood, Z. A., Schroder, E., Robin Harris, J., and Poole, L. B. (2003). Structure, mechanism and regulation of peroxiredoxins. Trends in biochemical sciences *28*, 32-40.

Wu, Q., Huang, S., Sun, Y., Gu, S., Lu, F., Dai, J., Yin, G., Sun, L., Zheng, D., Dou, C.*, et al.* (2006). Dual specificity phosphotase 18, interacting with SAPK, dephosphorylates SAPK and inhibits SAPK/JNK signal pathway in vivo. Frontiers in bioscience : a journal and virtual library *11*, 2714-2724.

Wu, W. S., Wu, J. R., and Hu, C. T. (2008). Signal cross talks for sustained MAPK activation and cell migration: the potential role of reactive oxygen species. Cancer Metastasis Rev *27*, 303-314.

Xing, L., Shieh, H. S., Selness, S. R., Devraj, R. V., Walker, J. K., Devadas, B., Hope, H. R., Compton, R. P., Schindler, J. F., Hirsch, J. L.*, et al.* (2009). Structural bioinformatics-based prediction of exceptional selectivity of p38 MAP kinase inhibitor PH-797804. Biochemistry *48*, 6402-6411.

Yeo, M., Lin, P. S., Dahmus, M. E., and Gill, G. N. (2003). A novel RNA polymerase II C-terminal domain phosphatase that preferentially dephosphorylates serine 5. J Biol Chem *278*, 26078-26085.

Young, T. W., Mei, F. C., Yang, G., Thompson-Lanza, J. A., Liu, J., and Cheng, X. (2004). Activation of antioxidant pathways in ras-mediated oncogenic transformation of human surface ovarian epithelial cells revealed by functional proteomics and mass spectrometry. Cancer research *64*, 4577-4584.

Zhou, G., Bao, Z. Q., and Dixon, J. E. (1995). Components of a new human protein kinase signal transduction pathway. J Biol Chem *270*, 12665-12669.

Zick, Y. (2005). Ser/Thr phosphorylation of IRS proteins: a molecular basis for insulin resistance. Science's STKE : signal transduction knowledge environment *2005*, pe4.

Appendix

Library of inhibitors

The InhibitorSelect™ 96-Well Protein Kinase Inhibitor Library III consists of 84 protein kinase inhibitors, the majority of which are cell-permeable and ATP-competitive. They are supplied in a 96 well-plate format (**Suppl. Fig. 1**) at a concentration of 10 mM in DMSO (except for 3 of them, which are 5 mM). Their target pathways are specified in **Suppl. Table 1**.

Suppl. Table 1. Pathways targeted by InhibitorSelect™ Protein Kinase Inhibitor Library III

Target kinases			
AK	DNA-PK	MLCK	PKG
Akt	eEF2	Myt1	Plk
Aurora	GSK-3	p90RSK	Ras/Rac
c-Abl	IKK	PAK	Rho
CaMK	IP3K	PI3K	RIPK1
Cdks	Lck	PIKfyve	Src
CK1,2	MEK	PIM	Ste11
c-kit	MAPK	PKA	Tpl2
Chk1	MAPKAPK2	PKC	Wee1

	1	2	3	4	5	6	7	8	9	10	11	12
A	116890 Adenosine Kinase Inhibitor A1	124029 Akt Inhibitor XII, Isozyme-Selective, Akti-2 A2	181305 Arcyriaflavin A, Synthetic A3	191500 1-Azakenpaullone A4	203294 Bisindolylmaleimide III, Hydrochloride A5	203303 Bisindolylmaleimide V A6	203881 CR8, (R)-Isomer A7	203882 CR8, (S)-Isomer A8	208922 CaMKII Inhibitor, CK59 A9	217699 Cdk1 Inhibitor IV, RO-3306 A10	217707 c7/Cdk9 Inhibitor A11	BLANK 0 A12
B	218697 Casein Kinase II Inhibitor I B1	218713 Keratinocyte Differentiation Inducer B2	218714 Casein Kinase II Inhibitor IV B3	219445 Cdk2 Inhibitor II B4	219448 Cdk2/5 Inhibitor B5	219457 Cdk Inhibitor, p35 B6	220485 Chk2 Inhibitor B7	234501 Compound 401 B8	238806 Cdk2/9 Inhibitor B9	238811 Cdk9 Inhibitor II B10	238900 4-Cyano-3-methylisoquinoline B11	BLANK 0 B12
C	324515 eEF-2 Kinase Inhibitor, NH125 C1	361556 GSK-3 Inhibitor IX, Control, MeBIO C2	365252 Gö 7874, Hydrochloride C3	371958 H-8, Dihydrochloride C4	371964 HA 1004, Dihydrochloride C5	401482 IKK-2 Inhibitor V C6	401483 IKK-2 Inhibitor VI C7	401486 IKK Inhibitor VII C8	401487 IKK-2 Inhibitor VIII C9	401488 IKK-3 Inhibitor IX C10	401489 IKK Inhibitor X C11	BLANK 0 C12
D	401490 IKK-2 Inhibitor XI D1	402086 Indirubin-3'-monoxime, 5-Iodo- D2	406170 IP3K Inhibitor D3	407900 5-Iodotubercidin D4	420320 KT5720 D5	422709 KN-92 D6	440206 LY 294002, 4'-NH_2 D7	444965 MEK1/2 Inhibitor II D8	475864 MK-2 Inhibitor III D9	475880 ML-7, Hydrochloride D10	480065 Necroptotic Inhibitor, Nec-1 D11	BLANK 0 D12
E	DMSO 0 E1	495621 Olomoucine II E2	506106 p21-Activated Kinase Inhibitor III, IPA-3 E3	506153 p38 MAP Kinase Inhibitor IV E4	506157 p38 MAP Kinase Inhibitor VI, JX401 E5	506158 p38 MAP Kinase Inhibitor VII, SD-169 E6	506163 p38 MAP Kinase Inhibitor VIII E7	524611 PIKfyve Inhibitor E8	526520 PIM1 Inhibitor II E9	526522 PIM1 Kinase Inhibitor IV E10	526523 PIM1/2 Kinase Inhibitor V E11	BLANK 0 E12
F	DMSO 0 F1	526524 PIM1/2 Kinase Inhibitor VI F2	528111 PI 3-Kα Inhibitor IV F3	528112 PI 3-Kγ/CKII Inhibitor F4	528113 PI 3-Kβ Inhibitor VI, TGX-221 F5	528114 PI 3-Kγ Inhibitor VII F6	528116 PI 3-Kα Inhibitor V F7	528282 Plk Inhibitor I F8	528283 Plk Inhibitor II F9	539644 UCN-01 F10	551590 Quercetagetin F11	BLANK 0 F12
G	DMSO 0 G1	553509 Ras/Rac Transformation Blocker, SCH 51344 G2	554717 Reversine G3	555550 Rho Kinase Inhibitor G4	555551 Rho Kinase Inhibitor II G5	555555 Rho Kinase Inhibitor V G6	557360 Roscovitine G7	557362 Roscovitine, (S)-Isomer G8	557520 Ro-31-8220 G9	559285 RSK Inhibitor, SL0101 G10	559399 SB 203580, Sulfone G11	BLANK 0 G12
H	DMSO 0 H1	559404 SB 239063 H2	565715 Scytonemin, *Lyngbya* sp. H3	569615 Stem-Cell Factor/c-Kit Inhibitor, ISCK03 H4	570100 Ste11 MAPKKK Activation Inhibitor H5	616404 Tpl2 Kinase Inhibitor II H6	655203 TX-1918 H7	681500 WHI-P180, Hydrochloride H8	681637 Wee1/Chk1 Inhibitor H9	681640 Wee1 Inhibitor H10	681641 Wee1 Inhibitor II H11	BLANK 0 H12

Suppl. Figure 1. Protein kinase inhibitor library array. 96 well-plate display of the 84 inhibitors.

A

WT	1	2	3	4	5	6	7	8	9	10	11	12
A	8686	8974	8517	9543	9018	8952	8909	8781	9889	9815	10147	
B	10818	3399	11853	12723	10331	8116	10204	9464	5212	9760	10517	
C	155	9636	5351	10717	10988	3687	9398	3893	9639	11279	10281	9919
D	7737	11072	11415	10142	10900	10922	6913	8399	9751	10616	10728	10101
E	9727	6709	9764	10345	10655	9813	10917	4581	11314	8597	9854	10183
F	10292	9143	5323	9051	7537	10246	5751	9738	11430	1415	10900	28744
G	10644	7792	5193	7590	9458	8899	7370	6665	5610	9588	10054	27877
H	9163	9976	7860	9575	9470	9452	9639	8027	5558	6517	8295	26971

B

WT+SB	1	2	3	4	5	6	7	8	9	10	11	12
A	7843	9767	8616	10167	8501	8767	8016	7832	9530	9245	9115	
B	10907	3153	10713	11143	10138	8058	9773	9380	6016	9503	10470	
C	63	8420	5445	9895	9706	5521	7952	3500	8275	10232	9954	9481
D	8586	9888	10297	7908	9340	8958	7888	7640	9865	10025	10587	9476
E	6868	7436	9701	9267	9052	9631	8146	5778	9975	9177	9482	9107
F	8372	8497	5950	8705	7035	8837	4769	9340	11009	2702	10189	25651
G	7559	8850	5335	8319	8970	8335	7324	6636	3990	9108	7664	24782
H	6894	8858	6614	6098	8716	8071	7972	6077	4994	5886	6239	23387

C

WT/WT+SB	1	2	3	4	5	6	7	8	9	10	11	12
A	1.11	0.92	0.99	0.94	1.06	1.02	1.11	1.12	1.04	1.06	1.11	
B	0.99	1.08	1.11	1.14	1.02	1.01	1.04	1.01	0.87	1.03	1.00	
C	2.46	1.14	0.98	1.08	1.13	0.67	1.18	1.11	1.16	1.10	1.03	1.08
D	0.90	1.12	1.11	1.28	1.17	1.22	0.88	1.10	0.99	1.06	1.01	
E		0.90	1.01	1.12	1.18	1.02	1.34	0.79	1.13	0.94	1.04	
F		1.08	0.89	1.04	1.07	1.16	1.21	1.04	1.04	0.52	1.07	1.13
G		0.88	0.97	0.91	1.05	1.07	1.01	1.00	1.41	1.05	1.31	
H	1.34	1.13	1.19	1.57	1.09	1.17	1.21	1.32	1.11	1.11	1.33	

D

KO	1	2	3	4	5	6	7	8	9	10	11	12
A	5677.5	8126.5	6710.5	6567.5	7088.5	5100.5	5360.5	5328.5	6056.5	4848.5	5737.5	
B	8348.5	1729.5	7930.5	7269.5	7596.5	5244.5	5511.5	6901.5	3625.5	7148.5	8836.5	
C	43.5	4942.5	6638.5	7945.5	7219.5	1432.5	4221.5	856.5	3139.5	7321.5	7947.5	6561.5
D	5990.5	6195.5	7607.5	5117.5	7556.5	6254.5	5231.5	9228.5	6319.5	8800.5	7839.5	6810.5
E	6497.5	4895.5	8410.5	8442.5	7040.5	7172.5	7204.5	3983.5	7525.5	4262.5	6316.5	6538.5
F	8305.5	6497.5	5725.5	6689.5	3592.5	6043.5	1703.5	6231.5	8081.5	1917.5	8100.5	21035.5
G	8609.5	5631.5	4707.5	2098.5	6914.5	3623.5	6259.5	5673.5	3103.5	7839.5	6983.5	20275.5
H	6982.5	7007.5	4536.5	6452.5	7664.5	7300.5	7340.5	7490.5	3298.5	3769.5	5789.5	18811.5

E

KO+SB	1	2	3	4	5	6	7	8	9	10	11	12
A	5074.5	8349.5	6023.5	6457.5	6368.5	6162.5	5017.5	4995.5	5964.5	5303.5	4712.5	
B	8466.5	2044.5	8555.5	7114.5	7443.5	5506.5	6232.5	6758.5	3574.5	5771.5	8411.5	
C	43.5	5209.5	4986.5	7685.5	6304.5	2265.5	3611.5	828.5	4745.5	6927.5	6594.5	7477.5
D	5896.5	6006.5	8565.5	5040.5	8260.5	6454.5	6941.5	7623.5	7001.5	7116.5	7396.5	9418.5
E	9306.5	5926.5	8681.5	7689.5	6025.5	6536.5	5981.5	4702.5	6776.5	5919.5	6880.5	6303.5
F	9163.5	5240.5	5114.5	5739.5	4919.5	6097.5	2994.5	5330.5	7712.5	4324.5	7783.5	19162.5
G	6463.5	5367.5	3755.5	3330.5	5888.5	4294.5	5344.5	4679.5	1872.5	6454.5	5665.5	16124.5
H	5524.5	5702.5	4600.5	4841.5	6411.5	6061.5	6995.5	7072.5	3113.5	3561.5	4552.5	15302.5

F

KO/KO+SB	1	2	3	4	5	6	7	8	9	10	11	12
A	1.12	0.97	1.11	1.02	1.11	0.83	1.07	1.07	1.02	0.91	1.22	
B	0.99	0.85	0.93	1.02	1.02	0.95	0.88	1.02	1.01	1.24	1.05	
C	1.00	0.95	1.33	1.03	1.15	0.63	1.17	1.03	0.66	1.06	1.21	1.08
D	1.02	1.03	0.89	1.02	0.91	0.97	0.75	1.21	0.90	1.24	1.06	
E		0.83	0.97	1.10	1.17	1.10	1.20	0.85	1.11	0.72	0.92	
F		1.24	1.12	1.17	0.73	0.99	0.57	1.17	1.05	0.44	1.04	1.13
G		1.05	1.25	0.63	1.17	0.84	1.17	1.21	1.66	1.21	1.23	
H	1.34	1.23	0.99	1.33	1.20	1.20	1.05	1.06	1.06	1.06	1.27	

Suppl. Figure 2. Screening data (10000 cells/well). Numbers in **blue** correspond to cells treated with DMSO and cisplatin; in **red** to cells treated with 1 mM doxorubicin; and in **green** to non-treated cells. Absolute values of cell survival (measured by resazurin) are indicated for HCT116 p53 WT cells **(A)**, p53 WT cells treated with SB203580 (SB) **(B)**, p53 KO cells **(D)**, KO cells treated with SB **(E)**; and the ratios vs. SB treatment were calculated for WT **(C)** and KO cells **(F)**. Significant differences are highlighted in yelow.

A

WT	1	2	3	4	5	6	7	8	9	10	11	12
A	25525	29624	24668	30879	23908	25451	23587	23629	26908	24983	27620	
B	32231	22632	34546	30844	33430	27377	25427	29743	18196	31007	32685	
C	13037	28974	27897	31731	31600	17291	25002	24183	31113	31799	30831	51303
D	27963	31600	33094	27512	29299	28444	27033	32532	24992	33841	32695	52017
E	31751	25004	34484	32582	32711	32295	34389	18436	31062	24116	27547	49988
F	30318	26547	23009	28412	29680	30019	23210	33413	32953	16312	30594	25741
G	50314	27413	24411	28798	29702	29184	26731	27216	21845	30565	28235	24515
H	50223	30397	29014	22562	25402	24087	22403	27804	17089	20844	24542	22448

B

WT+SB	1	2	3	4	5	6	7	8	9	10	11	12
A	26327	28875	23725	28092	22265	24250	22866	22898	25199	25393	23676	
B	30635	22223	31121	29494	29416	25653	24147	27419	18157	27553	29437	
C	6768	25876	27713	29973	31230	21479	25103	21861	30257	29099	28641	48917
D	27598	26393	30675	24818	29823	29432	28094	29742	25673	30586	28174	49275
E	29477	23721	32871	31455	27894	30188	29724	22239	29645	24023	25210	48766
F	49343	47121	22809	27179	28786	27673	21103	30819	33757	20159	28888	22944
G	50168	47556	35607	46605	49583	48928	44901	41298	21990	49132	47910	20194
H	47476	25004	26935	25292	27017	25954	26747	26800	18367	19342	29877	18882

C

WT/WT+SB	1	2	3	4	5	6	7	8	9	10	11	12
A	0.97	1.03	1.04	1.10	1.07	1.05	1.03	1.03	1.07	0.98	1.17	
B	1.05	1.02	1.11	1.05	1.14	1.07	1.05	1.08	1.00	1.13	1.11	
C	1.93	1.12	1.01	1.06	1.01	0.81	1.00	1.11	1.03	1.09	1.08	
D	1.01	1.20	1.08	1.11	0.98	0.97	0.96	1.09	0.97	1.11	1.16	1.04
E		1.05	1.05	1.04	1.17	1.07	1.16	0.83	1.05	1.00	1.09	
F	1.05	0.56	1.01	1.05	1.03	1.08	1.10	1.08	0.98	0.81	1.06	
G		0.58	0.69	0.62	0.60	0.60	0.60	0.66	0.99	0.62	0.59	1.17
H	1.03	1.22	1.08	0.89	0.94	0.93	0.84	1.04	0.93	1.08	0.82	

D

KO	1	2	3	4	5	6	7	8	9	10	11	12
A	22737	23747	21660	26562	22731	20493	16726	17536	21802	23019	25625	
B	27969	15938	30229	29469	27938	24638	25395	26178	13924	26482	26992	
C	4262	26611	27120	29754	27883	10406	22878	8847	22989	26934	28454	46422
D	24687	31535	29759	23013	29101	27406	23748	29284	23041	31285	28169	46883
E	29066	23356	32323	31791	30354	29797	29114	17914	28988	25058	24507	47055
F	29406	24244	21444	24780	22597	25749	17903	26251	29712	19829	28546	19116
G	49446	24349	17987	18983	26384	23240	22560	23640	18253	27827	24833	18256
H	44013	21343	19033	20182	25663	21004	23581	24708	12540	15078	21609	17992

E

KO+SB	1	2	3	4	5	6	7	8	9	10	11	12
A	24935.5	23130.5	20017.5	23715.5	20330.5	20472.5	16165.5	16779.5	20922.5	21083.5	19487.5	
B	27065.5	16444.5	27170.5	25868.5	25392.5	22518.5	24595.5	25276.5	13876.5	23815.5	26267.5	
C	3624.5	24744.5	24882.5	26965.5	27401.5	15786.5	21215.5	10933.5	22503.5	24846.5	26284.5	46113.5
D	23587.5	28000.5	28557.5	21640.5	26489.5	26588.5	23871.5	27105.5	23795.5	28002.5	25595.5	45903.5
E	27218.5	22175.5	31252.5	28762.5	25934.5	26059.5	25268.5	21926.5	27583.5	22265.5	23351.5	45558.5
F	25991.5	22618.5	21092.5	23462.5	24527.5	23829.5	17623.5	26706.5	28449.5	17885.5	26630.5	16715.5
G	47645.5	23888.5	18223.5	20335.5	24301.5	22857.5	21505.5	22180.5	16127.5	24515.5	22959.5	16249.5
H	42352.5	21084.5	22646.5	19115.5	23197.5	21374.5	23391.5	22867.5	13365.5	15517.5	20451.5	14123.5

F

KO/KO+SB	1	2	3	4	5	6	7	8	9	10	11	12
A	0.91	1.03	1.08	1.12	1.12	1.00	1.03	1.05	1.04	1.09	1.31	
B	1.03	0.97	1.11	1.14	1.10	1.09	1.03	1.04	1.00	1.11	1.03	
C	1.18	1.08	1.09	1.10	1.02	0.66	1.08	0.81	1.02	1.08	1.08	1.02
D	1.05	1.13	1.04	1.06	1.10	1.03	0.99	1.08	0.97	1.12	1.10	
E		1.05	1.03	1.11	1.17	1.14	1.15	0.82	1.05	1.13	1.05	
F	1.10	1.07	1.02	1.06	0.92	1.08	1.02	0.98	1.04	1.11	1.07	1.18
G		1.02	0.99	0.93	1.09	1.02	1.05	1.07	1.13	1.14	1.08	
H	1.04	1.01	0.84	1.06	1.11	0.98	1.01	1.08	0.94	0.97	1.06	

Suppl. Figure 3. Screening data (20000 cells/well). Numbers in **blue** correspond to cells treated with DMSO and cisplatin; in cyan to cells treated only with DMSO; in **red** to cells treated with 1 mM doxorubicin; and in **green** to non-treated cells. Absolute values of cell survival (measured by resazurin) are indicated for HCT116 p53 WT cells **(A)**, p53 WT cells treated with SB203580 (SB) **(B)**, p53 KO cells **(D)**, KO cells treated with SB **(E)**; and the

ratios vs. SB treatment were calculated for WT (C) and KO cells (F). Significant differences are highlighted in yelow.

Array of antioxidant enzymes

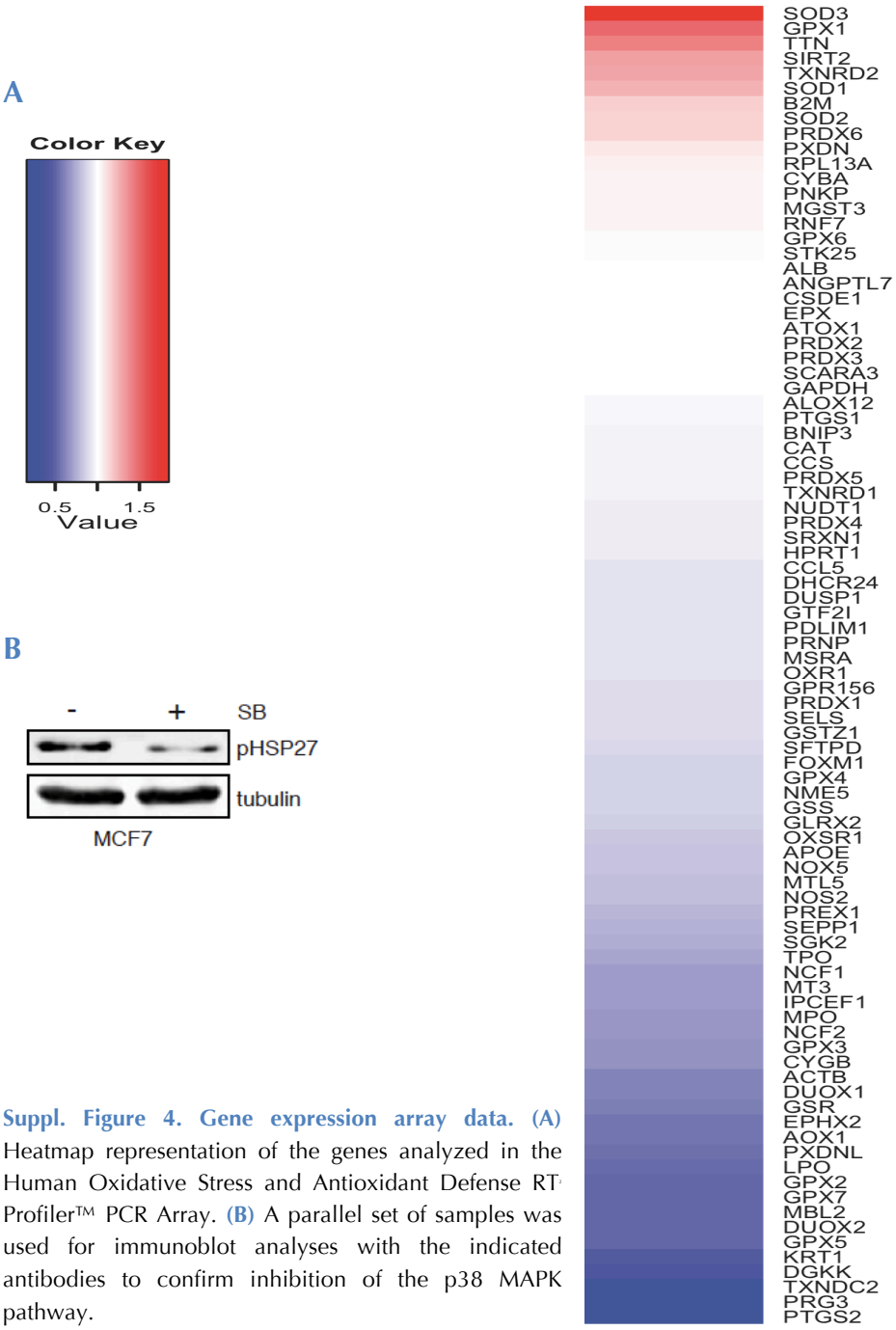

Suppl. Figure 4. Gene expression array data. (A) Heatmap representation of the genes analyzed in the Human Oxidative Stress and Antioxidant Defense RT² Profiler™ PCR Array. **(B)** A parallel set of samples was used for immunoblot analyses with the indicated antibodies to confirm inhibition of the p38 MAPK pathway.

Suppl. Table 2. Proteins identified in band 1

Band	Key	Gene	Protein
SB	Q6IFZ6	Krt77	Keratin, type II cytoskeletal 1b
SB	P05786	KRT8	Keratin, type II cytoskeletal 8
NT	Q1LSP0	tgt	Queuine tRNA-ribosyltransferase
NT	P08729	KRT7	Keratin, type II cytoskeletal 7
SB	P02533	KRT14	Keratin, type I cytoskeletal 14
SB	Q7SY65	krt18b	Keratin, type I cytoskeletal 18-B
SB	Q6EIY9	KRT1	Keratin, type II cytoskeletal 1
NT	Q9Z2K1	Krt16	Keratin, type I cytoskeletal 16
SB	Q6IMF3	Krt1	Keratin, type II cytoskeletal 1
SB	P08776	krt8	Keratin, type II cytoskeletal 8
NT	B2FN00	tgt	Queuine tRNA-ribosyltransferase
SB	Q5K2P2	-	Keratin, type I cytoskeletal 15
SB	Q6IFV3	Krt15	Keratin, type I cytoskeletal 15
SB	Q8BGZ7	Krt75	Keratin, type II cytoskeletal 75
SB	P51856	-	Keratin, type I cytoskeletal 19
SB	Q5FJN8	-	tRNA pseudouridine synthase B
SB	Q6P6Q2	Krt5	Keratin, type II cytoskeletal 5
SB	Q7SYF8	-	Keratin, type I cytoskeletal 18
SB	P04264	KRT1	Keratin, type II cytoskeletal 1
SB	Q8TBZ0-2	CCDC110	Isoform 2 of Coiled-coil domain-containing protein 110
SB	P13549	eef1a-s	Elongation factor 1-alpha, somatic form
SB	Q8VED5	Krt79	Keratin, type II cytoskeletal 79
SB	Q29S21	KRT7	Keratin, type II cytoskeletal 7
NT	Q2M2I5	KRT24	Keratin, type I cytoskeletal 24
SB	P45983-4	MAPK8	Isoform 4 of Mitogen-activated protein kinase 8
NT	Q8LPC4	-	Elongation factor 1-alpha
SB	Q4FZU2	LOC683313	Keratin, type II cytoskeletal 6A
SB	P08727	KRT19	Keratin, type I cytoskeletal 19
NT	P34825	-	Elongation factor 1-alpha
NT	A5A6M6	KRT1	Keratin, type II cytoskeletal 1
SB	O57607	LOC100136778	Keratin, type I cytoskeletal 18
SB	P04259	KRT6B	Keratin, type II cytoskeletal 6B
SB	Q3SZV3	EEF1G	Elongation factor 1-gamma
SB	P27592	-	Elongation factor 1-alpha
SB	P24789	vim1	Vimentin-1/2
SB	P35908	KRT2	Keratin, type II cytoskeletal 2 epidermal
SB	P13647	KRT5	Keratin, type II cytoskeletal 5
NT	P16878	xenck55	Keratin, type II cytoskeletal

Suppl. Table 3. Proteins identified in band 2

Band	Key	Gene	Protein
NT	P48674	vim	Vimentin
NT	P02533	KRT14	Keratin, type I cytoskeletal 14
NT	Q29426	-	Keratin, type II cytoskeletal 3
NT	Q6IMF3	Krt1	Keratin, type II cytoskeletal 1
NT	Q6EIZ0	KRT10	Keratin, type I cytoskeletal 10
NT	Q9NRL2-2	BAZ1A	Isoform 2 of Bromodomain adjacent to zinc finger domain protein 1A
SB	P08777	MGC68905	Keratin, type I cytoskeletal 47 kDa
NT	Q3TTY5	Krt2	Keratin, type II cytoskeletal 2 epidermal
NT	Q8BGZ7	Krt75	Keratin, type II cytoskeletal 75
SB	P51856	-	Keratin, type I cytoskeletal 19
NT	P19013	KRT4	Keratin, type II cytoskeletal 4
NT	Q95JF4	-	DnaJ homolog subfamily A member 1
SB	P08515	-	Glutathione S-transferase class-mu 26 kDa isozyme
NT	Q7SYF8	-	Keratin, type I cytoskeletal 18
SB	P08730	Krt13	Keratin, type I cytoskeletal 13
NT	P49411	TUFM	Elongation factor Tu, mitochondrial
NT	A1KQY9	-	Keratin, type I cytoskeletal 18-A
NT	O95678	KRT75	Keratin, type II cytoskeletal 75
NT	Q29S21	KRT7	Keratin, type II cytoskeletal 7
NT	Q5XQN5	KRT5	Keratin, type II cytoskeletal 5
NT	P38989	SMC2	Structural maintenance of chromosomes protein 2
SB	P06394	KRT10	Keratin, type I cytoskeletal 10
SB	P25030	Krt20	Keratin, type I cytoskeletal 20
SB	Q6PVZ1	KRT14	Keratin, type I cytoskeletal 14
NT	Q4FZU2	LOC683313	Keratin, type II cytoskeletal 6A
SB	Q63279	Krt19	Keratin, type I cytoskeletal 19
SB	P08727	KRT19	Keratin, type I cytoskeletal 19
NT	Q22909	ceh-30	Homeobox protein ceh-30
SB	Q6IFX2	Krt42	Keratin, type I cytoskeletal 42
NT	P48677	-	Glial fibrillary acidic protein
NT	O93532	LOC395772	Keratin, type II cytoskeletal cochleal
SB	P04104	Krt1	Keratin, type II cytoskeletal 1
NT	Q5XKE5	KRT79	Keratin, type II cytoskeletal 79
NT	P08728	LOC514812	Keratin, type I cytoskeletal 19
SB	P35661	-	Glutathione S-transferase class-mu 26 kDa isozyme
NT	P08728	LOC514812	Keratin, type I cytoskeletal 19
SB	O18740	KRT9	Keratin, type I cytoskeletal 9
NT	P13647	KRT5	Keratin, type II cytoskeletal 5

Suppl. Table 4. Proteins identified in band 3

Band	Key	Gene	Protein
NT	Q1LSP0	tgt	Queuine tRNA-ribosyltransferase
SB	Q6EIZ0	KRT10	Keratin, type I cytoskeletal 10
NT	P13646-3	KRT13	Isoform 3 of Keratin, type I cytoskeletal 13
NT	P08778	LOC397756	Keratin, type I cytoskeletal 47 kDa
NT	Q61781	Krt14	Keratin, type I cytoskeletal 14
NT	P19013	KRT4	Keratin, type II cytoskeletal 4
NT	Q6IFW6	Krt10	Keratin, type I cytoskeletal 10
SB	P08515	-	Glutathione S-transferase class-mu 26 kDa isozyme
NT	O77727	-	Keratin, type I cytoskeletal 15
NT	P19001	Krt19	Keratin, type I cytoskeletal 19
SB	A8GJ49	Spro_4044	Probable Fe(2+)-trafficking protein
SB	Q5XQN5	KRT5	Keratin, type II cytoskeletal 5
SB	P48672	-	Vimentin A2
NT	A7YWK3	KRT73	Keratin, type II cytoskeletal 73
NT	P11679	Krt8	Keratin, type II cytoskeletal 8
SB	P35661	-	Glutathione S-transferase class-mu 26 kDa isozyme
NT	P02538	KRT6A	Keratin, type II cytoskeletal 6A
SB	P84048	-	Histone H4
SB	Q89743	-	Uncharacterized protein DR7
NT	Q29426	-	Keratin, type II cytoskeletal 3
NT	P50446	Krt6a	Keratin, type II cytoskeletal 6A
NT	Q6IMF3	Krt1	Keratin, type II cytoskeletal 1
NT	B2FN00	tgt	Queuine tRNA-ribosyltransferase
NT	Q6IFV3	Krt15	Keratin, type I cytoskeletal 15
NT	Q6P6Q2	Krt5	Keratin, type II cytoskeletal 5
NT	Q7SYF8	-	Keratin, type I cytoskeletal 18
NT	O95678	KRT75	Keratin, type II cytoskeletal 75
NT	Q61414	Krt15	Keratin, type I cytoskeletal 15
NT	P48668	KRT6C	Keratin, type II cytoskeletal 6C
NT	P08779	KRT16	Keratin, type I cytoskeletal 16
NT	O76013-2	KRT36	Isoform 2 of Keratin, type I cuticular Ha6
NT	Q22909	ceh-30	Homeobox protein ceh-30
NT	O93532	LOC395772	Keratin, type II cytoskeletal cochleal
SB	P24789	vim1	Vimentin-1/2
SB	P04104	Krt1	Keratin, type II cytoskeletal 1
NT	P19012	KRT15	Keratin, type I cytoskeletal 15
NT	A1L317	Krt24	Keratin, type I cytoskeletal 24
NT	P13647	KRT5	Keratin, type II cytoskeletal 5
NT	P16878	xenck55	Keratin, type II cytoskeletal
NT	Q9QWL7	Krt17	Keratin, type I cytoskeletal 17

Resumen en castellano

Título

Regulación de la supervivencia de las células cancerígenas por p38 MAPK.

Sinopsis

La regulación del estado redox es esencial para mantener la homeostasis celular. De hecho, la desregulación de la producción de especies reactivas de oxígeno (ROS) ha sido asociada con un incremento de la tumorogenicidad en células epiteliales. Sin embargo, los efectos pro-tumorogénicos de la acumulación de ROS pueden resultar un arma de doble filo, ya que altos niveles de estas especies pueden disminuir el umbral apoptótico para la citotoxicidad. Por tanto, la regulación redox juega un papel importante en la supervivencia de la célula tumoral.

La proteína kinasa p38α is una reguladora importante de muchos procesos celulares. Está bien establecido que la señalización de p38α regula negativamente la transformación de la célula epitelial, pero un aumento de su actividad kinasa ha sido correlacionado con un mal pronóstico clínico en algunos tipos de tumores. Esto, junto con el hecho de que se ha mostrado que p38α es necesaria para la proliferación de algunas líneas celulares de cáncer, nos indujo a pensar que esta proteína podría ser una buena diana para la terapia contra el cáncer.

Por tanto, llevamos a cabo un *screening* para identificar compañeros letales sintéticos de p38α, pero estos resultados todavía tienen que terminar de ser validados. No obstante, proporcionamos evidencia basada en inhibidores químicos y en depleciones génicas, de que p38α coopera con cisplatino para matar a las células tumorales. Aquí mostramos que la inhibición de p38α resulta en el aumento de ROS, que a su vez activa la ruta de JNK mediante la inactivación de sus fosfatasas, y así sensibiliza a las células tumorales humanas a la apoptosis inducida por cisplatino. Además, usando un modelo animal de cáncer de mama, mostramos que la inhibición de p38α coopera con el tratamiento de cisplatino para reducir el tamaño de los tumores y su malignidad *in vivo*. En su conjunto, nuestros resultados revelan una nueva función de p38α que ayuda a las células

tumorales a sobrevivir a los tratamientos quimioterapéuticos, manteniendo la expresión de enzimas antioxidantes, y muestran que la combinación de inhibidores de p38α con cisplatino podría ser potencialmente explotada en la terapia contra el cáncer.

Introducción

1. El cáncer, una enfermedad antigua y mundial

Se podría pensar que el cáncer es una enfermedad moderna, sin embargo ha existido durante siglos. Ha sido claramente identificado en estudios de momias egipcias (Granville, 1825) e incluso representado en obras de arte a lo largo de los siglos (Vaidya, 2007). No obstante, hoy en día es un fenómeno más común, principalmente por el crecimiento de la población mundial, el incremento de la esperanza de vida y los avances en la civilización.

La tumorogénesis es un proceso de múltiples pasos de alteraciones genéticas que conducen la transformación progresiva de células normales en otras altamente malignas, la cuales poseen defectos en los circuitos regulatorios que gobiernan su proliferación y homeostasis. El cultivo de células tumorales *in vitro* y la disección de sus componentes moleculares ha generado gran parte del conocimiento que actualmente poseemos sobre los procesos moleculares subyacentes al desarrollo del cáncer. Hanahan y sus compañeros sugirieron que el amplio repertorio de genotipos celulares observados es la manifestación de seis alteraciones esenciales en la fisiología celular, que colectivamente dictan el crecimiento maligno: auto-suficiencia de señales de crecimiento, insensibilidad a las señales inhibidoras del crecimiento, evasión de la apoptosis, potencial replicativo ilimitado, angiogénesis mantenida e invasión tisular, y metástasis (Hanahan and Weinberg, 2000) (**Fig. 1**).

El ratón de laboratorio (*Mus musculus*) ha revolucionado nuestra capacidad de estudiar las funciones génicas *in vivo* y entender los mecanismos moleculares de la patogénesis del cáncer. Hoy en día existen numerosas técnicas para su manipulación genética (Cheon and Orsulic, 2011) y esto ha permitido la generación de un gran número de modelos animales para recapitular las

enfermedades humanas (Frese and Tuveson, 2007). Aquí nos centraremos en un modelo animal de cáncer de mama, el MMTV-PyMT.

El cáncer de mama es sin duda el más comúnmente diagnosticado en mujeres alrededor del mundo (pasando a ser el segundo si combinamos las estadísticas de ambos sexos), ya que representa casi un cuarto (23%) de todos los cánceres diagnosticados en mujeres. Además, también es la causa más común de muerte en mujeres a nivel mundial (Cancer Research UK, 2011). Los modelos animales de cáncer de mama modificados genéticamente exhiben muchas características del cáncer humano, y por tanto son valiosos para investigar la biología y patogénesis de esta enfermedad. Sin embargo, dada la complejidad y heterogeneidad del cáncer de mama, no hay un único modelo que recapitule todos los aspectos de esta enfermedad.

El poliomavirus murino (PyV) puede causar una gran variedad de tumores en diferentes tipos de células (Dawe et al., 1987; Fluck and Haslam, 1996). La proteína transformante más importante que producen es la oncoproteina MT, cuya expresión trangénica puede causar tumores en un gran rango de tejidos (Cecena et al., 2006; Guy et al., 1992; Rassoulzadegan et al., 1990; Tehranian et al., 1996). Cuando PyMT se expresa bajo el control del promotor de la glándula mamaria, MMTV, se inducen carcinomas metastáticos (Guy et al., 1992). Las primeras lesiones hiperplásicas surgen a edades muy tempranas y están localizadas próximas al pezón. Tras el crecimiento prepubertal, los ductos se elongan todavía más bajo la influencia hormonal y nuevas lesiones aparecen en los brotes terminales distales, que se fusionan con los tumores próximos a los pezones en estadíos tardíos. Se indentificaron cuatro estadíos con similitudes a los tumores humanos (hiperplasia, adenoma o neoplasia mamaria intraepitelial (MIN), carcinoma *in situ* y carcinoma invasivo), que aparecen descritos en la **figura 2**. Análisis de agrupación jerárquica han emplazado a los tumores del modelo MMTV-PyMT en un grupo luminal subtipo B (Fluck and Schaffhausen, 2009) (**Fig. 3**).

2. Las cascadas de señalización MAPK

Las células necesitan estar constantemente alerta de los cambios en el medio extracelular para responder en consecuencia, de modo que han desarrollado una gran variedad de mecanismos para recibir señales, transmitir la información y coordinar las respuestas apropiadas. Estas normalmente están mediadas por la activación de factores de transcripción, los cuales inducen los procesos celulares necesarios. Sin embargo, la mayoría de agentes extracelulares no pueden cruzar la membrana plasmática para activar a los genes correspondientes. Por el contrario, estos genes usan "líneas de comunicación", conocidas como "rutas de señalización", para transmitir las señales a sus objetivos citoplasmáticos y nucleares. En muchos casos, las rutas de señalización operan a través de fosforilaciones secuenciales y son llamadas "cascadas de proteínas kinasas". Este tipo de mecanismo de señalización es usado por las proteínas kinasas activadas por mitógenos (MAPK), que son una familia evolutivamente conservada de proteinas serina treonina de la que se han descrito principalmente cuatro rutas canónicas en los últimos 20 años: las kinasas reguladas por señales extracelulares 1 y 2 (ERK1/2) (Boulton et al., 1991), kinasas N-terminales de Jun 1-3 (JNK 1-3), p38 MAPK α, β, γ, ∂ (p38α-∂) (Freshney et al., 1994; Han et al., 1994; Rouse et al., 1994) y las ERK5 (Lee et al., 1995; Zhou et al., 1995) (**Fig. 4**).

Las cuatro p38 MAPK descritas están codificadas por cuatro genes diferentes y varían en sus patrones de expression tisular, siendo p38α la única expresada ubícuamente y en cantidades significativas en la mayoría de los tipos celulares, mientras que las otras suelen ser más tejido-específicas (Cuadrado and Nebreda, 2010). A pesar de su alta homología de secuencia, las isoformas de p38 MAPK difieren en su sensibilidad a inhibidores químicos (Coulthard et al., 2009). El descubrimiento de las condiciones patológicas en que las p38 MAPK están involucradas (**Fig. 5**) apoya el potencial interés terapéutico de modular la actividad de estas kinasas. Drogas del tipo piridinil-imidazol, como SB203580, fueron los primeros inhibidores identificados y se caracterizan porque encajan en el sitio de unión del ATP (**Fig. 6**), de modo que compiten con éste por la unión.

En los últimos años, se ha visto que los miembros de la familia de p38 MAPK

estaban involucrados en varios de los procesos de transformación tumoral, siendo asociados sobre todo con funciones supresoras de la tumorogénesis. En el caso de p38α, estas funciones supresoras parecen operar principalmente en el inicio del proceso de transformación (Dolado et al., 2007; Hui et al., 2007; Ventura et al., 2007), ya que se ha correlacionado un incremento de la fosforilación de p38 MAPK con baja supervivencia general en pacientes con cánceres de mama negativos para HER-2 (Esteva et al., 2004) o con carcinoma hepatocelular (Wang et al., 2012). Sin embargo, el papel pro-tumorogénico de p38α no sólo está basado en correlaciones, sino que también se ha visto que puede contribuir a la proliferación de líneas celulares de cáncer de mama (Chen et al., 2009), colorrectales (Chiacchiera et al., 2009), de próstata (Ricote et al., 2006) o piel (Schindler et al., 2009).

Las tres proteínas JNK descritas también están codificadas por genes diferentes y pueden llegar a generar hasta diez isoformas diferentes (Dreskin et al., 2001; Gupta et al., 1996). Mientras que JNK1 y JNK2 se expresan en casi todos los tipos celulares, JNK3 está principalmente localizada en cerebro y, en menor medida, en corazón y testículos (Bode and Dong, 2007).

La ruta de JNK se activa en respuesta a estrés, pero su señalización dependerá del contexto celular, ya que ha sido implicada tanto en procesos apoptóticos como de supervivencia (Ip and Davis, 1998). Uno de los estímulos que activa a JNK es el cisplatino (CDDP), un pequeño complejo inorgánico neutro que se activa tras entrar en la célula, donde reemplaza sus ligandos cis-cloro con moléculas de agua (el-Khateeb et al., 1999; Kelland, 2000). Esta forma acuosa es muy reactiva hacia los centros nucleofílicos de las proteinnas, RNA, DNA, fosfolípidos de membrana y microfilamentos, aunque en general sus propiedades antitumorales están asociadas a su capacidad de unirse al DNA y generar roturas de cadena simple en última instancia (Fuertes et al., 2003; Jamieson and Lippard, 1999). Hoy en día se usa frecuentemente en la clínica para tratar tumores sólidos.

Las proteínas implicadas en el reconocimiento de la unión del cisplatino al DNA son las que disparan la señalización de las MAPK, que son las últimas responsables de llevar a cabo los efectos citotóxicos de esta droga. En la mayoría de los sistemas celulares investigados, la activación de JNK en respuesta a cisplatino induce la muerte celular (Koyama et al., 2006; Krilleke et al., 2003; Li et al., 2005; Mansouri et al., 2003; Sanchez-Perez et al., 2002; Sanchez-Perez et al., 1998; Sanchez-Perez and Perona, 1999). De hecho, la falta de activación sostenida de JNK en células resistentes a cisplatino determina su supervivencia tras tratamiento con este compuesto, cosa que no sucede en el caso de las células sensibles a cisplatino (Li et al., 2005).

3. La familia de proteínas tirosina fosfatasas

Puesto que las MAPK son mediadoras esenciales de muchos de los procesos celulares inducidos por estimulación, su inactivación es crítica para alcanzar tan sólo una activación transitoria y poder regular así la intensidad de señal, que determinará respuestas específicas. El cese de la actividad kinasa implica la activación de la familia de las proteínas tirosina fosfatasas (PTP), que están agrupadas en cuatro subfamilias según la secuencia aminoacídica de su dominio catalítico: las de tipo I, II y III (todas basadas en cisteína) y las basadas en aspártico (Alonso et al., 2004) (**Fig. 8**). Las PTP de tipo I se pueden dividir a su vez en dos grupos según la similitud de sus dominios catalíticos: las PTP clásicas, que son tirosina específicas; y las fosfatasas de especificidad dual (DUSP). Las de tipo II sólo contienen un tipo de fosfatasas, las PTP de bajo peso molecular (LMWPTP), que están relacionadas con fosfatasas bacterianas de bajo peso molecular, evolutivamente conservadas (Alonso et al., 2004). El tipo III son tirosina y treonina específicas (Alonso et al., 2004; Russell and Nurse, 1986) y consisten en reguladores del ciclo celular: Cdc25A, Cdc25B y Cdc25C, que defosforilan a ciclinas dependientes de kinasas (Karlsson-Rosenthal and Millar, 2006). Finalmente, las PTP basadas en aspártico, incluyen las fosfatasas específicas de tirosina EyA ("eyes absent") y las haloácido deshalogenasas (HAD) (Moorhead et al., 2007). Estas últimas son un grupo heterogéneo de fosfatasas que pueden ser específicas tanto de tirosina (Rebay et al., 2005) como de serina (Gohla et al.,

2005; Yeo et al., 2003) y tienen sustratos muy diversos. Aquí nos centraremos únicamente en las PTP tipo I.

Las PTP clásicas son de tipo I y pueden ser proteínas tipo receptor (RPTP, que están ancladas a membrana) o solubles (**Fig. 9**). Las RPTP tienen el potencial de regular la señalización mediante defosforilaciones controladas por ligando. Muchas de ellas presentan características de moléculas de adhesión celular en su segmento extracelular y han sido implicadas en procesos involucrados en contactos célula-célula y célula-matriz. Las PTP solubles, o citoplasmáticas, se caracterizan por la presencia de secuencias reguladoras que flanquean el dominio catalítico y controlan su actividad, tanto directamente, como mediante interacciones en el sitio activo que modulan su actividad o controlan la especificidad del sustrato.

Las DUSP son un grupo muy grande y heterogéneo, que también pertenecen al tipo I, y se caracterizan por su habilidad para defosforilar tanto residuos de tirosina como de serina treonina dentro de un mismo sustrato. Uno de los grupos mejor caracterizado es el de las fosfatasas de kinasas activadas por mitógeno (MKP), formadas por 10 proteínas (**Table 1**). Cada una de las MKP muestran especificidad de sustrato por una o varias de las MAKP ERK, JNK o p38 (**Fig. 10**).

Las PTP pueden ser objeto de modificaciones postraduccionales, como por ejemplo la oxidación. La presencia de una cisteína catalítica de bajo pKa (den Hertog et al., 2005; Salmeen and Barford, 2005; Tonks, 2005) en su sitio activo, hace que las PTP sean especialmente sensibles a la inactivación por oxidación de esta cisteína, que induce profundos cambios en la arquitectura del sitio catalítico. Los estímulos fisiológicos provocan la producción localizada de especies reactivas de oxígeno (ROS), que llevan a la oxidación e inactivación de aquellas PTP que normalmente están atenuando la respuesta de señalización. Esta oxidación es transitoria, de modo que las PTP son reducidas de nuevo para volver a sus estado activo gracias a la acción de agentes reductores como la tiorredoxina o el glutatión.

4. El estrés oxidativo

Definimos estrés oxidativo como una situación de desbalance entre los factores pro-oxidantes y antioxidantes celulares, que están controlados por múltiples factores y pueden conducir al daño celular. Las especies reactivas de oxígeno (ROS), como el anión superóxido (O_2^-), el peróxido de hidrógeno (H_2O_2) y el radical hidroxil (HO·), son especies de oxígeno, radicales y no radicales, que están formadas por la reducción parcial del oxígeno y juegan un papel clave en el estrés oxidativo, el cual provoca daños en ácidos nucleicos, lípidos y proteínas.

Los altos niveles de ROS en las células cancerígenas pueden ser resultado de su incrementada actividad metabólica, disfunción mitocondrial, actividad peroxisomal, actividad oncogénica, actividad incrementada de oxidasas, y otras, junto con su interacción con células inmunes infiltrantes (Storz, 2005; Szatrowski and Nathan, 1991). En la mitocondria, las ROS son producidas como un producto inevitable de la fosforilación oxidativa (**Fig. 11**).

En situaciones fisiológicas normales, los niveles intracelulares de ROS están controlados para impedir el daño celular. Esto es posible gracias tanto a moléculas no enzimáticas (glutatión, flavonoides, vitaminas A, B y C…) como a enzimas antioxidantes (catalasa, glutatión peroxidasas -GPX-, superóxido dismutasas -SOD-, tiorredoxinas…), que específicamente capturan diferentes tipos de ROS (**Fig. 11**). Sin embargo, puesto que las células cancerígenas producen altos niveles de ROS y además están expuestas a muchos oxidantes exógenos, son capaces de adaptarse a altos niveles de estrés oxidativo (Kim et al., 2006; Schneider and Kulesz-Martin, 2004) y promover rutas de supervivencia (Irmak et al., 2003) o expresar altos niveles de antioxidantes (Young et al., 2004). Esta capacidad antioxidante incrementada probablemente les sea útil como mecanismo evasor de la apoptosis (Trachootham et al., 2006) (**Fig. 12**).

Objetivos

Se ha demostrado que p38α tiene un papel supresor de tumores basado en su habilidad para regular negativamente la proliferación celular y por inducir muerte celular. Sin embargo, la mayoría de estos estudios se han limitado a la investigación de las funciones de p38α durante la iniciación tumoral, pero todavía no entendemos completamente las funciones de p38α en la progresión tumoral.

Por tanto, el objetivo de este trabajo es determinar si p38α podría ser una potencial diana terapéutica para la quimioterapia siguiendo estas dos aproximaciones:

- realizar un *screening* para identificar compañeros sintéticos letales de p38α
- determinar si la inhibición de p38α podría sinergizar con los tratamientos quimioterapéuticos para inducir la muerte de las células cancerígenas.

Resultados

Para determinar si p38α podría ser una diana terapéutica de interés, seguimos dos enfoques diferentes: buscar compañeros letales sintéticos de p38 MAPK y estudiar si su inhibición podría sinergizar con agentes quimioterapéuticos para inducir la muerte de la célula cancerígena.

1. p38 MAPK como un compañero letal sintético

El concepto de letalidad sintética surgió como una alternativa prometedora a los inespecíficos, y por tanto agresivos, tratamientos quimioterapéuticos en algunos tipos de cáncer. De hecho, ya existen resultados destacables al respecto usando este abordaje, como es el caso del tratamiento con inhibidores de la poli(ADP-ribosa) polimerasa (PARP) para el tratamiento de tumores de mama portadores de mutaciones en BRCA (Fong et al., 2009). Dos genes se consideran como sintéticos letales si la mutación de ambos es letal, pero no así su mutación independiente (Kaelin, 2005).

Con el objetivo de encontrar compañeros letales sintéticos de p38 MAPK, combinamos su inhibición con la de otras rutas importantes para la supervivencia de la célula cancerígena, como ERK y mTOR. Medición de la apoptosis celular nos indicó que no había ningún sinergismo que eficientemente matara a las células cancerígenas, ni en condiciones basales (**Fig. 16A**), ni tras el tratamiento con agentes quimioterapéuticos (**Fig. 16B**). Los mismos resultados fueron obtenidos al medir el porcentaje de viabilidad celular en diferentes líneas de cáncer, también en condiciones basales (**Fig. 17A**) y estimuladas (**Fig. 17B**).

Puesto que ninguna de las rutas testadas resultaron ser sintéticos letales de p38 MAPK decidimos realizar un *screening* para comprobar 84 inhibidores (**Suppl. Fig. 1**) que afectan a 36 rutas de señalización diferentes (**Suppl. Table 1**). Se compararon células HCT116 y HCT116 p53-/- sin tratar con las tratadas con SB203580, un inhibidor químico de p38 MAPK, en todos los casos estimuladas con cisplatino (una droga ampliamente usada en la clínica para el tratamiento de tumores sólidos), ya que se vio que respondían a esta droga (**Fig. 18**). Tras comparar el incremento de viabilidad relativo a las células tratadas con SB203580 (los datos originales se pueden contrar en la **Suppl. Figure 2**), identificamos 3 rutas que presentaban cambios significativos: IKK2, PKCs y eEF2 (**Fig. 19**). Aunque tan sólo la última se podría considerar un compañero sintético letal de p38 MAPK, ya que las dos primeras incrementaban la viabilidad celular combinar su inhibición con la de p38 MAPK en vez de reducirla. Parece que la letalidad sintética de eEF2 kinasa funciona sólo en el caso de células que tienen un p53 salvaje, aunque todavía se necesita caracterizar adecuadamente esta candidata.

2. Sensibilización a quimioterapia por inhibición de p38 MAPK

En la búsqueda de compañeros letales sintéticos de p38 MAPK advertimos que sólo con inhibir esta ruta ya disminuíamos la viabilidad de la célula tumoral tras el tratamiento con agentes quimioterapéuticos (**Figs. 16-18**). Para determinar el papel de la señalización de esta proteína en la supervivencia celular, expusimos varias células de cáncer de mama (MCF7) y colon (HT-29 y SW620) al tratamiento con cisplatino y el inhibidor SB203580. Tras medir la apoptosis de estas células

mediante diferentes técnicas, vimos que el tratamiento combinado producía un efecto aditivo a la hora de inducir la muerte de las células tumorales (**Fig. 20**). Este mecanismo era independiente del papel que p38 MAPK desempeña en la proliferación de algunas células cancerígenas (**Fig. 21**), y no está relacionado con el estado de p53 (**Table 2**). Además, hemos visto que la incubación con SB203580 no induce daño en el DNA (**Fig. 22**).

Varios estudios indican que la señalización de p38 MAPK puede regular negativamente la ruta de JNK en diferentes contextos, principalmente en células no transformadas (Perdiguero et al., 2007b; Wagner and Nebreda, 2009). Puesto que JNK juega un papel importante en la inducción de apoptosis (Davis, 2000), investigamos si esta ruta estaba también implicada en el aumento de apoptosis observado en las células cancerígenas tratadas con cisplatino. Efectivamente comprobamos la correlación inversa entre las rutas de JNK y p38 MAPK **Fig. 23A**) y su sensibilización a apoptosis tanto con el uso de inhibidores (**Fig. 23B**) como de herramientas genéticas (siRNA y shRNA) (**Fig. 24**).

Se sabe que la señalización de JNK puede ser activada por ROS (Shen and Liu, 2006) y al revés, que altos niveles de ROS correlacionan con activación de JNK en células cancerígenas humanas (Dolado et al., 2007). Además, parece que p38 MAPK también puede impedir la acumulación de ROS en células no transformadas y la inhibición de esta ruta ha sido correlacionada con un patrón de expresión génica relacionado con estrés oxidativo (Mateescu et al., 2011). Por tanto, imaginamos que la inhibición de p38 MAPK podría resultar en un aumento de los niveles de ROS, que a su vez activarían la ruta de JNK. Y esto es exactamente lo que encontramos, como se puede observar en las figuras **figure 25** y **figure 26** , respectivamente.

Nos preguntamos si la inhibición de p38 MAPK también podría sensibilizar células con altos niveles basales de ROS a apoptosis, de modo que comparamos las células de cáncer de mama MDA-MB-231 y MCF7, ya que las primeras tienen mayores niveles basales de ROS que las segundas (**Fig. 27A**). Resultó muy

interesante descubrir que el mismo mecanismo operaba en estas células, es decir, la inhibición de p38 MAPK induce la acumulación de ROS, lo que activa a JNK y sensibiliza a apoptosis tras el tratamiento con cisplatino.

Para determinar el mecanismo por el cual p38 MAPK regula la producción de ROS, realizamos un *array* de expresión de 84 genes implicados en estrés oxidativo (**Suppl. Fig. 3**), y descubrimos que había 8 genes de enzimas antioxidantes cuya expresión se reducía al inhibir p38 MAPK. No obstante, sólo 3 de ellos se mantenían significativamente reducidos al inhibir p38 MAPK en dos líneas celulares de cáncer de mama y colon (**Table 3**). Uno de estos genes, *PTGS2*, que codifica para la proteína antiinflamatoria COX-2, a pesar de estar regulado por p38 MAPK, demostró no estar implicado en la regulación de ROS (**Fig. 28A**). Pero sí observamos que los dos restantes, *GPX5* y *TXNDC2*, que codifican para una glutatión peroxidasa y una tioredoxina, respectivamente, regulan los niveles basales de activación de JNK (**Fig. 28B**), simulando los resultados obtenidos cuando aumentan los niveles de ROS al inhibir p38 MAPK. Asimismo, también comprobamos que la producción de ROS tras la inhibición de p38 MAPK también podría ser mitocondrial, pero no regulada por Nox (**Fig. 28C**). Finalmente, ha sido interesante descubrir que los mecanismos de regulación por p38 MAPK de las enzimas antioxidantes catalasa y SOD que ha sido observada en células no tumorales (Gutierrez-Uzquiza et al., 2012), no se mantiene en nuestras células cancerígenas (**Fig. 28D**), sugiriendo que la regulación de ROS por p38 MAPK es diferente en células transformadas y en las que no lo son.

Otros trabajos han mostrado que ROS puede inhibir la actividad de fosfatasas, debido a que su cisteína catalítica puede ser inactivada por oxidación (Kamata et al., 2005; Teng et al., 2007). Así, pensamos que la activación de la ruta de JNK tras la inhibición de p38 MAPK podría ser debida a la inhibición de la actividad fosfatasa tras el aumento de ROS. De este modo demostramos que tanto tirosina fosfatasas como serina treonina fosfatasas pueden estar implicadas en la regulación de JNK tras la inhibición de p38 MAPK dependiendo del tipo celular

(**Fig. 30**), y que muy probablemente los activadores de JNK no estuviesen implicados en este proceso de activación (**Fig. 31**).

Para determinar si nuestras observaciones podían tener alguna relevancia *in vivo*, usamos un modelo de ratón de cáncer de mama, el MMTV-PyMT, mediante el cual los animales desarrollan tumores de mama de forma espontánea en torno a los 2.5 meses de edad. Tras aplicar tres tratamientos diferentes (el inhibidor de p38 MAPK PH-797804, cisplatino, o la combinación de los dos) y compararlos con la evolución de los tumores de los animales control (sólo tratados con el vehículo de los tratamientos), observamos que el doble tratamiento provocaba una reducción del tamaño de los tumores de más del 90% a los 18 días de seguimiento, mientras que el cisplatino sólo los reducía un 50% (**Fig. 32A**). Análisis inmunohistoquímicos de las muestras a 7 días revelaron que la ruta de JNK se activaba tras la inhibición de p38 MAPK y que esto correlacionaba con un aumento de apoptosis, menor malignidad del tumor y reducción de la proliferación (**Fig. 32B-D**). También ha sido interesante descubrir que había un aumento de oxidación celular al tratar con PH-797804 (**Fig. 32E**). Los tumores también fueron analizados por inmunohistoquímica al final del experimento, lo que confirmó que éstos mantenían reducido su nivel de proliferación en el doble tratamiento y, lo que es más importante, la malignidad de los tumores seguí siendo menor (**Fig. 33**). Tras esta observación, pensamos que en el caso eventual de una recidiva, estos tumores más pequeños y menos proliferativos tardarían más en volver a crecer, comparados con los tratamientos independientes, y fue exactamente lo que observamos al repetir el experimento en las mismas condiciones pero cesando los tratamientos a día 15 (**Fig. 34**).

Hemos visto que otros tipos de células cancerígenas humanas también presentaban activación de la ruta de JNK tras la inhibición de p38 MAPK (**Fig. 35**), y que esto sensibilizaba a apoptosis (**Fig. 36**), indicando que el mecanismo aquí descrito podría aplicar a un amplio abanico de células tumorales. Además, ha sido interesante observar que la activación de JNK tras la incubación con SB203580

era eminentemente citoplasmática, contrastando con la intensa activación nuclear que produce la radiación UV (**Fig. 37**).

Discusión

Se sabe que las ROS juegan un papel muy importante en la homeostasis de la célula tumoral, pero muchos estudios han descrito cómo altos niveles intracelulares de éstos están asociados con apoptosis. JNK es un importante mediador de la inducción de apoptosis en respuesta a diferentes agentes quimioterapéuticos, en particular a cisplatino. Nosotros hemos encontrado que la inhibición de la señalización de p38α en las células cancerígenas es suficiente para aumentar los niveles de ROS, que a su vez estimulan la apoptosis mediada por JNK en respuesta a cisplatino. Trabajos previos han mostrado que las rutas de JNK y p38 MAPK pueden interactuar a muy diversos niveles, principalmente en células no transformadas (Wagner and Nebreda, 2009), pero esta es la primera vez que se muestra que esta conexión puede estar mediada por ROS en células tumorales. También proporcionamos evidencias de la relevancia biológica de este mecanismo en la respuesta de las células cancerígenas a los tratamientos quimioterapéuticos, ampliando otras publicaciones donde mencionaban la implicación de ROS en la apoptosis mediada por JNK (Hou et al., 2008; Kamata et al., 2005).

ASK1 se ha propuesto como un regulador clave de la apoptosis en respuesta a estrés oxidativo a través de la activación de MKK4 y MKK7 (Takeda et al., 2008). Sin embargo, estos activadores de JNK no parecen estar implicados en el proceso de activación de JNK que describimos aquí. Nuestros resultados indican que la inhibición de fosfatasas de JNK por la acumulación de ROS intracelulares es la responsable de la activación de esta proteína tras la inhibición de p38 MAPK. Tampoco hemos encontrado ninguna evidencia de que esta inhibición afecte a la expresión de la fosfatasa nuclear inducible MKP1 (Keyse, 2008), la cual, basándose en experimentos de sobreexpresión, ha sido propuesta como reguladora de la activación de JNK inducida por cisplatino (Sanchez-Perez et al., 2000). Sin embargo, analizando las fosfatasas citoplasmáticas que regulan JNK

(Dickinson and Keyse, 2006), hemos visto que DUSP8 controla los niveles basales de fosforilación de JNK en las células MCF7 de cáncer de mama. Además, se ha descrito que DUSP8 puede interaccionar con células no estimuladas (Sanchez-Perez et al., 2000). Curiosamente, también proporcionamos evidencia de que esta fosfatasa no parece jugar un papel relevante a la hora de regular la fosforilación basal de JNK en otras líneas de cáncer humanas. Por tanto, nuestros resultados indican que las fosfatasas implicadas en la regulación de la actividad basal de JNK varían dependiendo del tipo de línea celular.

También hemos abordado la cuestión de cómo la inhibición de p38α aumenta los niveles de ROS en las células cancerígenas. Experimentos usando rotenona sugieren que el transporte de electrones a través de la cadena respiratoria mitocondrial podría contribuir a la generación de ROS tras la inhibición de p38α. Además hemos identificado dos genes antioxidantes, *GPX5* y *TXNDC2*, que están positivamente regulados por p38α en células cancerígenas y que controlan los niveles de actividad basal de JNK. Por tanto, p38α podría regular negativamente la acumulación de ROS a diferentes niveles. Interesantemente, ha sido mostrado que la señalización de p38α regula negativamente la acumulación de ROS en MEFs a través del incremento de expresión de catalasa y superóxido dismutasa (Gutierrez-Uzquiza et al., 2012), pero nosotros no hemos encontrado ninguna evidencia de que estas dos enzimas estén reguladas por p38α en las células cancerígenas que hemos analizado. Esto indica que la señalización de p38α puede regular la acumulación de ROS por diferentes mecanismos en células transformadas. De hecho, la diferente sensibilidad de las células transformadas y las que no lo son, ha sido propuesto como un hecho terapéuticamente relevante de forma potencial (Mateescu et al., 2011; Raj et al., 2011; Shaw et al., 2011).

En este trabajo demostramos que la actividad aumentada de JNK sensibiliza a las células cancerígenas a apoptosis inducida por tratamientos quimioterapéuticos y, además, esta respuesta parece estar conservada en diferentes tipos de células tumorales, sugiriendo que podría ser potencialmente explotado para terapia antitumoral en combinación con agentes inductores del estrés oxidativo (Engel

and Evens, 2006). Así, la inhibición de p38α sensibilizaría a las células tumorales al tratamiento con estos agentes.

Usando un modelo animal de cáncer de mama y un inhibidor de p38α que está en ensayos clínicos para procesos antiinflamatorios (Goldstein et al., 2010; Hope et al., 2009), hemos confirmado *in vivo* que la inhibición de p38α coopera con el cisplatino para matar a las células tumorales. Además, no sólo los tumores de mama eran más pequeños, sino que también se veían histológicamente menos malignos. La proliferación celular también había sido reducida, indicando que la inhibición de p38α podría ralentizar probablemente el crecimiento de nuevos tumores en el caso de una recidiva, como efectivamente hemos corroborado.

Se ha publicado que la inhibición de p38 MAPK podría ayudar a algunos agentes quimioterapéuticos a matar a las células cancerígenas. Este es el caso de células de mieloma tratadas con bortezomib (Navas et al., 2006), células de linfoma tratadas con etoposida (Kurosu et al., 2005), o gliomas tratados con temozolomida (Demuth et al., 2007). En estos casos, el incremento del efecto citotóxico observado tras la inhibición de p38 MAPK estaba asociado a una parada defectiva del ciclo celular en G2. Se ha propuesto que la señalización de p38α podría tener un papel importante para regular la expresión de proteínas implicadas en la supervivencia de células paradas en G2 (Phong et al., 2010). En cambio, nosotros mostramos que la inhibición de p38α resulta en la acumulación de ROS y activación de JNK, sensibilizando a las células tumorales a apoptosis inducida por cisplatino, tanto en líneas celulares de cáncer humanas como en un modelo animal de cáncer de mama. Parece poco probable que la parada de ciclo celular sea requerida para la acumulación de ROS en respuesta a la inhibición de p38α, aunque no podemos descartar que la parada en G2 contribuya a la reducción en proliferación de las células tumorales tras incubación con el inhibidor de p38α. Nuestros resultados también indican que el efecto cooperativo de la inhibición de p38α junto con el tratamiento de cisplatino probablemente sea independiente de

p53, ya que hemos observado este efecto pro-apoptótico en células cancerígenas con distintos estados de p53.

En su conjunto, estos resultados revelan un nuevo mecanismo mediante el cual p38α contribuye a la supervivencia de la célula tumoral manteniendo bajos los niveles de ROS, y sugieren que la combinación de inhibidores de p38α con agentes quimioterapéuticos podrían ser considerados para la terapia antitumoral.

Conclusiones

1. La kinasa eEF2 podría ser una compañero letal sintético de p38 MAPK en células cancerígenas con p53 salvaje en respuesta al tratamiento con cisplatino.

2. p38 MAPK no es necesaria para la proliferación basal de todas las células cancerígenas.

3. Disfunción de p38α activa la ruta de JNK en células cancerígenas en condiciones basales y las sensibiliza a apoptosis, independientemente del estado de p53.

4. La inhibición de p38 MAPK regula negativamente la producción de enzimas antioxidantes, incrementando así los niveles de ROS en la célula cancerígena, lo que conduce a la inactivación de las fosfatasas de JNK.

5. La inhibición de p38 MAPK coopera con el cisplatino para reducir el tamaño y malignidad de los tumores en un modelo de ratón de cáncer de mama.